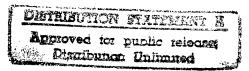


# JPRS Report



# Science & Technology

Central Eurasia: Materials Scient

DTIC QUALITY INSPECTED 2

19980120 051

REPRODUCED BY
U.S. DEPARTMENT OF COMMERCE
NATIONAL TECHNICAL
INFORMATION SERVICE
SPRINGFIELD, VA 22161

# Science & Technology Central Eurasia: Materials Science

JPRS-UMS-92-003

#### **CONTENTS**

16 March 1992

#### **ANALYSIS, TESTING**

Simulation of Sintered SmCo <sub>5</sub> Magnet Polarity Reversal [A.M. Gabay, A.S. Lileyev, et al.; IZVESTIYA VYSSHIKH UCHEBNYKH ZAVEDENIY: CHERNAYA	. 1
METALLURGIYA, Sep 91]	•
Strength Analysis of Collapsible Diamond Dies	
[V.N. Kissyuk, V.N. Lvov, et al.; IZVESTIYA VYSSHIKH UCHEBNYKH ZAVEDENIY: CHERNAYA	
METALLURGIYA, Sep 91]	. 1
Investigation of Effect of Impurity Elements on Photometric Identification of Aluminum in Alloyed	l
Investigation of Effect of Impurity Elements on Photometric Identification of Administration in Analysis	
Steels IT N Zakharova I.M. Kuzmin, et al.: ZAVODSKAYA LABURATOKIYA, Dec 91]	. 1
Computer-Aided MTI-3M Complex for Measuring Microhardness of Materials and Coats	
[V.N. Skvortsov, R.M. Matveyevskiy, et al.; ZAVODSKAYA LABORATORIYA, Dec 91]	. 2
[V.N. Skvortsov, R.M. Matveyevskiy, et al., 2AVODSKATA LABORATORIA, Physical and Mochanical	
Computer-Aided Collection and Processing System for Experimental Data on Physical and Mechanical	٠ _
Properties of Metal IA A Perfilov, Ye.D. Panov, et al.: ZAVODSKAYA LABORATORIYA, Dec 911	. 2
Crack Resistance Characteristics of Welded Joints: Assessment, Design, and Statistical Analysis	
[A.M. Lepikhin, V.V. Moskvichev; ZAVODSKAYA LABORATORIYA, Dec 91]	. 2
[A.M. Lepikhin, V.V. Moskvichev, ZAVODSKATA LABORATORITA, Det 31]	_
Crack Growth Criterion Under Creep Conditions	•
[S.I. Olkin; ZAVODSKAYA LABORATORIYA, Dec 91]	. 2
Computer Aided Compley for High-Temperature X-Kay Studies	
[A.V. Terukov, O.M. Ivasishin, et al.; ZAVODSKAYA LABORATORIYA, Dec 91]	. 3
[A.V. Terukov, O.M. Ivasisnin, et al., EAVODSKATA Laboration Bushors by Atomic Absorption	
Identification of Microscopic Co Quantities in SKD-KP Butadiene Rubber by Atomic Absorption	٠ ،
Method [Ye.M. Volchikhina, A.P. Garshin, et al.; ZAVODSKAYA LABORATORIYA, Dec 91]	, 3
Atomic Absorption Identification of Impurities in Chromium (III) Chloride	
[D.I. Kurbatov, G.A. Bolshakova, et al.; ZAVODSKAYA LABORATORIYA, Dec 91]	. 3
D.I. Karbatov, G.A. Dolsimova, Et al., 221 V Obstantial Land	
Atomic Absorption Analysis of Natural and Waste Water	Δ
[N.N. Basargin, N.V. Chernova, et al.; ZAVODSKAYA LABORATORIYA, Dec 91]	, ,
Coulometric Identification of Generic Iron in Iron ()re Materials	
IA N. Magiloughiy, I.S. Shlyaranko, et al.: 74VODSKAYA LABORATORIYA, Dec 911	. 4
Chamical Atomic Emission Analysis of High-Purity Ga and In With Breakdown by Bromine Vapors III	1
Confined Volume [L.L. Baranova, L.D. Berliner, et al.; ZAVODSKAYA LABORATORIYA, Dec 91]	. 4
Confined Volume [L.L. Baranova, L.D. Bertiner, et al., 247 Obstatil Eliboration Allows	
Proximate Photometric Antimony Identification in Nonferrous Alloys	5
[I.S. Novikova, V.V. Fedorov, et al.; ZAVODSKAYA LABORATORIYA, Dec 91]	ر ,
Photomechanical Identification of Palladium in Aminochloride Electrolytes	
[Ye.P. Parkhomenko, N.F. Falendysh, et al.; ZAVODSKAYA LABORATORIYA, Dec 91]	. 5
Tin Identification Within Broad Concentration Range in Nonferrous Metal Alloys	
[S.V. Toporov, N.L. Olenovich; ZAVODSKAYA LABORATORIYA, Dec 91]	5
[S.V. Toporov, N.L. Olenovich; ZAV ODSKATA LABORATORITA, Det 9]	
Investigation of Composite Material Failure by Mechanoluminescence Method Within Broad Loading	, ,
Pote Dange III F Krawa PP Kalnin et al PROBLEMY PROCHNOSTI, Sep 911	. ,
Second All Penublic Seminar on Dynamic Strength and Crack Resistance of Structural Materials Under	Γ
One-Time Impulse Loading [G.V. Stepanov; PROBLEMY PROCHNOSTI, Sep 91]	. 6
One-Time Impulse Dodding 10.7. Stepanov, Incommission in Strong Magnetic Fields	
Phase and Structure Changes in Metals Under Pulse Straining in Strong Magnetic Fields	6
[A.V. Stepuk; PROBLEMY PROCHNOSTI, Sep 91]	
Experimentally Analytical Method of Determining Strength Characteristics of Material Under	Ī
Ouggietatic Tensile Conditions	
[M.M. Astakhov, A.V. Loginov, et al.; PROBLEMY PROCHNOSTI, Sep 91]	. 6
Effect of High-Speed Straining and Temperature on Strength and Ductility Characteristics of Cr-Ni-Mo	)
Effect of riigh-speed straining and reinperature on strength and Ductinty Characteristics of Criticity	6
Steel [A.P. Vashchenko, V.P. Leonov, et al.; PROBLEMY PROCHNOSTI, Sep 91]	, U
Effect of Artificial Surface Defects on Steel Slab Failure During Contact Loading by Explosive Layer	
Detonation [A.S. Ispatyev; PROBLEMY PROCHNOSTI, Sep 91]	. 7
Estimation of Comment Contract Of Page Clab During Evaloring Welding	
[V.G. Resinov, S.G. Tsybochkin, et al.; PROBLEM WALLING WALLING	. 7
[V.G. Resinov, S.G. Isyoochkin, et al., FRODELM I INCOMINGSII, Sep 71]	•
[V.P. Bartenev, G.V. Stepanov; PROBLEMY PROCHNOSTI, Sep 91]	. /
•	

Approximation Model of Structural Material Failure and Failure Wave Problem  [A.S. Kravchuk, A.V. Malashkin; PROBLEMY PROCHNOSTI, Sep 91]	S
Analysis of Rapid-Quenched Strip Surface Configuration and Quality	
[B.V. Molotilov, N.M. Zapuskalov, et al.; STAL, Dec 91]	8
Testing of 32G2F Steel for High-Strength Drill Pipe Shells	•
[Ye.A. Solomadina, D.A. Akhmedova, et al.; STAL, Dec 91]	8
ZrO <sub>2</sub> -Y <sub>2</sub> O <sub>3</sub> -Sc <sub>2</sub> O <sub>3</sub> System's Liquidus Surface	Ĭ
[A.V. Shevchenko, L.M. Lopato, et al.; IZVESTIYA AKADEMII NAUK SSSR: SERIYA	
NFORGANICHESKIYE MATERIALY Dec 911	8
Magnetoelectric Properties of Piezoelectric and Magnetostrictive Materials' Mixtures With Polymer	
Binder	
[T.G. Lupeyko, S.S. Lopatin, et al.; IZVESTIYA AKADEMII NAUK SSSR: SERIYA	
NEORGANICHESKIYE MATERIALY, Dec 91]	9
Phase Composition and Photoconductivity of TlIn <sub>1-x</sub> Dy <sub>x</sub> S <sub>2</sub> Crystals	
[E.M. Kerimova, G.B. Gasymov, et al.; IZVESTIYA AKADEMII NAUK SSSR: SERIYA	
NEORGANICHESKIYE MATERIALY, Dec 91]	9
Effect of Magnetic Field on Residual Impurity and Dopant Distribution in InSb	
[A.N. Popkov, V.S. Vekshina, et al.; IZVESTIYA AKADEMII NAUK SSSR: SERIYA	_
NEORGANICHESKIYE MATERIALY, Dec 91]	9
Effect of Transverse Magnetic Field on Residual Impurity Concentration in InSb	
[A.N. Popkov, V.S. Vekshina, et al.; IZVESTIYA AKADEMII NAUK SSSR: SERIYA	
	10
Growing of Ge-Doped InSb Crystals Under Effect of Transverse Magnetic Field on Melt	
[A.N. Popkov, A.Ya. Polyakov, et al.; IZVESTIYA AKADEMII NAUK SSSR: SERIYA	10
NEORGANICHESKIYĖ MATERIALY, Dec 91]	10
On Interrelation of Electric Conductivity and Porosity of Quasi-Isotropic Carbon Materials  [I.Ya. Levintovich, A.S. Kotosonov, et al.; IZVESTIYA AKADEMII NAUK SSSR: SERIYA	
NEORGANICHESKIYE MATERIALY, Dec 91]	10
Investigation of Thermoelectric Materials Based on Solid Solutions of Bi <sub>2</sub> Te <sub>3</sub> -Bi <sub>2</sub> Se <sub>3</sub> and Sb <sub>2</sub> Te <sub>3</sub> -Bi <sub>2</sub> Te <sub>3</sub>	10
Systems Doped With Copper and Nickel	
[A.A. Mageramov, A.T. Tilavoldiyev, et al.; IZVESTIYA AKADEMII NAUK SSSR: SERIYA	
NEORGANICHESKIYE MATERIALY, Dec 91]	11
Interrelation Between Conductivity, Thermoelectric Coefficient, and Magnetic Susceptibility of	
Semiconductor Melts	
[V.M. Glazov, A.I. Faradzhov; IZVESTIYA AKADEMII NAUK SSSR: SERIYA	
NEORGANICHESKIYE MATERIALY, Dec 91]	11
Lu-Lu <sub>2</sub> S <sub>3</sub> System	
[O.V. Andreyev, N.N. Parshukov; IZVESTIYA AKADEMII NAUK SSSR: SERIYA	
NEORGANICHESKIYE MATERIALY, Dec 91]	11
Structure and Electric Properties of Rapidly Quenched InSb Foils and InSb-InBi System Solid Solutions	
[V.G. Shepelevich; IZVESTIYA AKADEMII NAUK SSSR: SERIYA NEORGANICHESKIYE	
MATERIALY, Dec 91]	11
The Physicochemical Properties of a Cd <sub>1-x</sub> Mn <sub>x</sub> Te Surface With Varying Mn Contents	
[Ye.V. Buzaneva, T.A. Vdovenkova, et al.; PÖVERKHNOST: FIZIKA, KHIMIYA, MEKHANIKA,	12
	12
Determination of the Dependence of Acoustic Emission Parameters on Deformation During the Simple Bending of Composites Consisting of Materials With Different Strengths	
	12
The Effect of a Free Surface on the Distribution of Point Defects in a Metal	12
[Yu.N. Devyatko, O.V. Tapinskaya; POVERKHNOST: FIZIKA, KHIMIYA, MEKHANIKA, Dec 91]	13
Phase Transformations in Cd <sub>0.2</sub> Hg <sub>0.8</sub> Te due to the Effect of Pulsed Laser Radiation of Nanosecond	13
Duration	
[P.V. Goloshikhin, K.Ye. Mironov, et al.; POVERKHNOST: FIZIKA, KHIMIYA, MEKHANIKA,	
Dec 911	13
Effective Strength Parameters of Matrix Composites	
[V.A. Buryachenko, Yu.S. Skorbov, et al.; PROBLEMY PROCHNOSTI, Dec 91]	13
Generalizing the Solution of a Prandtl Problem of the Compression of a Plastic Layer With Two Rough	
	14
The Deformation and Fracture of Boron-Aluminum Composite in a Complex Stressed State	
[S.V. Tsvetkov, P.A. Zinovyev, et al.; PROBLEMY PROCHNOSTI, Dec 91]	14

	Mathematical Modeling of the Destruction of Brittle Inhomogeneous Mineral Ores	1 4
	[I.A. Sveshnikov, L.Ya. Mishnayevskiy; PROBLEMY PROCHNOSTI, Dec 91]	14
	The Link Between Critical Embrittlement Temperature and Stress Concentrator Geometry and Loading Rate [M. Mishin, I.V. Kislyuk, et al.; PROBLEMY PROCHNOSTI, Dec 91]	1.5
	The Arrest and Propagation of a Brittle Crack in Construction Steels. Communication 1	1.5
	[Z. Bilek, M. Cherny; PROBLEMY PROCHNOSTI, Dec 91]	15
	The Arrest and Propagation of a Brittle Crack in Construction Steels, Communication 2	
	IM Cherny Z. Rilek: PRORLEMY PROCHNOSTI, Dec 911	16
	Temperature Dependences of the Propagation Rate of Longitudinal Ultrasound Waves in Aluminum	
	Oxide and Zirconium Dioxide Monocrystals	
	[V.A. Borisenko, A.I. Troyanskiy; PROBLEMY PROCHNOSTI, Dec 91]	16
	An Investigation of Structural and Phase Transformations in Carbon Steels Subjected to the Combined	
	Effects of Laser Radiation and a Magnetic Field	
	[I.V. Suminov, Ye.V. Klopikov, et al.; FIZIKA I KHIMIYA OBRABOTKI MATERIALOV, No 3,	15
	May-Jun 91]	1 /
	An Investigation of the Destruction of Composites by Laser Radiation in a Vacuum and at Atmospheric	
	Air Pressure	
	[V.T. Karpukhin, M.M. Malikov, et al.; FIZIKA I KHIMIYA OBRABOTKI MATERIALOV, No 3,	17
	May-Jun 91]  A Study of the Microstructure and Mechanical Characteristics of 40Cr10C2Mo Steel After Laser	1 /
	Treatment	
	[A.G. Grigoryants, S.I. Aleksenko, et al.; FIZIKA I KHIMIYA OBRABOTKI MATERIALOV, No 3,	
	May-Jun 91]	18
	The Interaction of Radiation Defects With Lithium Impurity Atoms in Aluminum	
	IV.L. Arbuzov, A.E. Davletshin, et al.; FIZIKA I KHIMIYA OBRABOTKI MATERIALOV, No 3,	
	Mav-Jun 911	18
	The Effect of a Metal's Defect Structure on Interstitial Ion Distribution Profile	
	[V.I. Boyko, B.Ye. Kadlbovich, et al.; FIZIKA I KHIMIYA OBRABOTKI MATERIALOV, No 3,	
	May-Jun 91]	18
	Damage to Tungsten Monocrystal by Fast Heavy Ions	
	[V.N. Bugrov, S.A. Karamyan; FIZIKA I KHIMIYA OBRABOTKI MATERIALOV, No 3,	1.0
	May-Jun 91]	19
	The Dissolution of Aluminum and Its Alloys in Mineral Acid Solutions [V.P. Kochergin, L.V. Paderova, et al.; IZVESTIYA VYSSHIKH UCHEBNYKH ZAVEDENIY:	
	TSVETNAYA METALLURGIYA, No 2, Apr 91]	19
	TOVETNATA METALLOROTTA, NO 2, Apr 31j	• •
CO	ATINGS	
	The High-Temperature Oxidation of a Composite Material Consisting of 80% TiB <sub>2</sub> and 20% TiC	
	IV.S. Shestitko. P.V. Polvakov, et al.: IZVESTIYA VYSSHIKH UCHEBNYKH ZAVEDENIY:	• •
	TSVETNAYA METALLURGIYA, No 2, Apr 91	20
	Selected Features of Pulsed Laser Hardening of Titanium Alloys	
	[A.P. Lyubchenko, Ye.A. Satanovskiy, et al.; FIZIKA I KHIMIYA OBRABOTKI MATERIALOV, No 6,	20
	Nov-Dec 91]	20
	[A.N. Bekrenev, Ye.A. Morozova; FIZIKA I KHIMIYA OBRABOTKI MATERIALOV, No 6,	
	Nov-Dec 91]	20
	Protective Diamondlike Films on Quartz	
	[S.M. Klotsman, A.S. Kovsh, et al.; FIZIKA I KHIMIYA OBRABOTKI MATERIALOV, No 6,	
	Nov-Dec 911	21
	Morphologic Changes in the Structure of Composite Conglomerated Powders During Plasma Sputtering	
	and Their Effect on Coating Structure	
	[A.K. Tolstobrov, M.Yu. Zashlyapin, et al.; FIZIKA I KHIMIYA OBRABOTKI MATERIALOV, No 6,	
		21
	Improving the Quality of Chemical Coatings of the System Ni-P on Tool Steels by Laser Irradiation	
	[G.I. Brover, V.N. Varavka, et al.; FIZIKA I KHIMIYA OBRABOTKI MATERIALOV, No 3,	22
		22
	Laser-Stimulated Chemical Deposition of Nickel Films [M.R. Bruk, Ye.A. Morozova, et al.; FIZIKA I KHIMIYA OBRABOTKI MATERIALOV, No 3,	
	[M.K. Bruk, Ye.A. Morozova, et al.; FIZIKA I KHIMITA OBKABOTKI MATERIALOV, NO 5, May-Jun 91]	22
	1414y-3411 71J	

The Porosity and Electrical Strength of Thin Alumina and Zirconia Films Produced by High-Frequency Magnetron Sputtering	<b>/</b>
[V.G. Padalka, I.V. Lunev, et al.; FIZIKA I KHIMIYA OBRABOTKI MATERIALOV, No 3,	
May-Jun 91]	. 23
The Formation Mechanism of Crystal Lattice Defects in Electrodeposited Nickel Films	21
[T.A. Tochitskiy, A.V. Bolutshkin; POVERKHNOST: FIZIKA, KHIMIYA, MEKHANIKA, Dec 91] Laws Governing the Growth of a Gold Film on a Benzene Substrate at 77 K	. 2:
[V.L. Karnatsevich, B.S. Kaverin, et al.; POVERKHNOST: FIZIKA, KHIMIYA, MEKHANIKA,	
	. 24
The Formation Mechanism of Films Produced by Reactive Ion-Plasma Deposition [A.N. Pilyankevich, V.Yu. Kulikovskiy, et al.; POVERKHNOST: FIZIKA, KHIMIYA, MEKHANIKA Dec 91]	
Dielectric Layer Formation on InP by Thermal Oxidation of InP/PbS Structures	
[I.Ya. Mittova, V.V. Pukhova, et al.; IZVESTIYA AKADEMII NAUK SSSR: SERIYA NEORGANICHESKIYE MATERIALY, Dec 91]	. 25
COMPOSITE MATERIALS	
Calculation of the Adhesion Characteristics of a System of Two Different Metals Separated by	
Dielectric Layer	
[A.N. Vakilov, V.V. Prudnikov; POVERKHNOST: FIZIKA, KHIMIYA, MEKHANIKA, Dec 91]	
Irradiation [R.G. Khanbekov, Kh.M. Rasulkulov, et al.; IZVESTIYA AKADEMII NAUK SSSR: SERIYA NEORGANICHESKIYE MATERIALY, Dec 91]	
An Investigation of Destruction of Composite Materials by Laser Radiation and a Supersonic Nitroger Flow	. 20 1
[A.A. Betev, V.T. Karpukhin, et al.; FIZIKA I KHIMIYA OBRABOTKI MATERIALOV, No 6, Nov-Dec 91]	. 26
FERROUS METALS	
The Effect of Argon Ion Channeling on the Sputtering of a Niobium Monocrystal Surface	
[A.A. Kosyachkov, V.T. Cherepin, et al.; POVERKHNOST: FIZIKA, KHIMIYA, MEKHANIKA,	
Dec 91]  Development and Implementation of Low-Sulfur Steel-Making Pig Iron Smelting Under Southern USSR	. 28
Conditions [S.N. Pryadko, V.I. Malkin, et al.; STAL, Dec 91]	. 28
Metal Jet Drop Height During In-Line Vacuum Degassing of Continuously Cast Steel: Discussion	
[A.A. Smirnov; STAL, Dec 91]	. 28 . 29
MONEEDDOUG METALS ALLOWS DRAZES SOUDEDS	
NONFERROUS METALS, ALLOYS, BRAZES, SOLDERS	
The Nitriding of a Nickel Alloy and Its Properties	
[Yu.V. Levinskiy, A.A. Nuzhdin, et al.; FIZIKA I KHIMIYA OBRABOTKI MATERIALOV, No 6,	
Nov-Dec 91] The Formation of Mg <sub>32</sub> (Al, Zn) <sub>49</sub> and Al-Mg-Zn Phases in an Unsaturated Aluminum-Magnesium-Zinc	. <b>3</b> 0
Solid Solution Upon Electron Irradiation in a Diffraction Channeling Mode [V.V. Ivanov, V.M. Lazorenko, et al.; FIZIKA I KHIMIYA OBRABOTKI MATERIALOV, No 6,	
Nov-Dec 91]	
Gold Extraction With Low-Basicity Anion Exchangers	
[G.A. Stroganov, V.Ye. Dementyev, et al.; TSVETNYYE METALLY, Jun 91]	30
Producing Silicon Single Crystals With Uniformly Distributed Oxygen [Z.A. Salnik, Ye.S. Levshin, et al.; TSVETNYYE METALLY, Jun 91]	31
Electrolyzer for Carnallite With Wider Separation Zone Between Products of Electrolysis	<i>J</i> 1
[P.A. Donskikh, V.A. Kolesnikov, et al.; TSVETNYYE METALLY, Jun 91]	31
Results of Test Performed on Model of Cooler for Anodes of Magnesium Electrolyzer [V.F. Yalovoy, A.M. Sizonenko, et al.; TSVETNYYE METALLY, Jun 91	21
Behavior of Lead Anodes in Sulfuric Acid Solutions Containing Cobalt	
[A.A. Kucherov, A.D. Artemyev, et al.; TSVETNYYE METALLY, Jun 91]	32

#### **PREPARATIONS**

Efficiency of the Absorption of Radiation Point Defects by Pores Surrounded by [S.B. Kislitsin, Yu.S. Pyatiletov, et al.; FIZIKA I KHIMIYA OBRABOTKI Nov-Dec 91]	I MATERIALOV, NO 0,
Use of Cryogenic Technology To Produce Powders  [A.F. Alekseyev, K.K. Palekha, et al.; FIZIKA I KHIMIYA OBRABOTKI  May-Jun 911	MATERIALOV, No 3,
Preparation and X-Ray Phase Analysis of Thin Zinc Arsenide Films  [N.S. Zhalilov, G.S. Yuryev, et al.; IZVESTIYA AKADEMII N. NEORGANICHESKIYE MATERIALY Dec 911	AUK SSSR: SERIYA
ZnSe Production by Self-Propagating High-Temperature Synthesis Method and [S.V. Kozitskiy, D.D. Polishchuk, et al.; IZVESTIYA AKADEMII [NEORGANICHESKIYE MATERIALY, Dec 91]	ZnSe Properties NAUK SSSR: SERIYA
Photoluminescence of ZnSe/GaAs (100) Heterostructures [N.V. Bondar, A.V. Kovalenko, et al.; IZVESTIYA AKADEMII N NEORGANICHESKIYE MATERIALY, Dec 911	NAUK SSSR: SERIYA
Eu <sub>2</sub> Ti <sub>2</sub> O <sub>7</sub> Phase Produced at High Pressures and Its Ferroelectric Properties [A.M. Sych, S.Yu. Stefanovich, et al.; IZVESTIYA AKADEMII NEORGANICHESKIYE MATERIALY, Dec 91]	NAUK SSSR: SERIYA
Growing of Single Crystals of CuI and Its Certain Properties  [V.I. Popolitov; IZVESTIYA AKADEMII NAUK SSSR: SERIYA  MATERIALY, Dec 911	NEORGANICHESKIYE
Growing of MgGa <sub>2</sub> S <sub>4</sub> Single Crystals and Their Photoelectric Properties [N.A. Moldovin; IZVESTIYA AKADEMII NAUK SSSR: SERIYA MATERIALY Dec 011	NEORGANICHESKIYE
Production of Promising Types of Metal Products by Continuous Horizontal Tv [V.M. Sinitskiy, A.I. Mayorov, et al.; STAL, Dec 91]	
Correcting Titanium Content Within Narrow Range in Continuous Casting Making [A.I. Trotsan, B.F. Belov, et al.; STAL, Dec 91]	achine During Pipe Steel
Amorphous Precision Alloys: Technology, Properties, Applications  [A.M. Glezer, A.G. Kozlov; STAL, Dec 91]  Mathod of Making Wire From Low Carbon Steel	
[V.Ya. Chinokalov, V.P. Kolpak, et al.; STAL, Dec 91]	
TREATMENTS	
The Effect of Cycling on the Crack Formation of Austenite Chromium Mang Use in a Controlled Thermonuclear Reactor [S.Ye. Gurevich, Ye.V. Demina, et al.; FIZIKA I KHIMIYA OBRABOTKI May-Jun 91]	MATERIALOV, No 3,
Structural Changes in Polycrystalline Scandium Oxide Upon Ion Irradiation [A.Ye. Solovyeva, E.M. Diasamidze, et al.; FIZIKA I KHIMIYA OBRABOTK Nov-Dec 911	XI MATERIALOV, No 6,
The Erosion of Quartz Under the Effect of High-Power Nanosecond Ion Beams [V.P. Krivobokov, O.V. Pashchenko, et al.; FIZIKA I KHIMIYA OBRABOTK	I MATERIALOV, No 6,
Sets of Radiation Effect Functions in the Problem of Predicting the Sta Instruments in Ionizing Radiation Fields [V.I. Ostroumov, G.G. Solovyev, et al.; FIZIKA I KHIMIYA OBRABOTKI	MATERIALOV, No 6,
Nov-Dec 91]	
[S.Ā. Baryshev, G.A. Yermakov, et al.; FIZIKA I KHIMIYA OBRABOTKI	MATERIALOV, No 6,
The Properties and Use of Uranium Fluoride Plasma  Yu.N. Tumanov, K.V. Tsirelnikov; FIZIKA I KHIMIYA OBRABOTKI MATEL	RIALOV, No 6,
Nov-Dec 91]	4

An Experimental Investigation of the Discharge Occurring During the Effect of Continuous-Wave Radio-Frequency Radiation on Dielectric Materials  [Yu.V. Bykov, A.G. Yeremeyev, et al.; FIZIKA I KHIMIYA OBRABOTKI MATERIALOV, No 6, Nov-Dec 91]	10
Nov-Dec 91]	
[B.A. Kolachev, Yu.B. Yegorova, et al.; IZVESTIYA VYSSHIKH UCHEBNYKH ZAVEDENIY: TSVETNAYA METALLURGIYA, No 2, Apr 91]4	11
EXTRACTIVE METALLURGY, MINING	
The Problem of Creating an Integrated Technology To Reprocess Platinum-Bearing Chromatites—A New Mineral Ore Containing Platinum Metals	
[L.V. Razin, T.N. Greyver, et al.; IZVESTIYA VYSSHIKH UCHEBNYKH ZAVEDENIY: TSVETNAYA METALLURGIYA, No 2, Apr 91]	12
Operation of the Nonreturn Valve in a Separator for Regenerating Magnetic Fluids  [V.N. Gubarevich, S.V. Vidsota; IZVESTIYA VYSSHIKH UCHEBNYKH ZAVEDENIY: TSVETNAYA  METALLURGIYA, No 2, Apr 91]	12
An Analytic Method of Calculating the Parameters of the Magnetic Field in the Live Zone of a Magnetic-Gravitation Separator Based on Permanent Magnets	
[A.B. Solodenko; IZVESTIYA VYSSHIKH UCHEBNYKH ZAVEDENIY: TSVETNAYA METALLURGIYA, No 2, Apr 91]4	12
The Effect of pH on the State of Fatty Acid Collectors of Heavy Metal Ions in Solutions [L.D. Skrylev, V.F. Sazonova, et al.; IZVESTIYA VYSSHIKH UCHEBNYKH ZAVEDENIY: TSVETNAYA METALLURGIYA, No 2, Apr 91]	13
MISCELLANEOUS	
Learning To Use the First Domestically Manufactured Ladle Furnace [V. P. Denisenko, Yu. A. Koval, et al.; PROBLEMY SPETSIALNOY ELEKTROMETALLURGII, No 4 91]	14
Data Bank for Electroslag Remelting and Related Technologies [V. M. Litvinchuk; PROBLEMY SPETSIALNOY ELEKTROMETALLURGII, No 4, 91]	14

## Simulation of Sintered SmCo<sub>5</sub> Magnet Polarity Reversal

927D0082G Moscow IZVESTIYA VYSSHIKH UCHEBNYKH ZAVEDENIY: CHERNAYA METALLURGIYA in Russian No 9, Sep 91 pp 72-75

[Article by A.M. Gabay, A.S. Lileyev, S.A. Melnikov, V.P. Menushenkov, Moscow Institute of Steel and Alloys]

#### UDC 621.318.12

[Abstract] Extensive applications of SmCo<sub>5</sub> magnets are noted and an attempt is made to determine the parameters which characterize the magnetic polarity reversal of the elementary microvolumes and establish the relationship between these parameters and the hysteretic characteristics of the magnets. The model applicability is checked by experimentally measuring minor hysteresis loops (ChPG) of sintered magnets with various coercive forces and magnetic prehistories. The dependence of the maximum magnetization of minor hysteresis loops of a sintered magnet in a low coercivity state and the adjusted maximum magnetization calculated for the low coercivity ensemble on the magnetizing current amplitude and the dependence of the maximum magnetization of minor hysteresis loops of a sintered magnet in a high coercivity state and the adjusted maximum magnetization calculated for the high coercivity ensemble on the magnetizing current amplitude are plotted. The proposed model makes it possible to analyze minor hysteresis loops and magnetization curves of sintered magnets demagnetized by various methods and confirms that demagnetization is determined by the nucleation and growth of reverse magnetization domains. It is shown that the distribution of parameters characterizing the magnetization polarity reversal of individual elementary microvolumes may be determined from the properties of real magnets and that the magnetostatic interaction of sintered magnet grains is manifested in the behavior of minor hysteresis loops after the sample demagnetization by a static field. Although the study is performed for SmCo<sub>5</sub> sintered magnets, the results are applicable to other materials with a similar magnetization reversal mechanism. Figures 2; references 7: 2 Russian; 5 Western.

#### Strength Analysis of Collapsible Diamond Dies

927D0082F Moscow IZVESTIYA VYSSHIKH UCHEBNYKH ZAVEDENIY: CHERNAYA METALLURGIYA in Russian No 9, Sep 91 pp 61-64

[Article by V.N. Kissyuk, V.N. Lvov, G.P. Maltsev, All-Union Polytechnic Correspondence Institute]

UDC 621.778.1.07

[Abstract] The expediency of increasing the operating resistance of dies by developing leading compressive stresses on the outer contour of the diamond blank is

discussed and the issue of strength analysis of the holderdiamond system is considered. The computational procedure is aimed at ensuring joint operation of the holder and the diamond die and preventing separation on the contact boundary on the one hand and investigating the stressed state of the holder, usually made from a metal or alloy with a high yield strength, in order to select an appropriate material on the other. The holder-diamond system is simulated by two thick-walled cylinders inserted one into another. The proposed procedure for analyzing the strength of the holder-diamond and chuckholder-diamond systems makes it possible to avoid separation at the contact between the diamond and the holder or the holder and the chuck and increase the operating stability of diamond dies by precrimping the diamond beforehand. The latter measure opens up the possibility of using cheaper low carat raw materials and even synthetic diamonds. Figures 2; references 4.

#### Investigation of Effect of Impurity Elements on Photometric Identification of Aluminum in Alloyed Steels

927D0081A Moscow ZAVODSKAYA LABORATORIYA in Russian Vol 57 No 12, Dec 91 pp 1-3

[Article by T.N. Zakharova, I.M. Kuzmin, L.V. Vasilevskaya, L.S. Fokina, Institute of Standard Samples at the Central Scientific Research Institute of Ferrous Metallurgy imeni I.P. Bardin, Sverdlovsk]

UDC 546.62:543.432

[Abstract] The interfering effect of associated elements on chemical analysis methods can be assessed by the value of systematic error which is calculated allowing for the standard deviation of a single measurement result characterizing the analysis's random error. Since the effect of individual components may not be additive, an approach to examining the joint effect of all potential interfering components based on the factorial experiment design procedure is developed. In so doing, the ratio of the difference between the mass fraction of the component under study added to the solution and that determined from the results of the analysis to the normative standard deviation which characterizes the reproducibility of the results is used as the criterion of the measurement accuracy. Each experiment is conducted twice to estimate the random linear spread of initial data and experimental data are processed by the iterative regression analysis with subsequent examination of linear and quadratic models. The associated elements are selected according to existing standards as follows: 0.01-1.5% Nb, 3% V, Cu, and Ti, 5% Mo, 10% W, 25% Cr, and 35% Ni. It is shown that vanadium is the principal interfering associated element for identifying aluminum in the presence of the other components. The reliability of the method is checked by reproducing the values of certified aluminum concentrations in standard steel samples. Tables 1; references 8: 7 Russian; 1 Western.

## Computer-Aided MTI-3M Complex for Measuring Microhardness of Materials and Coats

927D0081N Moscow ZAVODSKAYA LABORATORIYA in Russian Vol 57 No 12, Dec 91 pp 55-57

[Article by V.N. Skvortsov, R.M. Matveyevskiy, V.A. Borodkin, Institute of Science of Machines imeni A.A. Blagonravov at the USSR Academy of Sciences, Moscow]

#### UDC 620.178.15.65.011.56

[Abstract] The MTI-3M computer-aided complex intended for investigating the micromechanical properties of products and samples from various materials by forcing the indenter into the specimen and automatically recording the indentation diagram in the forceindentation depth coordinates is described. Two microhardness testing procedures specified by GOST and COMECON standards are outlined and the conclusion is drawn that the method based on the depth of indentation is the most promising, objective, and reproducible. The use of the MTI-3M system for plotting the kinematic diagram of indentation and its advantages are outlined and a typical indentation diagram obtained by the new system is cited. In addition to the indenter and sensors, the new complex contains an IBM PC microcomputer and an RS/232 interface; the specifications of the indenter are cited. The proposed complex may be useful in physical metallurgy, mechanical engineering, metallurgy, fracture mechanics, mineralogy, and tribology. Figures 2: tables 1: references 3.

# Computer-Aided Collection and Processing System for Experimental Data on Physical and Mechanical Properties of Metal

927D0081M Moscow ZAVODSKAYA LABORATORIYA in Russian Vol 57 No 12, Dec 91 pp 53-55

[Article by A.A. Perfilov, Ye.D. Panov, S.N. Kabuzenko, M.V. Pirusskiy, Central Scientific Research Institute of Ferrous Metallurgy imeni I.P. Bardin]

#### UDC 620.172.224.65.011.56

[Abstract] A computer-aided system of mechanical tensile tests which is capable of collecting, processing, and storing experimental data as well as printing the results in the form of a test log, displaying them graphically on a color screen, and sending them to a graphics plotter is described. The system is developed at the Central Scientific Research Institute of Ferrous Metallurgy imeni I.P. Bardin and is characterized in that it can automatically identify the type of the diagram of conditional or physical yield strength and calculate the metal's strength parameters. The system is aimed at using conventional CAMAC, SM 1420, MERA 660, MERA 1300, and PC XT/AT computers and an ICHAC interface or a built-in interface board. The hardware components, system

architecture, and software are described in detail and an example of a tensile diagram is cited. The development of the system made it possible to automate the tedious and skill-demanding task of obtaining and processing experimental data on the physical and mechanical characteristics of metals, eliminate the subjective factor, increase the data reliability, and eliminate manual data entry. Figures 2.

#### Crack Resistance Characteristics of Welded Joints: Assessment, Design, and Statistical Analysis

927D0081L Moscow ZAVODSKAYA LABORATORIYA in Russian Vol 57 No 12, Dec 91 pp 48-51

[Article by A.M. Lepikhin, V.V. Moskvichev, Computer Center of the Siberian Department of the USSR Academy of Sciences, Krasnoyarsk]

UDC 620.192.46:621.791.052

[Abstract] The role of incipient and propagating cracks in the mechanics of fracture necessitates a study of the characteristics of crack resistance and such specific factors as the notch sensitivity index and critical crack apex divergence. In determining the crack resistance of welded joints, it is necessary to take into account the mechanical inhomogeneity of the joints due to the local character of thermal and mechanical metal "excitation" during the welding process which leads to the development of residual stress and strain, a change in the phase composition and structure, and the development of micro- and macrodefects. The results of mechanical tests of 3 mm-diameter samples and templates of welded joints from steel 10KhSND demonstrating the behavior of mechanical properties are examined: the ultimate strength, conditional yield strength, percentage reduction in area, and elongation and changes in the grain size and microhardness. As a result, the crack resistance behavior in the welded joint cross section, the dependence of crack resistance on the testing temperature, and the crack resistance distribution function in the welded joint are plotted. A study of the effect of structural and mechanical nonuniformity of welded joints on the crack resistance characteristics and the statistical patterns of their behavior as well as the possibilities of their simulation can be used in designing welded joints and analyzing their crack resistance and reliability on the basis of failure criteria. Figures 6; tables 1; references 20: 17 Russian; 3 Western.

#### Crack Growth Criterion Under Creep Conditions 927D0081K Moscow ZAVODSKAYA LABORATORIYA in Russian Vol 57 No 12, Dec 91 pp 42-45

[Article by S.I. Olkin, Central Aerohydrodynamic Institute imeni N.Ye. Zhukovskiy, Zhukovskiy, Moscow oblast]

UDC 620.178.38

[Abstract] The shortcomings of traditional approaches to describing the crack growth process are outlined and an approach based on the assumption that the crack growth rate (s.r.t.) under combined static and slow cyclical loading is a function of partial corrosion growth rates of the individual creep and fatigue conditions is proposed. Stress relaxation curves at the crack apex are plotted in the cases where the steady-state stress is lower and higher than the long-term strength and the stress distribution in the crack cross section is examined. Criterial relations are derived for the steady-state stress near the crack apex and creep tests of high-temperature aluminum alloy AK4-141 and nickel-based alloy KhN45MVTYuBR are conducted to check them. Crack growth curves in samples from the AK4-141 and KhN45MVTYuBR alloys are plotted. A procedure for calculating the notch sensitivity index of a slab with a central crack under the conditions of long-term static loading which makes it possible to determine the magnitude of local steady-state stress near the crack apex at the end of the relaxation process is proposed. The results also make it possible to conclude that the criterion of slow crack growth (or lack thereof) under creep conditions has been experimentally corroborated. Figures 3; references 13: 11 Russian; 2 Western.

## Computer-Aided Complex for High-Temperature X-Ray Studies

927D008IJ Moscow ZAVODSKAYA LABORATORIYA in Russian Vol 57 No 12, Dec 91 pp 32-33

[Article by A.V. Terukov, O.M. Ivasishin, I.A. Zabelina, A.M. Kats, V.V. Petkov, Institute of Physics of Metals at the Ukrainian Academy of Sciences, Kiev]

#### UDC 539.26.65.011.56

[Abstract] The difficulties of investigating the phase transformations occurring during he continuous heating of steels and alloys by conventional methods of X-ray diffractometry with the help of a DRON unit with a point detector and a high-temperature adapter chamber due to the noninstanteneous recording exposure are outlined and it is shown that the recording exposure may be shortened considerably by using a linear coordinate detector contained in the commercial RKD-1-01 system if its diffraction angle recording range of 5° is widened. An attempt to widen the diffraction angle recording range by recording several successive diffraction pattern segments on magnetic tape and subsequently outputting them to a plotter is reported and a computer-aided system developed for this purpose is described. The system uses an Iskra-1256 computer and a new application software package. The system architecture is cited and diffraction patterns of hardened titanium alloy VT23 are plotted. Each frame has an 80 s exposure. The proposed complex makes it possible to shorten the

recording time considerably and automate the experimental data collection and processing. Figures 2; references 3.

## Identification of Microscopic Co Quantities in SKD-KP Butadiene Rubber by Atomic Absorption Method

927D0081I Moscow ZAVODSKAYA LABORATORIYA in Russian Vol 57 No 12, Dec 91 pp 22-23

[Article by Ye.M. Volchikhina, A.P. Garshin, V.V. Krivoshein, All-Union Science Research Institute of Synthetic Rubber imeni Academician S.V. Lebedev, Voronezh]

#### UDC 543.422:546.73

[Abstract] The use of the atomic absorption analysis of butadiene rubber for microscopic quantities of cobalt which makes it possible to measure the Co concentration within a 10<sup>-4</sup>-10<sup>-3</sup>% by mass both during the production process and in the ready product is reported. SKD-L250 rubber (containing no cobalt) produced with a lithium catalyst and SKD-KP rubber produced with a cobalt catalyst are analyzed in an AAS-IN atomic absorption spectrophotometer (Carl Zeiss Jena). The optimum photometry conditions which ensure a high sensitivity and reproducibility of the results are determined and the reagents, solutions, and analytical procedure are described in detail. The results of an analysis of artificial mixtures of rubber with cobalt nitrate and the material balance of the cobalt distribution in water-flushed SKD-KP rubber are summarized. Data of statistical processing at a 0.95 confidence level are cited. The proposed technique is sufficiently simple and together with sample preparation, takes only 2 h. Tables 3; references 5.

## Atomic Absorption Identification of Impurities in Chromium (III) Chloride

927D0081H Moscow ZAVODSKAYA LABORATORIYA in Russian Vol 57 No 12, Dec 91 pp 21-22

[Article by D.I. Kurbatov, G.A. Bolshakova, G.A. Nikitina, Chemistry Institute at the Urals Department of the USSR Academy of Sciences, Sverdlovsk]

#### UDC 543.422:546.76

[Abstract] The difficulties of identifying chromium (III) chloride used as catalysts in making low-pressure polyethylene are noted and the development of a new technique for determining the mass fraction of Fe, Co, Cu, Mn, Al, Ca, and Mg impurities in chromium (III) chloride without separating it from the base is reported. The study is performed in a mod. 503 Perkin-Elmer atomic absorption spectrophotometer and shows that the use of polyatomic alcohols for dissolving chromium (III) chloride produces satisfactory results. The analytical procedure is described in detail and mass fractions of impurity

elements from ethylene glycol model solutions of chromium (III) chloride in the presence of ethanol or acetone and water measured by the proposed method are summarized. A formula is derived for determining the mass fraction of the impurity elements. The new method is capable of identifying iron, nickel, cobalt, copper, manganese, and calcium impurities at concentrations of up to 0.005%, magnesium at up to 0.0005%, and aluminum at up to 0.05%. Tables 1; references 2.

## Atomic Absorption Analysis of Natural and Waste Water

927D0081G Moscow ZAVODSKAYA LABORATORIYA in Russian Vol 57 No 12, Dec 91 pp 19-20

[Article by N.N. Basargin, N.V. Chernova, Yu.G. Rozovskiy, Ye.V. Petrunovskaya, Institute of Ore Deposit Geology, Petrography, Mineralogy, and Geochemistry at the USSR Academy of Sciences, Moscow]

#### UDC 543.422:543.3

[Abstract] The importance of the analytical task of identifying heavy metal ions in natural and waste water and the outlook for using chelating polymer sorbents for concentrating the microelements from natural waters are discussed and the possibility of using new chelating sorbents, particularly polystyrene-azo-4-oxy-3-arsonobenzene and polystyre-azo-3-sulfophenol-4 as well as polystyrene-methylene-imino-4-nitro-6-sulfophenol-1 and polyorgs VII m for concentrating heavy metals and comparing the data on group concentration with subsequent atomic absorption identification for various elements, is investigated. The synthesis of polymer chelate sorbents and optimal group concentration conditions are outlined and the analytical procedure is described in detail. The optimum conditions of measuring absorption using an AAS-IN spectrometer are determined and the results of atomic absorption identification of elements in drinking water with additions and in ground water and waste water are summarized. The outcome of the experiments makes it possible to compare the selectivity, sorption completeness, and sorption capacity of various reagents and shows that the new sorbents exceed the polyorgs VII m sorbent by a factor of 12-13 as well as ensure quantitative and selective extraction of a sum of microelements at a lower concentration level than other reagents. Tables 3; references 5.

## Coulometric Identification of Generic Iron in Iron Ore Materials

927D0081F Moscow ZAVODSKAYA LABORATORIYA in Russian Vol 57 No 12, Dec 91 pp 14-16

[Article by A.N. Mogilevskiy, I.S. Sklyarenko, T.N. Chubukova, S.L. Bychinskiy, A.A. Komarov, L.I. Kolomoyets, Geochemistry and Analytical Chemistry Institute imeni V.I. Vernadskiy at the USSR Academy of Sciences, Moscow and State Ore Quality Inspection Gikyuzhruda, Krivoy Rog]

UDC 546.72:543.258

[Abstract] The shortcomings of popular titrimetric, chelatometry, and potentiometry methods of identifying iron in iron-containing materials with the help of standard titrants are discussed and a coulometric method with monitored potential (KKP) is proposed. The method is based on employing Faraday's law and is absolute, i.e., does not call for using standard samples. The results of generic iron identification with the help of a PKU-2 precision coulometer unit in various standard iron-containing material samples from the Krivoy Rog basin at a 0.95 confidence are presented and a block diagram of the PKU-2 unit is cited. The analytical procedure is described in detail and the curves for determining the formal redox potential of the Fe3+/Fe2+ system in 1 M HCl are plotted. It is noted that the proposed method is characterized by its low error and good reproducibility and reliability and may be used for large-scale monitoring of iron-containing materials. Figures 2; tables 1; references 7: 6 Russian; 1 Western.

#### Chemical-Atomic-Emission Analysis of High-Purity Ga and In With Breakdown by Bromine Vapors in Confined Volume

927D0081E Moscow ZAVODSKAYA LABORATORIYA in Russian Vol 57 No 12, Dec 91 pp 10-12

[Article by L.L. Baranova, L.D. Berliner, B.Ya. Kaplan, M.G. Nazarova, State Scientific Research and Design Institute of Rare Metals Industry, Moscow]

UDC [543.681+543.683]:543.423

[Abstract] Ways of decreasing the detection threshold of impurities in high-purity metals by the chemicalatomic-emission analysis (KhAEA) method by using larger samples and the resulting symbatic increase in the correction of the check experiment are discussed and a new method of decreasing the check experiment correction in analyzing high purity indium and gallium by adding the oxidant—bromine in this case—through the gaseous phase in a confined reactor volume rather than in an autoclave is described. The base element is separated by extraction during the analysis. The correctness of the procedure for all impurities except silicon is verified by the additions method; silicon analysis could not be confirmed. The analytical procedure for In and Ga is outlined in detail and the analytical spectrum lines of all impurities in indium and gallium are summarized. A design drawing of the fluoroplastic vessel with a screw lid and a crucible base used in the analysis is presented. The method is capable of identifying 15 impurities in high-purity indium and gallium: Al, Bi, Cd, Ca, Co, Si, Mg, Mn, Cu, Ni, Pb, Ag, Ti, Cr, and Zn. Figures 1; tables 1; references 1.

## Proximate Photometric Antimony Identification in Nonferrous Alloys

927D0081D Moscow ZAVODSKAYA LABORATORIYA in Russian Vol 57 No 12, Dec 91 pp 9-10

[Article by I.S. Novikova, V.V. Fedorov, N.S. Yershova, V.V. Orlov, V.M. Ivanov, Central Scientific Research Institute of Materials Science, Kaliningrad, Moscow oblast]

#### UDC [546.86+546.19]:543.432

[Abstract] The shortcomings of known methods of antimony identification in nonferrous metals and alloys and the difficulty of antimony identification in the presence of tin are addressed and a new photometric method of antimony (III) identification is proposed. The method is based on forming a red-dyed complex compound of antimony with 9-(n-dimethylaminophenyl)-2,3,7-trioxylfluorone-6 (PDMAFF). The reagent forms a stable chelate compound with antimony in a 1:2 metal-:reagent ratio (measured by the isomolar method). The complex has the peak light absorption at 560 nm and the reagent—at 460 nm; the color reaction contrast is 100 nm and the chelate compound's molar absorptance is 5.2 x 10<sup>4</sup>. A standard antimony solution prepared from a 99.99% metallic antimony is used; it is shown that the method's optimum antimony (III) chelation region is pH 1.0-1.5 and that the presence of Zn, In, Ga, Al, Cu, and Mn (II) virtually does not impede antimony identification while Sn. Ge. Fe. Nb. and Ti does. The analytical procedure is described and the results of an analysis of several nonferrous alloy samples are summarized. The method has an adequate accuracy and sensitivity and makes it possible to identify antimony in alloys without separating it from the base, as well as in alloys with a high tin concentration. Tables 1; references 3.

## Photomechanical Identification of Palladium in Aminochloride Electrolytes

927D0081C Moscow ZAVODSKAYA LABORATORIYA in Russian Vol 57 No 12, Dec 91 pp 7

[Article by Ye.P. Parkhomenko, N.F. Falendysh, A.T. Pilipenko, Colloidal Chemistry and Water Chemistry Institute imeni A.V. Dumanskiy at the Ukrainian Academy of Sciences, Kiev]

#### UDC 546.98:543.062

[Abstract] The need for simple and proximate palladium identification techniques necessitated by extensive palladium-coating applications in today's technologies is discussed and a simple and proximate photometric method of palladium identification in aminochloride electrolytes is proposed. The new method is based on measuring the light absorption of palladium's chloride complex [PdCl<sub>2</sub>]<sup>2-</sup>. The underlying principles of the method and the analytical procedure are described in

detail and the results of an analysis of palladium-containing solutions are summarized. The resulting data are compared to the results of gravimetric palladium identification with dimethylglyoxime. Although the new method's metrological characteristics are somewhat inferior to those of the gravimetric method, it is much simpler and more proximate. The method is also distinguished by its adequate reproducibility and correctness of the analysis results and may be recommended for monitoring the palladium concentration in electrolytes and palladium-coating flushing water. Tables 1; references 4.

#### Tin Identification Within Broad Concentration Range in Nonferrous Metal Alloys

927D0081B Moscow ZAVODSKAYA LABORATORIYA in Russian Vol 57 No 12, Dec 91 pp 5-6

[Article by S.V. Toporov, N.L. Olenovich, Odessa State University imeni I.I. Mechnikov]

#### UDC 669.2/8:546.814:543.432

[Abstract] The difficulties of tin identification in the course of certification analysis of nonferrous metal alloys due to the poor selectivity of the methods used is discussed and a new extractive photometric method based on extracting a complex of tin (IV) with benzoylphenylhydroxylamine (BFGA) or its analogues and measuring the light absorption of the heteroligand complex with phenylfluorone forming in the organic phase is described. The method has been used to identify tin in copper-, zinc-, and magnesium-based nonferrous metal alloys and commercial aluminum. To check the veracity of the results, standard samples are analyzed and method of additions is used, and data are compared to the results obtained by other methods. The analytical procedure is outlined in detail and the conclusion is drawn that the new method is characterized by relative simplicity, high selectivity, and sensitivity and makes it possible reliably and quickly to identify tin in samples of copper-, zinc-, and magnesium-based nonferrous metals and alloys. Tables 3; references 14: 13 Russian; 1 Western.

#### Investigation of Composite Material Failure by Mechanoluminescence Method Within Broad Loading Rate Range

927D0063A Kiev PROBLEMY PROCHNOSTI in Russian No 9(267), Sep 91 pp 48-52

[Article by U.E. Krauya, P.P. Kalnin, Ya.L. Yansons, A.A. Strukovskis, Polymer Mechanics Institute at the Latvian Academy of Sciences, Riga]

#### UDC 620.17:678.01

[Abstract] The mechanoluminescence (ML) method—the appearance of glow during the loading of various materials, primarily polymer and composite, due to several microprocesses—is explained and the use of

modern photomultiplier (FEU) photodetectors which are fast and virtually instantaneous for recording the ML phenomenon is discussed. A procedure for examining the failure of a laminar glass-reinforced plastic with a given reinforcement arrangement by the mechanoluminescence method under static (at 3 mm/min) and dynamic tension is presented. A block diagram of the mechanoluminescence recording device on the basis of a photomultiplier and a block diagram of a computeraided recording and processing device are cited. The behavior of the mechanoluminescence and stress intensity under static and dynamic loading of various types of samples is plotted. It is shown that static and dynamic tension in laminar glass reinforced plastic is accompanied by the development of mechanoluminescence which reflects the jump-like nature of the stage-by-stage failure of the composite material. Figures 5; references 16: 13 Russian: 3 Western.

#### Second All-Republic Seminar on Dynamic Strength and Crack Resistance of Structural Materials Under One-Time Impulse Loading

927D0062A Kiev PROBLEMY PROCHNOSTI in Russian No 9(267), Sep 91 pp 3-4

[Article by G.V. Stepanov]

[Abstract] The second all-republic scientific and engineering seminar on the Dynamic Strength and Crack Resistance of Structural Materials Under On-Time Impulse Loading was held in Kiev on 20-22 September 1988 at the Strength Problems Institute of the Ukrainian Academy of Sciences; it was organized by the Scientific Council on the problem of Mechanics of Deformable Rigid Bodies at the Ukrainian Academy of Sciences, the Strength Problems Institute of the Ukrainian Academy of Sciences, the Ukrainian Republican Center for Exhibits and Fairs, and Science Pavilion of the Ukrainian Academy of Sciences. Over 140 experts, 110 of them from out-of-town, and 53 organizations participated in the seminar. Thirty-five reports and 62 poster presentations covering various aspects of structural material behavior under impulse loading were made. They reflected today's state of research in this field and the level of research in the area of strength and fracture under loading. Some of the reports are published as a book. References 2.

#### Phase and Structure Changes in Metals Under Pulse Straining in Strong Magnetic Fields

927D0063B Kiev PROBLEMY PROCHNOSTI in Russian No 9(267), Sep 91 pp 77-79

[Article by A.V. Stepuk, Kharkov Polytechnic Institute]

UDC 620.192

[Abstract] Specific features of the dynamic processes occurring in structural materials—usually metals and alloys with a low resistivity—under pulsed magnetic

field are outlined and the thermal and mechanical effects of metal and alloy straining in pulsed strong magnetic fields (ISMP) in a submegaoersted range are considered and their behavior is analyzed. The contribution of thermal and mechanical effects is investigated and an attempt is made to describe the physical model of the metal structure formation in the pulsed strong magnetic field affected area (ZV ISMP). In particular, elastic and plastic deformation and magnetohydrodynamic (MGD) flow are examined and heat-effect and mechanical-effect zones are identified. The development of residual stress after the effect of the pulsed strong magnetic field and its distribution pattern are analyzed. It is shown that during the martensite transformation in steel, the interaction of the resulting martensite with the initial structure leads to the development of compressive stresses whose magnitude depends on the amount of retained austenite. X-ray patterns of samples from structural steel 65G and tool steel U8 recorded in K-radiation after the effect of pulsed strong magnetic field with a 4 µs duration and a 1.5 MOe amplitude are cited to illustrate the phase and structural changes in metals. Figures 1; references 5.

# Experimentally Analytical Method of Determining Strength Characteristics of Material Under Ouasistatic Tensile Conditions

927D0062G Kiev PROBLEMY PROCHNOSTI in Russian No 9(267), Sep 91 pp 26-28

[Article by M.M. Astakhov, A.V. Loginov, L.P. Loshmanov, O.G. Kudryavtsev, A.Ye. Trotsenko, Moscow Engineering Physics Institute]

**UDC 539.4** 

[Abstract] In order to avoid nonuniaxial strained states and decrease strength measurement errors during highspeed tensile tests, an experimentally analytical method is developed for calculating the strength characteristics of samples with a short effective member which does not have a uniaxial stressed state domain. To this end, the conditional yield strength of steel 12Kh18N10T is determined experimentally and analytically in samples of various effective member length within a 1-15 mm range under static and dynamic tension. The experimental load-time charts are plotted. The domains of nonuniaxial (offset) strained state along the sample's effective member length are established numerically by the finite elements method (MKE) using an AIDA-NEPTUN-KOMPAS software package. The experimental results are consistent with analytical data within the experiment's margin of error. The use of this method also makes it possible to expand the range of straining rates under study. Figures 4; references 2.

# Effect of High-Speed Straining and Temperature on Strength and Ductility Characteristics of Cr-Ni-Mo Steel

927D0062F Kiev PROBLEMY PROCHNOSTI in Russian No 9(267), Sep 91 pp 17-19

[Article by A.P. Vashchenko, V.P. Leonov, V.M. Tokarev, A.S. Eglit, Strength Problems Institute of the

Ukrainian Academy of Sciences, Kiev, and Central Scientific Research Institute of Structural Materials, St. Petersburg]

#### UDC 620.172.254

[Abstract] Available experimental data on the strength and ductility characteristics of alloyed structural steels under straining do not cover high straining rates; consequently, the results of mechanical tensile tests of secondary-hardenable chromium-nickel-molybdenum steel heat-treated for various static strength levels are presented. Dynamic tests at plastic deformation rates of up to 5 x 10<sup>4</sup> s<sup>-1</sup> were conducted in a 77-523K temperature range while static tests were carried out at a tensile rate of 2 mm/min in an Instron machine. The dependence of the strength and ductility characteristics of Cr-Ni-Mo steel heat-treated for various strength levels on the straining rate and temperature is investigated and plotted for various samples. The results are consistent with the dislocation model of plastic metal flow and may be divided into three ranges corresponding to different straining rates. An improvement in strength and ductility with the straining rate is demonstrated. The findings contradict the hypothesis of the equivalent effect of temperature drops and straining rate increases on the mechanical characteristics of metals. The conclusion is drawn that Cr-Ni-Mo steel is highly reliable for use under such operating conditions. Figures 3; references 9.

# Effect of Artificial Surface Defects on Steel Slab Failure During Contact Loading by Explosive Layer Detonation

927D0062E Kiev PROBLEMY PROCHNOSTI in Russian No 9(267), Sep 91 pp 11-14

[Article by A.S. Ispatyev, Special Design Office of Hydraulic Impulse Technology at the Siberian Department of the USSR Academy of Sciences, Novosibirsk]

#### UDC 620.192.7+621.7.044.2

[Abstract] The use of various explosion methods for cropping oversize metal items and their shortcomings are discussed and the effect of surface defects on the character of steel slab failure is investigated in order to produce a feasibility study for increasing the productivity of oversize item cropping and reduce the specific consumption of explosives (VV). The effect of noncontinuous surface defects on the failure characteristics is considered for both mechanically and explosion-induced defects. The failure of 75 and 150 mm-thick steel St.3 slabs with an artificial defect representing a set of individually drilled holes by a surface explosion charge is examined. A two-stage failure mechanism is suggested and corroborated. The results show that it is possible to substantially lower the specific explosive charge consumption by selecting the artificial defect shape (e.g., a set of shallow drilled holes); the explosive charge shape is optimized: the specific consumption of ammonite 6ZhV

is 15 and 19 g/cm for the 75 mm-thick slabs with different defect sizes. Figures 1; tables 1; references 3.

## Estimation of Strained State of Base Slab During Explosion Welding

927D0062D Kiev PROBLEMY PROCHNOSTI in Russian No 9(267), Sep 91 pp 9-11

[Article by V.G. Resinov, S.G. Tsybochkin, Yu.A. Konon, Scientific Production Association of the Altay Scientific Research Institute of Mechanical Engineering, Barnaul]

#### UDC 539.4

[Abstract] The need to determine the strain and velocities of slabs used in explosion welding, particularly in the case of oblique collision, in order to analyze the taut strained state of the base slab is identified; the processes of oblique collision of the projectile slab with the elastic base slab and explosion strengthening are generally simulated by a moving surface load locally distributed in a certain neighborhood of the point of contact and applied uniformly along a line on a surface. The boundary value problem under the conditions of planar strain is solved. The longitudinal strain on the slab's free surface is measured experimentally. The estimates make it possible to predict the behavior of materials sensitive to the straining rate under explosion welding loading conditions. The experimental results are found to be consistent with theoretical data. Figures 2; references 5.

## **Estimation of Stresses and Strain During Explosion Welding**

927D0062C Kiev PROBLEMY PROCHNOSTI in Russian No 9(267), Sep 91 pp 7-9

[Article by V.P. Bartenev, G.V. Stepanov, Scientific Production Association of the Altay Scientific Research Institute of Mechanical Engineering, Barnaul, and Strength Problems Institute at the Ukrainian Academy of Sciences, Kiev]

#### **UDC 539.4**

[Abstract] The inability of existing methods to analyze the taut strained state (NDS) after the compression wave reflection from the slab end and the dynamic loading during explosion welding which often leads to intense strain and failure near the ends of welded slabs is discussed and the methods developed earlier by the authors (*Problemy prochnosti* No. 9, 1988) is used to determine the dynamic field of the tensile stresses and shearing strain developing during explosion welding. The oblique collision of slabs is simulated by loading a layer of acoustic material of finite thickness and length moving at a given velocity by a locally distributed superficial load defined by an expansion into a double Fourier series. The boundary value problem is solved by

the method of separation of variables and the computation results are analyzed. The conclusion is drawn that the intensive strain and failure in the edge zone occur after the end of the explosion welding process and are caused by the reflected relief wave. The consistency of experimental and analytical results is noted. Figures 3; references 6.

## Approximation Model of Structural Material Failure and Failure Wave Problem

927D0062B Kiev PROBLEMY PROCHNOSTI in Russian No 9(267), Sep 91 pp 4-6

[Article by A.S. Kravchuk, A.V. Malashkin, All-Union Mechanical Engineering Correspondence Institute, Moscow]

#### **UDC 539.4**

[Abstract] Transmission of a failure wave through a structural material with discontinuities is analyzed by the continuous computation method whereby the discontinuity "spreading" procedure is interpreted in a physical sense as an accumulation of failures in a transition layer which results in a transition of the material into another with altered characteristics. The procedure is based on measuring the variations in the moduli of elasticity when crossing the wave front. The method is illustrated by an analysis of the spherical failure wave motion. Figures 2; references 4.

## Analysis of Rapid-Quenched Strip Surface Configuration and Quality

927D0061I Moscow STAL in Russian No 12, Dec 91 pp 68-71

[Article by B.V. Molotilov, N.M. Zapuskalov, V.T. Timofeyev, All-Union Scientific Research Institute of Ferrous Metallurgy and All-Union Science Research Institute of Metallurgical Machine-Building]

#### UDC 669-175.2

[Abstract] The results of an investigation carried out in an AMKL-150 double-roller unit using two sets of watercooled bronze rollers in order to establish the patterns of inhomogeneities appearing in rapidly quenched strip and determine their causes are presented. Surface roughness parameters were measured by a roughness indicator manufactured by the Kalibr plant as well as a Surtronic-3P instrument made by Taylor-Hobson, the strip thickness was measured under a micrometer, and the strip length by a ruler. The strip configuration variations during the process and the thickness distribution in a strip made in flexible and rigid roll sleeves are plotted. The effect of the roller's barrel shape on the strip scale width and thickness variation is examined. An analysis demonstrates that the width of the strip produced by the rapid quenching method in rollers is determined by the metal consumption rate and depends on the molten metal pool vibrations while the cross-sectional strip shape is determined by the design features of the continuous casting solidification rollers. Figures 7; references 5: 4 Russian, 3 Western.

## Testing of 32G2F Steel for High-Strength Drill Pipe Shells

927D0061H Moscow STAL in Russian No 12, Dec 91 pp 60-62

[Article by Ye.A. Solomadina, D.A. Akhmedova, A.I. Ramazanov, Ye.L. Vasilyev, A.S. Bondarenko, All-Union Scientific Research Institute of Tube Industry and Azeri Pipe Rolling Mill]

#### UDC 621.785.616.1:621.78.083]:621.791.052

[Abstract] Studies confirming that low alloy steel 32G2 is not suitable for making drill pipes of strength class L or higher are outlined and the need to use steel with higher stability of supercooled austenite is identified. As a result, steel 32G2F additionally alloyed with vanadium is studied and tested for the first time; to this end, the kinetics of austenite transformation in this steel are investigated and the continuous cooling transformation diagram is plotted with the help of a Linsize dilatometer. The mechanical properties of drill pipe shells from steel 32G2 and 32G2F are summarized and compared to each other and the microstructure of dilatometry samples cooled at different rates is analyzed. The continuous cooling transformation diagram of steel 32G2F demonstrates that in order to attain a martensite structure in drill pipes after quenching, the cooling rate must be at least 65 K/s. A study of mechanical properties of steel 32G2F shows that the mechanical properties of hot rolled tubes meet the requirements of strength class E with a considerable safety margin and meet the specifications of TU 14-3-1571-88. Work on improving the equipment and methods of heat treatment is underway at the Azeri Tube Rolling Mill. Figures 2; tables 2.

#### ZrO<sub>2</sub>-Y<sub>2</sub>O<sub>3</sub>-Sc<sub>2</sub>O<sub>3</sub> System's Liquidus Surface 927D0069A Moscow IZVESTIYA AKADEMII NAUK

92/D0069A Moscow IZVESTITA AKADEMII NAUK SSSR: SERIYA NEORGANICHESKIYE MATERIALY in Russian Vol 27 No 12, Dec 91 pp 2673-2675

[Article by A.V. Shevchenko, L.M. Lopato, I.M. Mayster, Institute of Materials Science Problems imeni I.N. Frantsevich at the Ukrainian Academy of Sciences]

#### UDC 548.651/659

[Abstract] Phase equilibria and constitution diagrams binary and ternary  $ZrO_2-Y_2O_3-Sc_2O_3$  system are discussed and an attempt to investigate the liquidus surface of the  $ZrO_2-Y_2O_3-Sc_2O_3$  ternary system which can be used for developing high-temperature refractory materials and clarify the liquidus curve which serves as the boundary of the binary  $Y_2O_3-Sc_2O_3$  system is described. The boundaries of the phase domains are determined

with the help of differential thermal analysis (DTA) in helium at a temperature of up to 2,500°C and on the basis of data of derivative thermal analysis (PTA) in the air at temperature of up to 3,000°C with the help of the helium unit. The projection of the liquidus surface of the ternary system upon the concentration triangle plane and the constitution diagrams of polythertmal cross sections of the ternary system are plotted. The analytical results confirm the presence of a minimum on the binary system's liquidus curve at a temperature of 2,050°C and show that the ternary system's liquidus surface consists of three primary phase crystallization domains; the maximum liquidus surface temperature is equal to the melting point of the sample containing 90% (mol.) of ZrO<sub>2</sub>. Figures 2; references 7: 4 Russian; 3 Western.

#### Magnetoelectric Properties of Piezoelectric and Magnetostrictive Materials' Mixtures With Polymer Binder

927D0068R Moscow IZVESTIYA AKADEMII NAUK SSSR: SERIYA NEORGANICHESKIYE MATERIALY in Russian Vol 27 No 12, Dec 91 pp 2678-2678

[Article by T.G. Lupeyko, S.S. Lopatin, I.V. Churikova, I.B. Lopatina, Rostov State University]

UDC 537.228.1

[Abstract] The mixtures of piezoelectric and magnetostrictive materials which serve as the active basic ingredient of hybrid composites, display the magnetoelectric effect (ME), and are used in instruments for recording static and alternating magnetic fields, in frequency doublers, sensory buttons, and shaft speed-to-code converters are discussed and data on the properties and composition optimization of mixed magnetoelectric composites with a polymer bonding agent are presented. The PRK-1 sintered piezoelectric ceramic made from lead zirconate-titanate with an addition of cadmium tungstate (an analogue of the TsTS-36 commercial product) was used in the experiments; the relative dielectric permittivity, dielectric loss tangent, radial coefficient of electromechanical coupling, thickness coefficient of electromechanical coupling, piezoelectric modulus, piezoelectric sensitivity, and speed of sound were measured. The concentration dependence of the dielectric permittivity, piezoelectric modulus, dielectric loss tangent, and piezoelectric sensitivity are plotted for a sample containing 75% of the mixture with ferrite and 25% fluoroplastic while the dependence of the magnetoelectric coefficient on the static magnetic bias field and the ferrite concentration is plotted for a sample containing 75% of the mixture with ferrite and 25% of fluoroplastic. The experiments were conducted in a unit at the Vitebsk branch of the Solid State Physics Institute at the Belarus Academy of Sciences. Although the PKR-1 composites are inferior to sintered ceramic materials with respect to their magnetoelectric coefficient, they can be used when high sensitivity is not required of the

transducer; in addition, the new composites are characterized by ductility and machinability. Figures 2; references: 1 Western.

## Phase Composition and Photoconductivity of $TlIn_{1-x}Dy_xS_2$ Crystals

927D0068P Moscow IZVESTIYA AKADEMII NAUK SSSR: SERIYA NEORGANICHESKIYE MATERIALY in Russian Vol 27 No 12, Dec 91 pp 2657-2658

[Article by E.M. Kerimova, G.B. Gasymov, F.G. Magerramova, R.A. Aliyev, Physics Institute at the Azeri Academy of Sciences]

UDC 546.683-682.644.15

[Abstract] TlIn<sub>1-x</sub>Dy<sub>x</sub>S<sub>2</sub> crystals with a monoclinic symmetry as well as other modifications are investigated by the X-ray phase analysis method; Debye powder pattern diagrams of Bridgeman synthesized ground TlIn<sub>1-</sub> xDy<sub>x</sub>S<sub>2</sub> samples are plotted in CuK<sub>a</sub>-radiation; diffraction patterns of TlIn<sub>1-x</sub>Dy<sub>x</sub>S<sub>2</sub> are summarized and the interplanar spacing data are presented. An analysis demonstrates that the TlIn<sub>1-x</sub>Dy<sub>x</sub>S<sub>2</sub> samples are singlephased and that diffraction reflections are uniquely induced on the basis of the monoclinic β-phase. The change in the TlIn<sub>1-x</sub>Dy<sub>x</sub>S<sub>2</sub> lattice cell parameters as a function of x, i.e., the number of Dy atoms in the molecule, and spectral photoconductivity distribution curves of  $TlIn_{1-x}Dy_xS_2$  and  $TlInS_2$  single crystals at 300K and 77K are plotted. The forbidden gap width of the above single crystals are equal 1.8 and 1.9 eV and 2.38 and 2.61 eV, respectively, at 300K and 77K. Figures 2; tables 1; references: 4 Western.

## Effect of Magnetic Field on Residual Impurity and Dopant Distribution in InSb

927D0068N Moscow IZVESTIYA AKADEMII NAUK SSSR: SERIYA NEORGANICHESKIYE MATERIALY in Russian Vol 27 No 12, Dec 91 pp 2653-2654

[Article by A.N. Popkov, V.S. Vekshina, O.V. Nagibin, N.I. Pepik, State Scientific Research and Design Institute of Rare Earth Metals Industry]

UDC 66.046.522

[Abstract] The factors affecting the impurity distribution in the length of growing crystal are outlined and the use of magnetic field in order to manipulate the mass and heat transfer processes during the growth of crystals and control the impurity distribution is discussed. The effect of magnetic field on the effective distribution coefficients of residual germanium and tellurium impurities in an indium antimonide crystal grown in the [211] direction with a transverse magnetic field applied to the melt is investigated in nondoped InSb grown by Czochralski's method with a magnetic flux density of up to 0.17 T. The dependence of the effective distribution coefficient of tellurium and residual impurities on the magnetic field

induction and the dependence of the effective germanium distribution coefficient on the magnetic field strength are plotted. An analysis demonstrates that an increase in the magnetic field to 0.17 T increases the effective distribution coefficient of residual impurities by more than twofold; moreover, the effective distribution coefficient increases with the magnetic field induction for both germanium and tellurium. Figures 2; references 4: 3 Russian; 1 Western.

## Effect of Transverse Magnetic Field on Residual Impurity Concentration in InSb

927D0068M Moscow IZVESTIYA AKADEMII NAUK SSSR: SERIYA NEORGANICHESKIYE MATERIALY in Russian Vol 27 No 12, Dec 91 pp 2651-2652

[Article by A.N. Popkov, V.S. Vekshina, O.V. Nagibin, N.I. Pepik, State Scientific Research and Design Institute of Rare Earth Metals Industry]

#### UDC 66.046.522

[Abstract] The use of the methods of magnetohydrodynamic treatment (MGD) of semiconductor melts in order to improve the quality of the resulting BCC crystals is discussed; in particular, the effect of transverse magnetic field on the concentration of residual impurities in indium antimonide is examined. To this end, nondoped crystals were grown by Czochralski's method in a quartz crucible with an MHD device for applying a transverse magnetic field. During the growing, the magnetic field was varied within 0-0.17 T. The resulting crystals had a diameter of close to 30 mm. The crystals were then sliced into wafers for studying the electric and physical parameters at a liquid nitrogen temperature; an analysis shows that the total concentration of ionized centers is within (1.5-2) x 10<sup>14</sup> cm<sup>-3</sup>, i.e., lower than that in crystals grown without the magnetic field by almost twofold. The use of magnetic field decreases the concentration of both n- and p-type centers while the concentration of the former decreases to a greater extent than that of the latter. The dependence of the charge carrier mobility on the charge carrier concentration in InSb with and without the magnetic field is plotted graphically. The charge carrier mobility values of crystals grown in a magnetic field fall within lower concentrations. Figures 1; tables 1; references 5: 1 Russian; 4 Western.

## Growing of Ge-Doped InSb Crystals Under Effect of Transverse Magnetic Field on Melt

927D0068L Moscow IZVESTIYA AKADEMII NAUK SSSR: SERIYA NEORGANICHESKIYE MATERIALY in Russian Vol 27 No 12, Dec 91 pp 2648-2650

[Article by A.N. Popkov, A.Ya. Polyakov, V.S. Vekshina, O.V. Nagibin, State Scientific Research and Design Institute of Rare Earth Metals Industry]

#### **UDC 548.55**

[Abstract] Since semiconductor materials are characterized by metallic conduction in a molten state, making it possible to use magnetohydrodynamic (MGD) treatment for controlling the hydrodynamic heat and mass transfer processes and thus determining the distribution uniformity of background impurities and dopants as well as the perfection of the resulting crystals, indium antimonide single crystals grown by Czochralski's method under the effect of a transverse magnetic field on the melt are investigated. Indium antimonide was doped in a vacuum and crystals were grown at a magnetic flux density of 0-0.17 T; the initial charge carrier concentration in indium antimonide was 1 x 10<sup>14</sup> cm<sup>-3</sup> while the growth rate was 0.5 mm/min. The charge carrier distribution and charge carrier mobility distribution in a germaniumdoped InSb crystal grown in a 0.17 T magnetic field and the dependence of the charge carrier mobility on the charge carrier concentration in InSb<Ge> with and without the transverse magnetic field application are plotted and the recombination characteristics of p-type InSb samples grown with and without magnetic field are summarized. An analysis demonstrates that in growing Ge-doped InSb crystals, the carrier concentration starts dropping with an application of a transverse magnetic field to the melt while the charge carrier mobility increases; the latter is attributed to a decrease in the concentration of deep centers with an energy of  $E_{\nu}+0.1$ eV. Figures 2; tables 1; references 5: 3 Russian; 2 Western.

#### On Interrelation of Electric Conductivity and Porosity of Quasi-Isotropic Carbon Materials

927D0068I Moscow IZVESTIYA AKADEMII NAUK SSSR: SERIYA NEORGANICHESKIYE MATERIALY in Russian Vol 27 No 12, Dec 91 pp 2546-2551

[Article by I.Ya. Levintovich, A.S. Kotosonov, G.M. Butyrin, State Scientific Research Institute of Graphite-Based Structural Materials]

#### UDC 661.66.3+537.311.3

[Abstract] The interrelation of electric conductivity and porosity of quasi-isotropic carbon materials (UM) obtained by the ceramics technology is investigated; to this end, the relationship between the electric resistivity σ and porosity, and especially the coefficient of connectivity—the ratio of the electric resistivity  $\sigma$  to the resistivity along the crystal grain layer  $\sigma_1$ —are examined. The dependence of various porous structure parameters of the samples on their sintering temperature, the dependence of the samples' electric resistivity on their microand macroporosity, and the dependence of specific resistivity of the samples on their total porosity with a change in temperature are plotted. An analysis of experimental data shows that the volume shrinking of coke-based materials during their heat treatment is uniform and the relative volume of macropores remains unchanged. A change in microporosity due to microstructural defects in carbon materials has a greater effect on their electric conductivity than a similar change in their macroporosity. A simple and sound method of assessing the electric conductivity of crystalline grains along the basal plane of the macroisotropic carbonized materials is proposed. The electric conductivity of GMZ-type carbonized materials is virtually the same as that of calcinated coke-based graphites. Figures 3; references 14: 8 Russian; 6 Western.

# Investigation of Thermoelectric Materials Based on Solid Solutions of Bi<sub>2</sub>Te<sub>3</sub>-Bi<sub>2</sub>Se<sub>3</sub> and Sb<sub>2</sub>Te<sub>3</sub>-Bi<sub>2</sub>Te<sub>3</sub> Systems Doped With Copper and Nickel

927D0068H Moscow IZVESTIYA AKADEMII NAUK SSSR: SERIYA NEORGANICHESKIYE MATERIALY in Russian Vol 27 No 12, Dec 91 pp 2533-2535

[Article by A.A. Mageramov, A.T. Tilavoldiyev, S.Sh. Kakhramanov, A.M. Muydinov, Fergana State Teachers College imeni Ulugbek]

#### UDC 536.212.2+537.322.8

[Abstract] The shortcomings of Bi<sub>2</sub>Te<sub>3</sub>- and Sb<sub>2</sub>Te<sub>3</sub>based materials used in thermocouples and thermal converters and ways of overcoming them by doping these compositions with copper and nickel are discussed and the effect of copper and nickel on the properties of solid solutions is examined. To this end, the properties of a Bi<sub>2</sub>Te<sub>2.88</sub>Se<sub>0.12</sub> solid solution doped with copper and nickel are investigated; in so doing, the copper concentration was varied within 0.1-0.05% by mass. The dependence of the thermoelectric coefficient a, electric conductivity  $\sigma$ , efficiency z, and compressive strength of Bi<sub>2</sub>Te<sub>2.88</sub>Se<sub>0.12</sub> and Sb<sub>1.5</sub>Bi<sub>0.5</sub>Te<sub>3</sub> solid solutions is analyzed and tabulated and the temperature dependence of electric conductivity  $\sigma$ , thermal conductivity  $\kappa$ , and efficiency z of the former solid solution is plotted. It is shown that an increase in the copper concentration alone hardens the alloy but its thermoelectromotive force decreases. Doping with nickel makes it possible to obtain hardened thermoelectric materials with both p- and *n*-type conduction. Figures 1; tables 1; references 3.

#### Interrelation Between Conductivity, Thermoelectric Coefficient, and Magnetic Susceptibility of Semiconductor Melts

927D0068G Moscow IZVESTIYA AKADEMII NAUK SSSR: SERIYA NEORGANICHESKIYE MATERIALY in Russian Vol 27 No 12, Dec 91 pp 2523-2526

[Article by V.M. Glazov, A.I. Faradzhov, Moscow Electronic Engineering Institute]

#### UDC 621.315.532

[Abstract] The interrelation between the electric conductivity  $\sigma$ , thermoelectric coefficient  $\alpha$ , and magnetic susceptibility  $\gamma$  of certain molten semiconductors, primarily

bismuth-selenium systems, are studied and the difficulties of calculating these values are addressed. The correlation of the values of  $\sigma$ ,  $\alpha$ , and  $\chi$  plotted as a function of temperature for a Bi<sub>2</sub>Se<sub>3</sub> melt is investigated. It is shown that experimental data may be used to assess certain melt parameters and thus obtain valuable data on the electron spectrum characteristics of semiconductor melts. Formulas for computing the conductivity, thermoelectric coefficient, and magnetic susceptibility in the diffusive transfer region are derived; an analysis demonstrates that given a weak electron scattering, these formulas do not differ from those describing metallic melts. Figures 1; references 8: 7 Russian, 1 Western.

#### Lu-Lu<sub>2</sub>S<sub>3</sub> System

927D0068D Moscow IZVESTIYA AKADEMII NAUK SSSR: SERIYA NEORGANICHESKIYE MATERIALY in Russian Vol 27 No 12, Dec 91 pp 2511-2515

[Article by O.V. Andreyev, N.N. Parshukov, Tyumen State University]

#### UDC 546.669'221:003.63

[Abstract] An attempt is made to fill in the gaps in the study of phase equilibria in the Lu-Lu<sub>2</sub>S<sub>3</sub> system and plot geometrical images of the high-temperature section of the Lu-Lu<sub>2</sub>S<sub>3</sub> system's constitution diagram Tx-projection. LyuM-1 lutetium and especially pure OSCh 14-4 sulfur are used in the experiments. Samples with a sulfur concentration of 40-59.5% are synthesized in two stages; the resulting ingots and sinters are then annealed at 1,870 or 2,070K for 25 or 15 min, respectively. The phase equilibrium is demonstrated by investigating the microstructure and phase composition of samples quenched at various stages. As expected, the Lu-Lu<sub>2</sub>S<sub>3</sub> system constitution diagram is similar to that of a Gd-Gd<sub>2</sub>S<sub>3</sub> system and shows that two congruently melting phases are formed in the structure: LuS and Lu<sub>2</sub>S<sub>3</sub>. The concentration dependence of the microhardness and lattice cell constant of a LuS-based solid solution for Lu-Lu<sub>2</sub>S<sub>3</sub> system samples annealed and quenched at 1,870K is examined and diffraction patterns of samples annealed and quenched at 1,870K are plotted. It is shown that in addition to the two congruently melting phases, two eutectic phases are also formed in the Lu-Lu<sub>2</sub>S<sub>3</sub> system. Figures 3; references 9: 6 Russian; 3 Western.

#### Structure and Electric Properties of Rapidly Quenched InSb Foils and InSb-InBi System Solid Solutions

927D0068C Moscow IZVESTIYA AKADEMII NAUK SSSR: SERIYA NEORGANICHESKIYE MATERIALY in Russian Vol 27 No 12, Dec 91 pp 2505-2507

[Article by V.G. Shepelevich, Belarus State University imeni V.I. Lenin]

UDC (548.5+537.311):621.315.5

[Abstract] InSb foils and InSb-InBi systems containing up to 4% InBi are produced by crystallizing a 0.3 g alloy drop splashed onto a polished inner surface of a rapidly spinning copper cylinder, resulting in 20 to 60 µm foils. Under such crystallization conditions, the cooling rate reaches 106K/s. The foils are investigated metallographically under an MMU-3 microscope and by an X-ray phase analysis in a DRON-3 diffractometer. The foil texture is examined by the inverse pole figures method. The pole density distribution of diffraction lines in rapidly quenched InSb foils and InSb-InBi systems is examined and summarized and the temperature dependence of their resistivity, Hall's coefficient, differential thermoelectromotive force, and Hall electron mobility is plotted. An analysis demonstrates that rapidly quenched InSb foils and InSb-InBi systems have a polycrystalline structure and are characterized by a crystallographic plane-111 + crystallographic plane-110 texture. A decrease in the electron mobility with an increase in the bismuth concentration in indium antimonide is attributed to the refining of the granular structure and, as a consequence, an enhancement of electron scattering on the grain boundaries and scattering on ionized bismuth atoms. Figures 1; tables 2; references 7: 6 Russian; 1 Western.

## The Physicochemical Properties of a Cd<sub>1-x</sub>Mn<sub>x</sub>Te Surface With Varying Mn Contents

927D0067B Moscow POVERKHNOST: FIZIKA, KHIMIYA, MEKHANIKA in Russian No 12, Dec 91 (manuscript received 22 Feb 90; after revision 19 Dec 90) pp 18-23

[Article by Ye.V. Buzaneva T.A. Vdovenkova, G.D. Popova, V.I. Strikha, A.I. Tsyganova, A. Rodzik, and E. Charnetska-Sukh, Kiev State University]

#### UDC 537.311.33

[Abstract] The authors of the study examined the physicochemical properties of  $Cd_{1-x}Mn_xTe$  (x = 0, 0.34, and 0.7) after spalling in air and after mechanical polishing, etching in a 12-15% or 3-5% solution of Br<sub>2</sub> in methanol, rinsing in methanol, and drying. The specimens' surface composition was studied by scanning Auger electron spectroscopy as described elsewhere. Etching the test specimens in a 12-15% solution of Br<sub>2</sub> in methanol was found to cause the specimen surfaces to become highly enriched in tellurium and to result in lower oxygen and tellurium oxide contents on the specimen surface than when a 3-5% Br<sub>2</sub>-in-methanol solution was used. The experiment results were found to be in good agreement with those predicted by a thermodynamic analysis of the possible reactions between Cd, Mn, Te, etching agent, oxygen, and water that the authors performed before conducting the actual experiments. Specifically, Cd, Te, and C were found to be more uniformly distributed in the specimen surfaces than Mn and O were. The sections with the highest manganese content also contained the highest amount of oxygen. In a near-surface layer about 10 angstroms thick, the etched specimens of  $Cd_{1-x}Mn_xTe$  studied were found to contain Te,  $TeO_2$ , and  $MnO_2$  with forbidden band widths that differed from those of the starting  $Cd_{1-x}Mn_xTe$  (x = 0, 0.34, 0.7). The two deeplevel bands discovered in specimens of  $Cd_{0.66}Mn_{0.34}Te$  were hypothesized to be linked not only to structural defects but also to the electron states in the conduction bands of Te,  $TeO_2$ , and  $MnO_2$ . Figure 1; references 8: 5 Russian, 3 Western.

#### Determination of the Dependence of Acoustic Emission Parameters on Deformation During the Simple Bending of Composites Consisting of Materials With Different Strengths

927D0066 Kiev PROBLEMY PROCHNOSTI in Russian No 12, Dec 91 (manuscript received 25 Jun 90) pp 51-56

[Article by Ye.Z. Korol, Mechanics Institute, Moscow State University, Moscow]

UDC 620.179

[Abstract] The author of the study worked to develop a series of formulas for use in determining the dependence of acoustic emission parameters on deformation during the simple bending of composites consisting of materials having different strengths. He develops a series of formulas that enable him to give consideration to the fact that the deformation properties of such materials depend on the type of stress-strained state (e.g., compression, tensile) in which the composite happens to be and that, under conditions of simple bending, such materials will have a nonuniform stress-strained state consisting of a tensile stress zone and a compression strength zone. The author derives a set of finite formulas for the case of degenerated nuclei. Formulas are presented for use in calculating the stresses that develop in composites consisting of materials having different strengths when the said composites are subjected to a specified bending moment and lengthwise force. Formulas are also presented for use in calculating the deformations developing in the outer fibers of any section. The author selects a laminar composite to study the particular cases of one acoustic emission source, two simultaneously acting acoustic emission sources, and two acoustic emission sources where the second follows the other after some specified delay. The author recommends that his new method and the diagrams resulting from its use be used in the nondestructive diagnosis and forecasting of the mechanical states of composite materials and structures such as those studied when they are in both uniform and nonuniform stress-strained states. Figures 3; references 2 (Russian).

4

## The Effect of a Free Surface on the Distribution of Point Defects in a Metal

927D0067E Moscow POVERKHNOST: FIZIKA, KHIMIYA, MEKHANIKA in Russian No 12, Dec 91 (manuscript received 5 Feb 90; after revision 12 Mar 91) pp 92-97

[Article by Yu.N. Devyatko and O.V. Tapinskaya, Moscow Physics Engineering Institute]

#### **UDC 536.76**

[Abstract] The authors of the study examined the effect of a free surface on the distribution of point defects in a metal in a state of thermodynamic equilibrium. They equate the generation of a point defect to the occurrence of a corresponding dilation space that enters into an elastic interaction with the surface. Through a series of calculations the authors show that the change in the chemical potential and, consequently, in the concentration of point defects in a metal is connected with the presence of far-reaching interatomic forces in the form of a long-wave electromagnetic field that is determined by the dielectric constant of the medium. They further show that close to the free surface of the said metal, there is an effective reduction in the energy of vacancy formation. Because of this reduction, the near-surface layer of the metal ends up containing between one and three orders of magnitude more vacancies than does the bulk of the metal. The authors' calculations indicate that for metals at a temperature of about 1,000 K, the change in chemical potential at their surface is somewhere between about 0.03 and 0.6 eV. This change in chemical potential is not explicitly dependent on temperature but rather is entirely determined by the following constants of the given matter: the coordination number N. the lattice constant a, and the conduction  $\delta$ . The characteristic length at which the change in vacancy concentration takes place for different metals is somewhere between 100 to 300 angstroms. Because the energy of the generation of interstitial atoms is between 3 and 5 eV, the presence of a surface does not noticeably alter the energy of the generation of interstitial atoms. Rather, their temperature concentration within the bounds of the solid phase remains as before. Figures 2; references 6 (Russian).

# Phase Transformations in Cd<sub>0.2</sub>Hg<sub>0.8</sub>Te due to the Effect of Pulsed Laser Radiation of Nanosecond Duration

927D0067A Moscow POVERKHNOST: FIZIKA, KHIMIYA, MEKHANIKA in Russian No 12, Dec 91 (manuscript received 13 Aug 90; after revision 5 Dec 90) pp 12-17

[Article by P.V. Goloshikhin, K.Ye. Mironov, and A.Ya. Polyakov, Physics Engineering Institute imeni A.F. Ioffe, USSR Academy of Sciences, Saint Petersburg]

UDC 621.315.592

[Abstract] The authors of the study examined the phase transformations occurring in Cd<sub>0.2</sub>Hg<sub>0.8</sub>Te subjected to the effects of pulsed laser radiation of nanosecond duration. Epitaxial layers (30 to 40 µm thick) of Cd<sub>0.2</sub>Hg<sub>0.8</sub>Te grown by the method of liquid epitaxy from telluriumenriched solutions were irradiated by a laboratory Nd laser in a Q-switching mode with a wavelength of 1.06 μm and a radiation intensity of 0.1 to 2.5 J/cm<sup>2</sup> in pulses lasting 100 ns. An MIM-7 optical microscope and BS-300 electron microscope (Tesla) were used to perform metallographic studies of the irradiated specimens. The specimens were also subjected to Auger electron spectroscopy (using an RN1-545-A Auger electron spectrometer). The studies performed established that beginning at a radiation energy of 0.15 J/cm<sup>2</sup>, pulsed radiation begins to affect layers of Cd<sub>0.2</sub>Hg<sub>0.8</sub>Te. At first the changes occur in islands and have the form of cylindrical waves. As the power-flow density increases, the "islands" become more dense and increase in area. By about 1 J/cm<sup>2</sup>, the cylindrical-wave structure of the surface begins to assume the form of plane waves. The standard distance between the "crests" of both types of waves was between 1 and 5 µm. When the specimens were irradiated under an angle other than 90°, the structure of the cylindrical waves was transformed into an ellipsoidal-wave structure. Beginning at a radiation intensity of 0.15 J/cm<sup>2</sup>, the specimens underwent a visually observable recrystallization of their surface and a noticeable redistribution of their solid-solution components up to a depth of 0.2 µm. The nonmonotonic distributions of components by depth were attributed to segregation at the crystallization front, vaporization of Hg from the surface, and subsequent partial condensation of the Hg. As the energy density increased, the nonequilibrium coefficient of the segregation of Cd decreased while that of Hg increased from 1.25 to 1.15 and from 0.93 to 0.96, respectively. The changes in surface morphology observed after the pulsed laser irradiation were determined to be caused by the interaction of the electromagnetic wave of the pulsed laser radiation with the melted layer of Cd<sub>0.2</sub>Hg<sub>0.8</sub>Te. Previous reports of analogous effects in Si and GaAs were cited as additional confirmation of the thermal nature of the changes caused by pulsed laser radiation. Figure 4; references 9: 4 Russian, 5 Western.

## Effective Strength Parameters of Matrix Composites

927D0066E Kiev PROBLEMY PROCHNOSTI in Russian No 12, Dec 91 (manuscript received 25 Apr 90) pp 47-51

[Article by V.A. Buryachenko, Yu.S. Skorbov, and S.V. Gunin, NIKhTI (not further identified), Lyubertsy]

#### UDC 539.218

[Abstract] The authors of the study worked to develop a method of calculating the effective strength surface of a composite material with consideration for the arbitrary elastic-strength anisotropy of the composite's components and the shape and orientation of the inclusions in its filler. The new method is based on the use of estimates of the mean values of the first and second moments of the stress tensors in the said components. The authors analyze a series of 23 equations illustrating the use of their proposed method. They also illustrate the difference between experimentally obtained and calculated (by their proposed method) values of the relative change in the strength of a composite based on BSK as a function of the degree to which it is filled with MT carbon black and then subjected to deformation rate of 0.637 m/s and temperature of 80°C. Figure 1; references 21: 14 Russian, 7 Western.

#### Generalizing the Solution of a Prandtl Problem of the Compression of a Plastic Layer With Two Rough Plates

927D0066G Kiev PROBLEMY PROCHNOSTI in Russian No 12, Dec 91 (manuscript received 3 Sep 90) pp 70-74

[Article by A.A. Ostsemin, Chelyabinsk Polytechnic Institute, Chelyabinsk]

UDC 539.374

[Abstract] The authors of the study worked to generalize the solution of a Prandtl problem of the compression of a sloping plastic layer between parallel rigid plates. Specifically, they worked to generalize the said problem for the case where the plastic layer is not orthogonal to the compressive force. On the basis of a partial differential equation, the authors derive a new fundamental solution for an ideally plastic body, stress tensor, and limiting compressive force. Classical Prandtl solutions are shown to follow from the new solution in the particular case of an orthogonal layer. A graphic interpretation of the dependences established is also presented. Figures 2; references 4 (Russian).

# The Deformation and Fracture of Boron-Aluminum Composite in a Complex Stressed State

927D0066C Kiev PROBLEMY PROCHNOSTI in Russian No 12, Dec 91 (manuscript received 4 Feb 91) pp 29-35

[Article by S.V. Tsvetkov, P.A. Zinovyev, A.N. Yeremichev, V.I. Tsyrul, V.Ye. Bukharin, and Yu.G. Bushuyev, Special Machine Building Scientific Research Institute, Moscow State Technical University imeni N.E. Bauman, Moscow, and USSR State Committee for Science and Technology]

UDC 539.4:678.067

[Abstract] The authors of the study conducted a series of experiments to determine the mechanical properties of

boron-aluminum composites containing 0.39 boron fibers by volume. The test specimens were manufactured by pressing in a vacuum at a temperature of 490 to 500°C. Single strips of boron fiber with AMg6 aluminum alloys sprayed on them were used as the starting intermediate product. Before pressing, the single strips were layered to form bundles 40 µm thick. A sleeve of the same alloy was used to form ends on the bundles. Ring-shaped specimens with a standard width of 10 mm were cut from the tube-shaped specimens by the electric spark method. Polished microsections were examined under a Neophot 30 optical microscope (magnification. 63x). Specimens were also subjected to axial compression and extension tests on EU-40 and TsDMU-30 testing machines. An I-1 experimental unit was used to produce stressed states in the specimens that could not be created by using conventional series-produced testing machines. The deformation diagrams obtained when the test boron-aluminum composite specimens were subjected to compression and shear stresses were not linear. The deformation diagrams obtained for the other types of stressed states examined were close to linear. When the test specimens were loaded with hydrostatic pressure and then released from its effects, they manifested residual deformations that were positive in the direction of the specimens' reinforcement and negative in the direction crosswise to the reinforcement. Of all the strength criteria considered, the criterion of maximum stresses was found to be in the best conformity to the experimental data. Loading the specimens with tensile forces and torque was found to result in a change in the mechanism of damage accumulation in the material and in the nature of the specimens' fracture. This change was found to depend on the relationships of the longitudinal stresses and shear stresses and to in turn result in a jumplike change in the strength of the given specimens. Figures 5, tables 2; references 6: 3 Russian, 3 Western.

## Mathematical Modeling of the Destruction of Brittle Inhomogeneous Mineral Ores

927D0066H Kiev PROBLEMY PROCHNOSTI in Russian No 12, Dec 91 (manuscript received 26 Jun 90) pp 75-78

[Article by I.A. Sveshnikov and L.Ya. Mishnayevskiy, Institute of Ultrahard Materials, UkSSR Academy of Sciences, Kiev]

#### **UDC 622.24**

[Abstract] The authors of the study worked to develop a mathematical model of the destruction of brittle inhomogeneous mineral ores. The said model is a probability model based on the mathematical apparatus of statistical physics. By using the theory of "nucleation center formation" and formulas developed by S.N. Zhurkov, the authors developed a description of a system of cracks formed in mineral ores when they are placed under a load. The cases of simultaneous and sequential loading of one space with several loads are compared: In the case

of sequential loading, the amount of damage incurred by mineral ores subjected to two instances of loading is additive. In the case of simultaneous loading, the equation used must contain an additional term  $\Delta R$ . This additional term represents the product of the probabilities of two independent events, i.e., no destruction at a given point due to the separate effect of each of two loads and destruction at the said point when the two loads act simultaneously. A formula was also derived to describe the size distribution of the cracks formed. The proposed model was used as a basis for deriving additional formulas for use in determining the energy intensity of the destruction of monolithic and cracked mineral ores. A probability model of the spalling of a ledge is also developed. On the basis of their proposed model, the authors showed that the destruction of mineral ore occurring in the case of simultaneous loading of one space with several loads is more intensive (by a factor of 1.7 to 2.3) than in the case of sequential loading by the same load. Figures 2; references 9 (Russian).

#### The Link Between Critical Embrittlement Temperature and Stress Concentrator Geometry and Loading Rate

927D0066D Kiev PROBLEMY PROCHNOSTI in Russian No 12, Dec 91 (manuscript received 27 Dec 90) pp 35-39

[Article by M. Mishin, I.V. Kislyuk, and V.I. Sarrak, Metal Science and Metal Physics Scientific Research Institute, and Central Scientific Research Institute of Ferrous Metallurgy imeni I.P. Bardin, Moscow]

UDC 539.4:620.178

[Abstract] The authors of the study worked to develop the physical principles of a method to determine the critical embrittlement temperature of a steel specimen or component with stress concentrators. Specifically, they set out to develop a method that would make it possible to tie the values of critical embrittlement temperature with the characteristics of local rupture strength, yield, and overstress and that would give consideration to the geometry of the specimen and the notch. Specimens (8.00 mm in diameter) of 10KP steel smelted in an open induction furnace were selected for the study. Three types of specimens were studied: smooth specimens; specimens containing annular grooves with a depth of 2.00 mm and a radius of curvature of 0.50 mm and with groove angles of 30, 60, and 120°; and specimens with a U-shaped notch. The specimens were heat-treated at 1,000°C for 60 minutes and cooled in air. The tensile strength tests were conducted on an Instron testing machine at loading rates of 2 and 20 mm/min at temperatures ranging from 77 to 293 K. The process of determining embrittlement temperature consisted of establishing the temperature at which the total-yield load equaled the breaking load. The experiments performed confirmed that critical embrittlement temperature (defined as the temperature at which local fracture at the

apex of a structural stress concentrator occurs) is directly linked to the characteristics of strength, yield, and overstress. The studies further confirmed that critical embrittlement temperature may be calculated by using the known critical maximum local tensile stress, the temperature dependence of the yield strength, and the overstress of the total yield. Finally, the authors concluded that their proposed calculation method may be used in developing a method of determining the critical embrittlement temperature of components with structural stress concentrators. Figures 4, tables 2; references 8: 7 Russian, 1 Western.

## The Arrest and Propagation of a Brittle Crack in Construction Steels. Communication 1

927D0066A Kiev PROBLEMY PROCHNOSTI in Russian No 12, Dec 91 (manuscript received 25 Jan 89) pp 15-21

[Article by Z. Bilek and M. Cherny, Brno, Czech and Slovak Federated Republic]

**UDC 539.4** 

[Abstract] The authors of the study examined the fracture toughness of three construction steels used in nuclear power plants (11.373, 11.483.1, and 15.313.5) in the stage of crack arrest at different temperatures. They measured the fracture toughness of the said steels by using the standard method of determining the critical coefficient of stress intensity in the stage of a running crack's arrest (K1a) as described in several other publications. The value of K<sub>1a</sub> of the individual construction steel was determined by loading a test specimen measuring 270 mm long x 100 mm wide x 24 in diameter x 20 mm thick or 270 x 100 x 52 mm in diameter x 30 mm thick with a wedge with an angle of 11° at its tip. The test temperature was varied from -196 to -60°C (nitrogen vapors were used to achieve these temperatures). The data obtained for all three construction steels tested demonstrated that their capability to arrest a running crack was below their rupture strength during initiation of the crack. The difference between these two indicators, which was found to increase with temperature, was interpreted as a reflection of the different micromechanisms of the initiation and arrest of fractures. Fractographic and metallographic studies of the specimens at the site of the end of the arrested cracks in the direction parallel to their propagation and perpendicular to the fracture surface revealed the presence of microdamage before the apex of the main crack. This was especially true in the cases of the ferrite-perlite steels 11.373 and 11.483.1, in which the growth of the main crack was determined to be due to the merger of individual microdamage. The values of  $K_{1a}$  that the authors determined by using a statistical approach were determined to reflect the capability of the test materials to arrest propagating brittle fractures. The studies performed led the authors to conclude that the planned American Society for Testing and Materials [ASTM] standard

regarding determining  $K_{1a}$  for ferrite steels may also be used successfully for steels having a bainite structure. The values of  $K_{1a}$  were found to be relatively independent of the rate of fracture before arrest and also to be relatively independent of the starting coefficient of stress intensity and crack length at time of arrest. The values of  $K_{1a}$  were found to provide a good approximation of minimum dynamic fracture toughness. The metallographic and fractographic studies performed also enabled the authors to derive a simple relationship between static fracture toughness and  $K_{1a}$ . Figures 17, table 1; references 16: 5 Russian, 11 Western.

## The Arrest and Propagation of a Brittle Crack in Construction Steels. Communication 2

927D0066B Kiev PROBLEMY PROCHNOSTI in Russian No 12, Dec 91 (manuscript received 25 Jan 89) pp 22-28

[Article by M. Cherny and Z. Bilek, Brno, Czech and Slovak Federated Republic]

#### **UDC 539.4**

[Abstract] The authors of the study worked to develop a laboratory method of determining the fracture toughness of construction steels in the crack propagation stage (K<sub>1D</sub>). For their studies, they used three construction steels typically used in nuclear power plant construction (i.e, types 11.373, 11.483.1, and 15.313.5). The fracture toughness determinations were made in a nitrogen-vapor cooled chamber at temperatures ranging from -196 to 20°C. A method based on interrupted conducting tracks was used to measure the rate of crack propagation. In essence, conducting tracks were produced in the specimens at specified distances apart in a direction perpendicular to the direction of crack propagation. The surface of each specimen was coated first with lacquer and then with an embrittled silver lacquer. The breaks occurring in the tracks during the course of the tests were recorded and analyzed to determine the crack propagation rate. The experimental crack propagation rate measurements made by the authors demonstrated that when the cracks of in test specimens were opened slowly, crack propagation occurred at a constant K<sub>1D</sub> such that the dependence of crack length on time was linear. The K<sub>1D</sub>-a [superimposed dot] (a [superimposed dot] being the rate of fracture propagation) plotted were not strictly linear. The studies further revealed that rate of crack growth, which remains constant for most of the length of the jump, may be controlled by adjusting the radius of the starting incision. The crack propagation rates (i.e., a [superimpodrf dot]) measured were found to correspond to theoretically calculated values. In the case of crack propagation rates ranging from 800 to 1,000 ms<sup>-1</sup>, the authors observed somewhat of a drop in the resistance of 15.313.5 steel to crack propagation. In the case of the steels 11.373 and 11.483.1, similar drops were initially observed in the crack propagation rate interval from 500 to 1,000 ms<sup>-1</sup>. This initial drop was followed by an increase when a [superimposed dot] became greater than 800 ms<sup>-1</sup>. The theory of the reverse merging of microcracks with the main crack was confirmed for steels with a ferrite-perlite structure. No such merging was found in the case of steel with a bainite structure. Comparisons of fracture toughness values found at different temperatures indicated that in the case of all three construction steels tested, the lowest values for resistance to the initiation of brittle fractures were found at the highest loading rates. The method developed by the authors to estimate dynamic fracture toughness during crack propagation eliminates the laborious propagation rate measurements generally required for such determinations and makes it possible to standardize the determination process. Figures 13; references 19: 8 Russian, 11 Western.

# Temperature Dependences of the Propagation Rate of Longitudinal Ultrasound Waves in Aluminum Oxide and Zirconium Dioxide Monocrystals

927D00661 Kiev PROBLEMY PROCHNOSTI in Russian No 12, Dec 91 (manuscript received 20 Feb 91) pp 81-82

[Article by V.A. Borisenko and A.I. Troyanskiy, Strength Problems Institute, UkSSR Academy of Sciences, Kiev]

#### UDC 534.22

[Abstract] The authors of the study conducted a series of experiments examining the propagation rate of longitudinal ultrasound waves in single crystals of aluminum oxide and zirconium dioxide within the temperature ranges from 10 to 100°C and -10 to +80°, respectively. The ultrasound echo-pulse method was used in the experiments with a relative error in determining ultrasound wave propagation speed that was no worse than +/-1 x 10<sup>-5</sup>. A system for heat stabilization of the acoustic line was used in which the temperature differential along the specimen did not exceed 0.1°C. The experimentation method used was distinguished by the fact that it entailed variable-by-variable sounding of the specimens by signals with different amplitudes. The nondoped aluminum oxide specimen had a height of 5 mm along the direction (001) and a diameter of 15 mm. It was heated at an average speed of 8 to 10°/h. The zirconium dioxide monocrystal used was stabilized in 10 mol% Y<sub>2</sub>O<sub>3</sub> and was in the form of a square measuring 9 mm on a side. It was heated at an average speed of 8 to 10°C/h. The temperature dependence of the phase propagation speed of an ultrasound wave through the aluminum oxide in the temperature range from 10 to 100°C exhibited three cascades of local extremums (containing three peaks each) and one individual local extremum. The temperature dependence of the propagation speed of an ultrasound wave in the ZrO2, as measured in the direction (110), contained three cascades of local extremums (containing four peaks each) in the temperature range from -10 to +80°C. The authors hypothesized that the number of peaks in the cascades of local extremums on the curves plotted for the temperature dependence of the elasticity characteristic of solids is linked to the number of valence bonds responsible for the attractive forces between the atoms of the lattice. They then proceeded to suggest that if this hypothesis is true, the electron subsystems of Al<sub>2</sub>O<sub>3</sub> and ZrO<sub>2</sub> contain three and four valence bonds, respectively, that play an important role in shaping the mechanical characteristics of these materials. Figures 2; references 4 (Russian).

#### An Investigation of Structural and Phase Transformations in Carbon Steels Subjected to the Combined Effects of Laser Radiation and a Magnetic Field

927D0049E Moscow FIZIKA I KHIMIYA OBRABOTKI MATERIALOV in Russian No 3, May-Jun 91 (manuscript received 12 Feb 90) pp 44-47

[Article by I.V. Suminov, Ye.V. Klopikov, N.A. Semenikhin, S.A. Pentyuk, and Yu.A. Zasetskiy, Moscow]

#### UDC 539.4.019.3.621.791.85

[Abstract] Specimens of U8 steel 15 mm in diameter and 1.5 mm thick were subjected to a series of experiments in order to determine the structural and phase transformations occurring in them when subjected to the combined effects of laser irradiation and a magnetic field. Before being subjected to laser hardening, the specimens were annealed in a vacuum of no worse than 10-3 Pa at a temperature of 750°C for 1 hour. The laser hardening was performed on a Kvant-12 unit in air with pulse energies of 0.5, 1.0, and 1.5 J and with pulse durations of 4 ms. A Polyus-600 unit was used to create a magnetic field. The magnetic induction lines were oriented coaxially to the laser radiation, and the magnetic induction on the specimens' surface was approximately 0.5 T. A YaGRS-4M spectrometer, gas-discharge detector, DRON-3M diffractometer, and Metalplan microhardness tester (manufactured by the firm Leitz) were used to study the laser radiation- and magnetic field-induced changes in the steel specimens. The Mossbauer spectra of all of the specimens tested were found to exhibit the characteristic sextet of lines corresponding to martensite. The Mossbauer spectra of those specimens that were not treated in a magnetic field were found to exhibit an additional central singlet associated with the presence of residual austenite in the surface layer. Disordering of the position of the carbon atoms in the martensite lattice following the treatment was found to cause a broadening of the lines constituting the sextet. In the absence of a magnetic field, the amount of residual austenite increased as the power of the laser pulse was increased, and a weak disordering of the carbon atoms could be observed. When a magnetic field was applied, residual austenite was absent. As the power of the laser radiation was increased, increasing disordering of the carbon atoms in the martensite could be observed. A layerby-layer analysis of the specimens treated at the maximum radiating power with no magnetic field showed

that the amount of residual austenite decreased deeper into the specimens. In the case of specimens irradiated in a magnetic field, the maximum disordering of the carbon in the matrix occurs at a depth of about 10 µm. X-ray crystallographic analysis confirmed these results. The application of a magnetic field at the moment of irradiation was found to increase specimens' microhardness somewhat; however, a magnetic field did not alter the basic profile of microhardness throughout the depth of the individual specimens treated. This increase in microhardness after the application of a magnetic field was attributed to the fact that the resultant elimination of residual austenite resulted in a greater relative amount of martensite in the treated specimens and thus in a corresponding increase in their microhardness. Figures 2; references 9: 8 Russian, 1 Western.

#### An Investigation of the Destruction of Composites by Laser Radiation in a Vacuum and at Atmospheric Air Pressure

927D0049D Moscow FIZIKA I KHIMIYA OBRABOTKI MATERIALOV in Russian No 3, May-Jun 91 (manuscript received 4 Apr 90) pp 38-43

[Article by V.T. Karpukhin, M.M. Malikov, N.V. Monakhov, A.P. Chernyshev, and N.I. Shalnova, Moscow]

UDC 539.4:678.067

[Abstract] The authors of the study examined the destructive effect of laser radiation on composites in a vacuum and at atmospheric pressure. A continuouswave CO<sub>2</sub> laser with an emissive power of up to 20 kW served as the radiation source. The pressure in the test chamber was varied from 1.3 x 10<sup>2</sup> to 10<sup>5</sup>Pa, and the specimen exposure time was varied from 1 to 20 seconds. A rectangle measuring 45 x 45 mm was irradiated in each specimen, and the power-flow density at the irradiated spot reached 10<sup>3</sup>/cm<sup>2</sup>. In a number of the experiments performed, a focusing lens made it possible to achieve a power-flow density of 0.5 to 1 x 10<sup>4</sup> W/cm<sup>2</sup>. Type STK glass-reinforced plastic, a carbon-plastic composite, and porous chlorosulfonated polyethylene with a filler served as the test composites. When materials of the same class as the test composites are subjected to irradiation at a radiating power of about 103 W/cm2 or less in atmospheric air, the predominant mechanisms of their destruction are thermal decomposition of the binder and the emission of solid coke particles in the form of gaseous products. The formation of these particles has been attributed to the destruction of the porous skeleton of the coke under the effect of thermal and mechanical loads during the filtration of pyrolysis gases. The experiments reported herein confirm that these same two mechanisms are the main mechanisms of the destruction of the type STK glass-reinforced plastic and carbon plastic composites tested. Decomposition of the binder makes a greater contribution to mass entrainment than particle emission does. Other researchers have shown that thermomechanical actions also affect the

composites tested herein. Specifically, thermomechanical actions result in deformations, stratification, and cracking of the surface layers of composites. The fusion of glass fiber occurring at an emissive power of about 400 W/cm<sup>2</sup> or more causes the fiber to break and thus diminishes the strength of the composite overall. The studies reported here demonstrated that the rates of graphite sublimation and glass vaporizaiton are low at temperatures less than or about 1,500 K and at pressures of 1.3 x 10<sup>2</sup> Pa or above. The studies further show that neither graphite sublimation nor glass vaporization make any significant contribution to the rate of mass entrainment. The effect of the heat of the exothermal reactions of the decomposition products with oxygen were also found to be insignificant. Figures 5; references 10 (Russian).

#### A Study of the Microstructure and Mechanical Characteristics of 40Cr10C2Mo Steel After Laser Treatment

927D0049I Moscow FIZIKA I KHIMIYA OBRABOTKI MATERIALOV in Russian No 3, May-Jun 91 (manuscript received 14 May 90) pp 102-107

[Article by A.G. Grigoryants, S.I. Aleksenko, and A.N. Safonov, Moscow]

#### UDC 621.785.54:669.14.018

[Abstract] The authors of the study examined the microstructure and mechanical characteristics of 40Cr10Si2Mo steel after laser treatment by a continuous-wave CO<sub>2</sub> laser in the radiating power interval from 0.5 to 2.1 kW. The test specimens were first hardened in oil at a temperature between 1,010 and 1,030°C and then tempered at a temperature between 760 and 780° to obtain a hardness (HRC) between 28 and 33. A Neophot-21 microscope was used for the metallographic analysis, a PMT-3 was used to measure microhardness under a load of 1 N. a DRON-3M diffractometer was used to determine the amount of residual austenite, and an SMTs-2 friction-testing machine was used to test durability. The experiments performed established that when 40Cr10C2Mo steel is subjected to laser treatment in modes involving fusion of the surface due to concentrated inhomogeneity, the fusion zone is made up of extrahard martensite cells surrounded by a thin grid of residual austenite. This structural pattern results in a significant improvement in the steel's mechanical characteristics. Laser treatment of 40Cr10C2Mo steel in a mode inducing surface fusion was also found to result in a jumplike increase in the durability of the laser paths analogous to the change in microstructure and hardness. The durability resulting from laser treatment involving surface fusion proved to be greater than the durability induced in steel by chromizing and laser surfacing with PG-SR3 powder but somewhat less than the durability resulting from ion nitriding. The best results were obtained by applying single paths at a 45° angle to the cylinder axis. The endurance limit of 40Cr10C2Mo

subjected to laser treatment until surface fusion occurred and then subjected to pure bending coupled with rotation was found to be 4 to 6% higher than before bending and 25 to 27% greater than the endurance of specimens subjected to galvanic chromizing. Figures 4, tables 3; reference 1 (Russian).

## The Interaction of Radiation Defects With Lithium Impurity Atoms in Aluminum

927D0049C Moscow FIZIKA I KHIMIYA OBRABOTKI MATERIALOV in Russian No 3, May-Jun 91 (manuscript received 11 Mar 90) pp 30-32

[Article by V.L. Arbuzov, A.E. Davletshin, I.Ye. Podchinenov, and S.M. Klotsman, Sverdlovsk]

#### UDC 539.1.043:069.71

[Abstract] The authors of the study examined the interaction occurring between radiation defects and lithium impurity atoms in aluminum. Diluted alloys of Al + 15 ppm Li and Al + 64 ppm Li based on type A999 aluminum were used for the studies. The alloys were prepared by remelting the Al-Li foundry alloy with pure Al in a graphite crucible in an atmosphere of pure helium. The specimens were irradiated in a continuoustype helium cryostat on a linear electron accelerator with an energy of 5.5 MeV at a temperature of 54 K. The studies performed indicated that lithium atoms in aluminum function as traps for interstitial atoms. The relative radius of the capture of the interstitial atoms by lithium impurity atoms at 54 K was found to equal 0.22 +/- 0.03, whereas the radius of capture of interstitial atoms by complexes consisting of an interstitial atom of the aluminum itself and a lithium atom equals 1.8 +/-0.2. The studies further revealed that the radii of the capture of interstitial atoms by impurity atoms can be correctly determined only at low irradiation doses ( $\Delta \rho$ 0.2 to 0.4 n $\Omega$  x cm depending on the impurity concentration [C<sub>1</sub>] and relative radius of the capture of the interstitial atoms of the metal itself by impurity atoms [R,]). Figures 2; references 8: 4 Russian, 4 Western.

## The Effect of a Metal's Defect Structure on Interstitial Ion Distribution Profile

927D0049B Moscow FIZIKA I KHIMIYA OBRABOTKI MATERIALOV in Russian No 3, May-Jun 91 (manuscript received 24 May 90) pp 27-29

[Article by V.I. Boyko, B.Ye. Kadlbovich, and I.V. Shamanin, Tomsk]

#### UDC 539.124

[Abstract] The correctness of ignoring "three-dimensional" structural defects when conducting research involving the bombardment of metal targets with ion beams is controversial. In an effort to clarify this matter, the authors of the study used the method of computer simulation to study the effect that the defect

structure of an aluminum target has on the distribution profile of H<sup>+</sup> and C<sup>6+</sup> ions throughout it. The experiments were designed to consider the case involving a bombardment energy of 1 MeV, particle concentrations between 10<sup>10</sup> and 10<sup>12</sup> cm<sup>-3</sup>, and volume defects ranging from 0.1 to 0.5 µm. The studies performed indicated that the presence of "three-dimensional" structural defects in metals results in a significant change in the distribution of stopped ions by penetration depth. The studies further indicated that the deviation in the run of an ion in aluminum with a dislocation density of about 10<sup>7</sup> cm<sup>-2</sup> from that calculated when defect structure is ignored may amount to tens of percentage points. The effect of "three-dimensional" structural defects on the process of an ion's passage through metal was found to be greatest in the case of heavy ions with an energy up to 1 MeV. "Three-dimensional" structural defects were found to cause a distortion of the Bragg distribution obtained when such defects are ignored and to thus result in a change in the parameters of the secondary processes accompanying the interaction of ions with metals and alloys. Figures 2, table 1; references 6 (Russian).

## Damage to Tungsten Monocrystal by Fast Heavy Ions

927D0049A Moscow FIZIKA I KHIMIYA OBRABOTKI MATERIALOV in Russian No 3, May-Jun 91 (manuscript received 11 Jun 90) pp 21-26

[Article by V.N. Bugrov and S.A. Karamyan, Dubna]

#### UDC 539.1.043

[Abstract] The authors of the study examined the damage inflicted on a tungsten monocrystal by irradiation with fast ions up to Xe+8 with an energy of approximately 0.9 MeV/amu. A direct crystallographic method based on the shadow effect was used for the studies. The studies were performed based on the following ions:  $^{16}\text{O}^{+3}$  (energy, 137 MeV),  $^{22}\text{Ne}^{+4}$  (energy, 175 MeV),  $^{40}\text{Ar}^{+2}$  (energy, 24 MeV), and  $^{129}\text{Xe}^{+8}$  (energy, 122 MeV). Polished monocrystalline specimens of W (110) were irradiated at room temperature by an ion beam along a direction not coinciding with their main crystallographic axes or planes. Heating of the specimens by the beams was insignificant. The beam parameters after passage through a collimator were as follows: diameter, 1 mm; divergence, <0.5°; intensity, <  $10^{10}$  s<sup>-1</sup>; and pulse intensity,  $\leq 1$  W. The main change discovered to occur when one type of bombarding particle was replaced by another was a change in dose scale. This fact was seen as an explanation of the fact that the anomalous damage that Xe+8 inflicts on semiconductors (Si and Ge) is not found in the case of tungsten. After analyzing the results of their experiments, the researchers concluded that the change in ions' ability to inflict damage corresponds to a model of generation of defects due to nuclear scattering. The experiments did not establish any contributions to tungsten damage resulting from ion energy electron losses. The experiments reported also confirmed that

direct crystallographic methods are most promising for use with monocrystalline specimens when studying the response of a condensed medium to the passage of highly ionizing particles. Figures 3, table 1; references 20: 5 Russian, 15 Western.

## The Dissolution of Aluminum and Its Alloys in Mineral Acid Solutions

927D0090E Ordzhonikidze IZVESTIYA VYSSHIKH UCHEBNYKH ZAVEDENIY: TSVETNAYA METALLURGIYA in Russian No 2, Apr 91 (manuscript received 8 Feb 90) pp 50-53

[Article by V.P. Kochergin, L.V. Paderova, G.Kh. Cherches, G.V. Kharina, O.M. Shevchenko, Inorganic Chemistry Department, Ural State University]

#### UDC 620.193.43

[Abstract] The authors summarize the results of a study of the anodic polarization and kinetics of the dissolution of A85 aluminum and its alloys D1, D16, and ML-5 in five different solutions. Solution 1 contained 200.00 g/dm<sup>3</sup> CrO<sub>3</sub> and 50.0 g/dm<sup>3</sup> H<sub>3</sub>PO<sub>4</sub>. Solution 2 contained 50.0 g/dm<sup>3</sup> HNO<sub>3</sub> and 10.0 g/dm<sup>3</sup> K<sub>2</sub>Cr<sub>2</sub>O<sub>7</sub> g/dm<sup>3</sup>. Solution 3 contained 200.0 g/dm<sup>3</sup> CrO<sub>3</sub> and 50.0 g/dm<sup>3</sup> H<sub>3</sub>PO<sub>4</sub>. Solution 4 consisted of 200.0 g/dm<sup>3</sup> CrO<sub>3</sub>, and solution 5 contained 700.0 g/dm<sup>3</sup> NaOH and 50 g/dm<sup>3</sup> NaNO<sub>3</sub>. Polarization curves were obtained in both galvanostatic and potentiodynamic modes on a P-5827M potentiostate using a YaSE-2 cell, silver chloride standard electrode, and a titanium auxiliary electrode. The gravimetric method was used to find the average dissolution rate and degree of protection afforded by the inhibitors. In concentrated HNO3 solutions aluminum was passivated, and its corrosion potential shifted to the range of electropositive values; however, this process was found to be impeded in the presence of F-, Cl-, Br-, and I- anions. Because of depassivation, the corrosion potential of A85 aluminum in the series NH<sub>4</sub>Cl-NH<sub>4</sub>F was found to shift to the side of electronegative values. The current density of the passivation of aluminum in a solution consisting of 10.0% HNO<sub>3</sub> and 3.0% NH<sub>4</sub>F turned out to be 1.8 times higher than the analogous value for metal in a solution containing 10.0% HNO<sub>3</sub> and 3.0% NH<sub>4</sub>Cl. Anodic oxidation of aluminum and its alloys and formation of protective and protective-decorative coatings were found to occur in solutions containing CrO<sub>3</sub>, H<sub>3</sub>PO<sub>4</sub>, H<sub>2</sub>SO<sub>4</sub>, HPO<sub>3</sub>, and H<sub>2</sub>C<sub>2</sub>O<sub>4</sub>. The dissolution rate of the aluminum alloys studied was found to increase as their melt temperature increased. The dissolution of the alloy D1 in solution 1 was, for example, 16 times more intensive than dissolution of the alloy D16. An analogous phenomenon was observed in tests conducted with solution 2. The anodic polarization curves recorded for the alloy MA-5 (which contains 7.5 to 9.5% Al and 0.2 to 0.8% Zn) in solutions 1, 4, and 5 did not contain any regions of active dissolution, which indicated that the electrode had passed into a passive state. Aluminum and its alloys were found to have a much lower corrosion resistance than magnesium and its alloys. The range of the anodic passive state of aluminum was found to be less than that for the magnesium alloy ML-5 by a factor of 1.6. Figures 3, tables 2; references 8 (Russian).

## The High-Temperature Oxidation of a Composite Material Consisting of 80% TiB<sub>2</sub> and 20% TiC

927D0090F Ordzhonikidze IZVESTIYA VYSSHIKH UCHEBNYKH ZAVEDENIY: TSVETNAYA METALLURGIYA in Russian No 2, Apr 91 (manuscript received 1 Mar 90) pp 59-63

[Article by V.S. Shestitko, P.V. Polyakov, and A.M. Golovanets, Light Metals Metallurgy Department, Krasnoyarsk Institute of Nonferrous Metals]

#### UDC 669.713.7

[Abstract] The authors of the study reported herein used the thermogravimetric method to examine the hightemperature oxidation of a composite consisting of 80% TiB<sub>2</sub> and 20% TiC. A preweighed specimen was hung on a nichrome suspension mounted on the bowl of an analytical scale and lowered into a shaft furnace that was then heated to a specified temperature for a specified time somewhere between 5 and 10 hours. The change in the specimen's mass as a result of high-temperature oxidation was then determined. The measurements were taken on hot-pressed specimens of the study composite with a close-to-theoretical density at five fixed temperatures (°C): 700, 800, 900, 1,000, and 1,100. The kinetic curves plotted for the different heating temperatures and times were not identical. In the initial legs of the curves for all of the study temperatures the researchers observed a reduction in specimen mass that was, upon first approximation, proportional to temperature. Also noteworthy was the fact that the "burnup peak" was in the range from 3 to 15 minutes from the beginning of the experiment at all temperatures except 900°C. In the case of heating to 900°C, the peak was shifted in time to the range of 25-30 minutes. In the cases of heating to temperatures of 700 and 800°C a protective film formed quickly after the "burnup peak," and the change in mass virtually ceased after the first 1-1.5 hours. At temperatures of 1,000 and 1,100°C, the oxidation curve assumed a parabolic form after a linear segment of mass increase in the interval from 15 to 30 minutes. Microphotographs of specimens heated to each of the different temperatures were compared. Heating at 700°C resulted in an increase in surface microirregularities and surface scarring. The specimens heated to 800°C exhibited smoothing of the surface and formation of vacancies between the individual conglomerates. At 900°C fusion and even more surface smoothing occurred along with the formation of fine grains with pores between them. At 1,000°C the grains became consolidated, and the zones of vacancies between them increased. At 1,100°C the grains on the specimens' surfaces became larger once again, fused particles became distinctly apparent, and the zone of the vacancies increased. Oxidation of the material was found to occur inside the pores of the forming protective film. The oxygen content of the different specimens was also compared. At 700°C the oxygen content dropped sharply farther from the surface. At 800°C the oxygen content deep within the specimens

increased. At 900°C the oxygen content decreased (evidently the film formed had greater protective properties). The oxygen content at the specimen surface reached a maximum at 1,000°C. Figures 4; references 8 (Russian).

## Selected Features of Pulsed Laser Hardening of Titanium Alloys

927D0089M Moscow FIZIKA I KHIMIYA OBRABOTKI MATERIALOV in Russian No 6, Nov-Dec 91 (manuscript received 26 Oct 90) pp 130-134

[Article by A.P. Lyubchenko, Ye.A. Satanovskiy, V.N. Pustovoyt, G.I. Brover, V.N. Varavka, and Ye.A. Katsnelson, Kharkov and Rostov-na-Donu]

#### UDC 669.14.018:621.785:535.211

[Abstract] The authors of the study reported herein examined selected characteristic features of the laser surface hardening of titanium alloys. Specimens of VT3-1 titanium alloy were subjected to pulsed laser treatment by a Kvant-16 laser with a power flux density of 100 to 150 kW/cm<sup>2</sup>. The following powders were used during the laser surface alloying: standard carburizer (birch tar oil), ferrochrome, Al<sub>2</sub>O<sub>3</sub>, T15K6, α-BN, and molecular boron. Coal-tar varnish was used as a binder. A Neophot-21 microscope was used for the metallographic studies, a PMT-3 hardness tester was used for the durability tests, and a DRON-.05 diffractometer was used for the x-ray crystallographic studies. The experiments conducted demonstrated that laser surface treatment can indeed harden the surface of titanium alloy specimens, with the degree of hardening depending on the alloying coating selected. Al<sub>2</sub>O<sub>3</sub>, ferrochrome, T15K6, and α-BN proved particularly effective in improving the basic performance characteristics of the titanium alloys treated. The laser surface treatment regimen tested was found to result in the formation of a rather deep (70 to 100 µm) hardened layer with a hardness exceeding that of the starting metal by a factor of 1.1 to 1.6. This effect was attributed to the concentration and morphological inhomogeneity of the solid solutions, the formation of a a' martensite phase, and saturation of the alloy with nitrogen and carbon from the air and from the coating. Figures 4; references 3: Russian, Western.

#### Change in the Structure and Properties of Surface Layers of Titanium Upon Laser Surface Alloying

927D0089L Moscow FIZIKA I KHIMIYA OBRABOTKI MATERIALOV in Russian No 6, Nov-Dec 91 (manuscript received 13 Feb 91) pp 117-123

[Article by A.N. Bekrenev and Ye.A. Morozova, Samara]

UDC 621.793.6:621.375.826

[Abstract] The authors of the study reported herein examined the changes in the structure and properties of

a titanium surface that occur when it is subjected to laser surface alloying with iron and nickel. Specimens of VT1-0 commercial-grade titanium prepared by annealing in a vacuum at a temperature of 970 K for 2 hours were studied. The electrolyte method was used to apply the alloying materials. To improve adhesion, a copper coating 0.3 to 0.4 µm thick was used as an underlayer. After coating the specimens were subjected to vacuum heating at a temperature of 870°C for 20 minutes. The resultant coating layer measured 10 µm in thickness. The coated specimens were fused by continuous-wave laser radiation at powers of 220 and 630 W. The treatment was conducted with fusion of the surface in a stream of commercial-grade nitrogen at a pressure of 0.25 atm. A Katun CO<sub>2</sub> laser and a spot diameter of 2 mm were used. The speed at which the beam was moved along the specimen surface was varied from 30 to 1,000 mm/min. The studies performed indicated that increasing the speed at which the beam is moved along the specimen surface results in a more uniform surface structure and makes it possible to produce a relatively finely disperse structure with improved physicomechanical properties. At high beam speeds no melt zones were observed (thanks to the low temperature factor). Figures 5, table 1; references 7: 6 Russian, 1 Western.

#### Protective Diamondlike Films on Quartz

927D0089K Moscow FIZIKA I KHIMIYA OBRABOTKI MATERIALOV in Russian No 6, Nov-Dec 91 (manuscript received 11 Mar 90) pp 113-116

[Article by S.M. Klotsman, A.S. Kovsh, L.M. Kovsh, Ye.V. Zuzmina, R.R. Mukhametkhaziyev, S.A. Plotnikov, I.Sh. Trakhtenberg, and L.M. Feygin, Sverdlovsk]

#### UDC 539.216.2:514.26-162

[Abstract] The authors of the study reported herein examined selected performance characteristics of protective diamondlike quartz coatings produced by the method of ion-condensation destruction of hydrocarbons. The said method, which is characterized by a high ion concentration in the beam, makes it possible to produce films with minimum internal stresses. A graphite chamber (cathode) containing two copper water-cooled anodes was used as the ion beam source. One of the chamber walls was fashioned in the form of a grid through which an ion beam measuring 70 x 150 mm<sup>2</sup> was drawn into the chamber. High-purity (99% pure) propane was used as the working gas. Fused polished quartz and quartz coatings on glass produced by electron beam sputtering served as substrates. Germanium substrates were also used in some of the experiments. The working chamber was evacuated to create a pressure no worse than 2 x 10<sup>-4</sup> Pa. Before the coating process began, the substrates were cleaned in an argon discharge. During the coating process the propane pressure was varied from 8 x 10<sup>-3</sup> to 5 x 10<sup>-2</sup> Pa, the discharge voltage was varied from 1.2 to 2 kV, and the discharge

current was varied from 0.15 to 0.66 A. After the sputtering the specimens were held in a vacuum for at least 30 to 40 minutes, after which air was allowed to enter the chamber. The method of nuclear reactions on a deuteron beam with an energy of 900 keV was used to determine the residual gas impurity (oxygen and nitrogen) profile of the diamondlike coatings. The optical properties of the diamondlike coating were found to be virtually independent of sputtering regimen. The diamondlike coatings applied to germanium had a higher refractivity than those on quartz (2.17 +/- 0.06 and 2.02 +/- 0.04, respectively). The diamondlike coatings' absorption was found to decrease as the wavelength was increased. The condensation rate was found to be a linear function of the discharge current. The diamondlike coatings on quartz were characterized by a refractivity of 2 and a transparency in the infrared range. The diamondlike coatings were found to afford a certain amount of protection to the quartz substrates to which they were applied. Specifically, they reduced the substrates' friction coefficient by a factor of 1.5, caused a severalfold increase in resistance to the effects of abrasive particles, and provided stability to moisture, heat shock, and heating to 200°C. The effectiveness of the diamondlike coating was not limited to the properties of the films themselves; rather, the quality of its mesh with the substrate (which increased as the ion beam energy increased) was also important. Figures 3, tables 2; references 6: 5 Russian, 1 Western.

#### Morphologic Changes in the Structure of Composite Conglomerated Powders During Plasma Sputtering and Their Effect on Coating Structure

927D0089I Moscow FIZIKA I KHIMIYA OBRABOTKI MATERIALOV in Russian No 6, Nov-Dec 91 (manuscript received 22 Jan 91) pp 84-89

[Article by A.K. Tolstobrov, M.Yu. Zashlyapin, and B.V. Mitrofanov, Nizhniy Tagil and Sverdlovsk]

#### UDC 621.793.72:533.9

[Abstract] The authors of the study examined the morphologic changes occurring in composite conglomerated powders during plasma sputtering and the effect of these changes on coating structure. Five conglomerated powders were tested. Their compositions (% by mass) were as follows: Powder 1,  $50\text{TiC}_{0.5}\text{N}_{0.5}$  + 50Ni; powder 2,  $50\text{TiC}_{0.5}N_{0.5} + 25\text{Ni} + 25\text{Mo}$ ; powder 3,  $35\text{TiC}_{0.5}N_{0.5} +$ 49Ni + 16Mo; powder 4,  $35\text{Ti}_{0.9}\text{Zr}_{0.1}\text{C}_{0.5}\text{N}_{0.5}$  + 49Ni + 16Mo; and powder 5,  $35\text{Ti}\text{C}_{0.5}\text{N}_{0.5}$  + 52Ni + 13Cr. The structure of particles produced by sputtering powders in a water bath from a distance of 200 to 300 mm was studied. The technique of plasma sputtering on a UPU-3D plasma unit was used to sputter the powders and apply composite coatings to substrates of type 45 steel. An argon-nitrogen mixture was used as the plasmaforming gas. A Neophot-21 microscope, Camebax x-ray spectroscope, and PMT-3 hardness tester were used for

the studies. Indenter loads of 50 and 100 g were used. The starting particles of all five test powders were spherical porous formations consisting of evenly distributed and sintered finely dispersed (particle size up to 10 um) subparticles of titanium carbonitrides and metals constituting the binder-alloy. All of the starting composites had a porosity of 40 to 55%. The technique of sputtering into water in a plasma stream was found to result in significant structural changes in each of the powders tested. The specific nature of the changes depended on a number of factors, including composition of the metallic component of the powder composites, the wettability of the refractory inclusions formed by the melts, and the density of the sputtered powders. The nature of the structure of the particles participating in the formation of the coatings was found to have a significant effect on the uniformity of the distribution of refractory inclusions in the field of the metal matrix of the composites, the quality of the boundary of fusion with the basic metal, and the porosity of the sputtered layers. Those coatings that were made of composites characterized by complete wetting of the surface of the refractory particles by the metal binder melt and formation of fused composite particles with a heterodisperse structure proved to have the highest-quality structure. Coatings made of powder 2 had the highest average microhardness (11.0 x 10<sup>3</sup> MPa), whereas coatings of powder 5 had the lowest microhardness (7.30 x 10<sup>3</sup> MPa). Coatings of powders 1, 3, and 4 had average microhardness values of 8.40, 8.50, and 8.70 x 10<sup>3</sup> MPa, respectively. In all cases, the microhardness of the center of the fused granules was much lower than that of the peripheral segments of the granules, thus indicating that the shells were filled primarily with refractory inclusions while the centers were filled primarily with binder-alloy. Figures 5, tables 3; references 3 (Russian).

## Improving the Quality of Chemical Coatings of the System Ni-P on Tool Steels by Laser Irradiation

927D0049H Moscow FIZIKA I KHIMIYA OBRABOTKI MATERIALOV in Russian No 3, May-Jun 91 (manuscript received 11 Mar 90) pp 90-94

[Article by G.I. Brover, V.N. Varavka, Ye.A. Katsnelsov, V.T. Loginov, G.Ye. Trofimov, and V.D. Kritin, Rostov-na-Donu]

#### UDC 621.785:669.14.018.29

[Abstract] The authors of the study explored the possibility of using laser irradiation to improve the quality of Ni-P chemical coatings on tool steels. Ni-P coatings were applied to the steels R6M5, R18, Cr12V1, and 4Cr5W2VSi by the technique of chemical deposition. A Kvant-16 laser unit was used at power-flow densities of 80 to 200 kW/cm². A Neophot-21 microscope was used for the metallographic analysis, a PMT-3 was used for the durability studies, and a DRON-0.5 diffractometer was used for the x-ray crystallographic analysis. The experiments performed revealed that the quality of the

chemical coatings deposited on the study steels and then treated by laser irradiation depends above all on the thickness of the coating and the power-flow density of the radiation. The optimal coating thickness was found to be 10 to 30 µm. When coating thickness was increased beyond 30 µm, the efficiency of the laser heat treatment process decreased. Power-flow densities above 100 kW/ cm<sup>2</sup> resulted in the formation of a crater-like zone that was deepest in the central portion of the spot. Cracking of the coating throughout virtually the entire area of the defocusing spot was also observed. Neither of these effects was observed when the power-flow density was kept below 100 kW/cm<sup>2</sup>. Laser treatment was found to produce a dendrite structure in the coated steel specimens, with the depth of the irradiated layer reaching 10-30 µm and the microhardness reaching 4-6 GPa (or even 8-9 GPa when the specimens were subjected to tempering for 1 hour at 300°C). Laser irradiation also increased the adhesion of the Ni-P coatings to the steel substrates tested. The experiments performed thus demonstrated that laser treatment is an effective method of improving the quality of Ni-P chemical coatings on tool steels. Figures 3; references 5 (Russian).

## Laser-Stimulated Chemical Deposition of Nickel Films

927D0049G Moscow FIZIKA I KHIMIYA OBRABOTKI MATERIALOV in Russian No 3, May-Jun 91 (manuscript received 12 Jan 90) pp 85-89

[Article by M.R. Bruk, Ye.A. Morozova, and G.A. Shafeyev, Moscow]

UDC 669.881:535.211

[Abstract] The authors of the study examined the laserstimulated chemical deposition of nickel films onto the following catalytically inactive substrates: Cu, GaAs, Si, Al<sub>2</sub>O<sub>3</sub>, and epoxy-resin glass-base textolite. A Cu vapor laser ( $\lambda$ , 0.51  $\mu$ m; P  $\simeq$  20 mW) and a YAG:Nd<sup>3+</sup> laser ( $\lambda$ , 1.06  $\mu$ m; P  $\simeq$  10 W) served as radiation sources. Both were used in pulse and continuous-wave modes. The coatings were precipitated from a chemical nickel plating solution. It main components were NiCl<sub>2</sub> and Na<sub>2</sub>H<sub>2</sub>PO<sub>2</sub>. The Ni-P coatings studied were deposited by the technique of scanning a beam along the substrate. When the test substrate was irradiated by a laser, deposition of the coating began after some activation time t<sub>a</sub>. Initially, the substrate temperature remained virtually unchanged. Then, at the moment ta, there was an avalanche-like increase in substrate temperature corresponding to the beginning of the deposition of the Ni onto the Cu. The deposition process was accompanied by the evolution of hydrogen gas. The time ta decreased as the fraction of the colloidal solution of metallic Ni in the starting solution was increased and was found to depend on the thickness of the solution over the target. A "running metallization" mode was detected in which the reaction was initiated at some arbitrary place on the copper path and then spread along the entire path of the

printed board. The researchers succeeded in producing Cu-Ni-P-Au printed circuit board contacts that meet the requirements established for contemporary circuit board technology. Experiments examining the exposure time dependence of the area of Ni-P deposited on Si revealed that while the area of a deposit does not initially depend on exposure time, it becomes very much dependent on exposure time further on into the process. Scanning the laser radiation along the substrate surface was found to result in the deposition of Ni-P pathways. Experiments related to direct laser metallization of epoxy-resin glassbase textolites resulted in the formation of paths that are little suited to use in actual practice because of their resistance (tens to hundreds of ohms). This problem was remedied by completing the growth of the deposited paths. After this was done, the path resistance decreased to 1  $\Omega$ . The researchers also succeeded in demonstrating the possibility of metallizing 100-um-diameter holes in polycorundum wafers 500 µm thick by laser-stimulated deposition of Ni-P coatings onto the hole walls. Figures 6; references 12: 9 Russian, 3 Western.

#### The Porosity and Electrical Strength of Thin Alumina and Zirconia Films Produced by High-Frequency Magnetron Sputtering

927D0049F Moscow FIZIKA I KHIMIYA OBRABOTKI MATERIALOV in Russian No 3, May-Jun 91 (manuscript received 2 Apr 90) pp 81-84

[Article by V.G. Padalka, I.V. Lunev, and V.I. Agafonov, Kharkov]

#### UDC 621.315.61

[Abstract] The authors of the study examined the porosity and electrical strength of thin alumina and zirconia films produced by high-frequency magnetron sputtering. Polycrystalline Al<sub>2</sub>O<sub>3</sub> and ZrO<sub>2</sub> films were produced by high-frequency magnetron sputtering in argon under a pressure of 1 to 2 Pa. Pure powders of the respective compounds that had first been annealed at 1,000°C in a vacuum of about 10-4 Pa were used as targets. The films were deposited onto standard pyroceram substrates that had been precoated with a layer of chromium 0.5 µm thick by thermal vaporization. The dependences of pore density, pore size distribution, and electrical strength of the films on the respective filmformation parameters were recorded at fixed values of the said parameters. In the case of the Al<sub>2</sub>O<sub>3</sub> films these parameters were as follows: film thickness, 200 nm; deposition rate, 17 nm/min; deposition temperature, 270°C; and substrate grid bias, -50 V. For the ZrO<sub>2</sub>, these same parameters were as follows: film thickness, 200 nm; deposition rate, 40 nm/min; deposition temperature, 300°C; and substrate grid bias, -40 V. The through porosity of the films was studied by the electrochemical method, and the films' electrical strength was determined by their volt-ampere characteristic. A sublayer of chromium and an external mercury contact served as electrodes. As the thickness of both types of films

increased, the density of the through pores tended to decrease. At thicknesses greater than 200 nm, this trend weakened noticeably, thus indicating the end of the process of build-up of aggregates of film nucleation centers. Through pore density was found to behave analogously as the deposition rate was increased. Increasing the speed at which the coating layer was deposited was found to result in a decrease in the ratio of the rate at which the condensation of argon and residual gases reached the surface to the rate at which particles of the deposited material reached it. This decrease in turn increased the mobility of the adatoms on the condensate surface and facilitated improved healing of the film defects that had formed. The density of the through micropores of both the alumina and zirconia films was found to decrease as the mobility of the adatoms increased. The pore size distribution functions of both the alumina and zirconia films studied had a normal distribution with a maximum in the range from 150 to 600 nm. As the deposition temperature was increased within the interval from 300 to 600°C, the electrical strength of both the alumina and zirconia films increased. Electrical strength decreased as film thickness increased, however. Increasing deposition speed also reduced electrical strength. The migration capability of the adatoms increased as the magnitude of the negative grid bias fed to the substrate during the film condensation process was increased. This increase in migration capability in turn resulted in the growth of a more perfect crystalline structure and in an increase in the films' electrical strength. Figures 2; references 5: 3 Russian, 2 Western.

#### The Formation Mechanism of Crystal Lattice Defects in Electrodeposited Nickel Films

927D0067H Moscow POVERKHNOST: FIZIKA, KHIMIYA, MEKHANIKA in Russian No 12, Dec 91 (manuscript received 13 Aug 90; after revision 5 Dec 90) pp 119-123

[Article by T.A. Tochitskiy and A.V. Bolutshkin, Solid-State Physics and Semiconductors Institute, BSSR Academy of Sciences, Minsk]

#### UDC 539.216.2.548

[Abstract] The authors of the study reported herein examined the mechanism of lattice defect formation in nickel films 20 nm to 10 µm thick that were precipitated from a sulfuric acid electrolyte onto copper substrates. Specifically, the films were precipitated from an electrolyte containing 280 g/l NiSO<sub>4</sub> x 7H<sub>2</sub>O, 120 g/l MgSO<sub>4</sub> x 7H<sub>2</sub>O, and 30 g/l H<sub>3</sub>BO<sub>3</sub>. The films were deposited at room temperature, a pH of 2 to 6, and a deposition current density of 5 to 70 mA/cm<sup>2</sup>. Saccharin in a concentration of 0 to 5 g/l was used as a surfactant. An EMV-100LM electron microscope and DRON-3 diffractometer were used to study specimens of the films. Specifically, the specimens subjected to x-ray crystallographic analysis consisted of 30 to 40 epitaxial layers

separated from the substrate. The crystalline lattice parameter was measured with an error of 0.01%. The studies performed established that when the electrolyte's acidity is reduced from a pH of 2 to a pH of 6 (with a current density of 15 mA/cm<sup>2</sup>), the (110) growth texture of the study films remains unchanged. The concentration of their subtraction-type stacking faults increases, however. Increasing the current from 5 to 70 mA/cm<sup>2</sup> (at a pH of 6) was found to facilitate an increase in the concentration of the specified defects and to cause the films' texture to be restructured in the sequence (100). (210), (110). Adding saccharin to the electrolyte was found to result in the formation of a (111) texture and a reduction in the concentration of stacking faults. The mismatch between the film lattice parameter and that of the substrate, as well as the incorporation of impurities during crystal growth, were determined to be the main causes of the stacking faults discovered. These results were determined to be in good agreement with data published in two other communications. The authors also proposed a formula for determining the probability of the appearance of stacking faults in electrodeposited coatings. Figures 2, table 1; references 14: 12 Russian, 2 Western.

## Laws Governing the Growth of a Gold Film on a Benzene Substrate at 77 K

927D0067F Moscow POVERKHNOST: FIZIKA, KHIMIYA, MEKHANIKA in Russian No 12, Dec 91 (manuscript received 4 Apr 90; after revision 19 Dec 90) pp 98-104

[Article by V.L. Karnatsevich, B.S. Kaverin, G.A. Domrachev, and V.I. Zaykovskiy, Organometallic Chemistry Institute, USSR Academy of Sciences, Nizhniy Novgorod]

#### UDC 539.234:537.533.35

[Abstract] The authors of the study used the electron microscopy method to study the laws governing the growth of gold films on benzene crystal substrates. The studies were conducted on a unit (described elsewhere) that made it possible to produce a benzene film at 77 K on a copper substrate and to then condense heatvaporized Au atoms onto it. The Au film formed on the benzene film-substrate complex was then extracted by using a carbon replica and analyzed by using a JEM-100CX high-resolution electron microscope. The laws governing the formation and growth of Au films were studied as a function of the degree of coating of substrate m as determined by the total number of atoms deposited on 1 cm<sup>2</sup> of a flat substrate parallel to the beam of atoms. First, the authors examined the condensation of Au onto molecularly smooth faces of crystals of a benzene substrate. The microscopy studies performed indicated that the said process occurs primarily by the mechanism of the union of the particles formed rather than by the formation of new nucleation centers. Two peaks were discovered in the size distribution of the said particles:

The first corresponded to close-to-spherical particles with a mean-weighted diameter of 3 nm, and the second corresponded to larger and longer particles with a meanweighted diameter of 11 nm. The two types of particles were designated as rank 1 and rank 2 particles, respectively. The rank 2 particles were determined to be the result of the union of rank 1 particles, with the formation of bridges between the latter in some cases. The rank 1 particles were found to include individual tetrahedra with (111) planes truncated by peaks and more complex particles (for example, with two systems of bands corresponding to (111) planes) that were either parallel to one another or else disoriented. The rank 2 particles were determined to be polyparticles formed when tetrahedral fragments and multiple twinning particles (icosahedra and decahedra) join together. Next, the authors turned their attention to the condensation of Au films on molecularly rough faces of the crystals of the benzene substrate. The microscopy studies performed revealed that the particles formed when Au is condensed on the molecularly rough faces are more isometric and more disperse than the particles formed on molecularly smooth surfaces given identical substrate coatings. The moment of onset of formation of a continuous film is earlier, and there are no signs of surface decoration (such signs are observed in the case of the particles on the molecularly smooth surfaces). Analysis of the size distribution of the particles formed on the molecularly rough faces revealed the presence of a maximum in the range of particles smaller than 2 nm in size. This finding was taken as an indication that the rate at which particles are generated exceeds the rate at which their shape changes owing to interaction in the ensemble of islands. Figures 4; references 12: 8 Russian, 4 Western.

## The Formation Mechanism of Films Produced by Reactive Ion-Plasma Deposition

927D0067C Moscow POVERKHNOST: FIZIKA, KHIMIYA, MEKHANIKA in Russian No 12, Dec 91 (manuscript received 20 Aug 90; after revision 24 Jan 91) pp 24-28

[Article by A.N. Pilyankevich (deceased), V.Yu. Kulikovskiy, and L.R. Shaginyan; Materials Science Problems Institute, Ukraine Academy of Sciences, Kiev]

UDC 539.216:661.55:669.29:621.793.7

[Abstract] The authors of the study worked to develop a methodology that would make it possible to estimate the contribution of chemically active gas particles to the process of synthesis of titanium nitride films. For the said studies, titanium nitride films were produced by using a planar magnetron system with an annular magnet and disk target with a constant current. Two sputtering techniques were used. In one, a titanium nitride disk produced by powder metallurgy techniques and sputtered in argon served as the target. In the other method, a titanium target was sputtered in a nitrogen-argon atmosphere. The targets were about 50 mm in diameter,

the target-to-base distance was 40 mm, and a discharge intensity of about 200 W was used. The argon and argon-nitrogen mixture were kept under a pressure of about 0.67 Pa. Formation of the nitride films began at a  $P_{N2}/P$  pressure of 0.29. The composition of the films and targets was studied by x-ray microanalysis, electron diffraction photography, and interferometry. Polished pyroceram plates and, in some cases, sheared surfaces of KCl monocrystals were used as the substrates. Essentially, the analysis method developed consisted of the following steps. The minimum partial nitrogen pressure in the nitrogen-argon mixture surrounding the target and, consequently, on which the titanium nitride is formed is determined experimentally. Because a state of dynamic equilibrium is known to exist on the target surface and because it is titanium nitride rather than titanium that is being sputtered, the pressure of the nitrogen during sputtering can, for all practical purposes, be assumed to equal the pressure established in the chamber before the discharge is turned on. Knowing this makes it possible to estimate the number of N<sub>2</sub><sup>+</sup> ions reaching the target. Comparing this figure with the number of nitrogen atoms sputtered in turn makes it possible to determine the contribution of the N2+ ions to the processes of the formation of titanium nitride on the target. A series of equations for use in making the calculations required for the numerical estimate are derived and presented along with a discussion of the assumptions underlying the proposed numerical analysis method. By applying their proposed method in the experiment conditions outlined above, the authors were able to establish that practically all of the nitrogen atoms reaching the substrate participate in the synthesis of titanium nitride. The N<sub>2</sub><sup>+</sup> molecular ions colliding with the surface of the titanium target, on the other hand, only partially participate in the formation of titanium nitride. At an energy of 430 eV, fewer than 15% of such ions contribute to the formation of titanium nitride. Figure 1; references 13: 7 Russian, 6 Western.

## Dielectric Layer Formation on InP by Thermal Oxidation of InP/PbS Structures

927D0068A Moscow IZVESTIYA AKADEMII NAUK SSSR: SERIYA NEORGANICHESKIYE MATERIALY in Russian Vol 27 No 12, Dec 91 pp 2484-2487

[Article by I.Ya. Mittova, V.V. Pukhova, V.N. Semenov, I.M. Soshnikov, Voronezh State University]

UDC 546.682.18:621.794.61

[Abstract] The pattern of dielectric layer formation on indium phosphide by thermal oxidation of InP/PbS structures and the composition and properties of the resulting dielectric layers are investigated. PbS layers are deposited by precipitation onto polished FIE-1a InP (100) wafers; thermal oxidation of the InP/PbS structures is performed in a quartz reactor with resistive heating while the layer thickness is measured by the ellipsometric method. The component distribution profiles in the films grown at 550°C and infrared transmission spectra of InP/PbS structures oxidized under various conditions are plotted. It is shown that thermal oxidation of InP/PbS structures accelerates the formation of dielectric layers with adequate characteristics. The film growth kinetics and mechanism are different from those of standard InP samples and GaAs/PbS structures. PbS oxidation to PbSO<sub>4</sub> is a dominant process; as the process temperature and duration increases, the InPO<sub>4</sub> formation starts to play an increasingly important role. Indium becomes bonded to sulfur on the interface which prevents excess indium accumulation in the film and ensures a considerable improvement in the layers' electrical properties. Figures 2; references 6: 5 Russian; 1 Western.

#### Calculation of the Adhesion Characteristics of a System of Two Different Metals Separated by a Dielectric Layer

927D0067D Moscow POVERKHNOST: FIZIKA, KHIMIYA, MEKHANIKA in Russian No 12, Dec 91 (manuscript received 3 Aug 90; after revision 24 Jan 91) pp 72-75

[Article by A.N. Vakilov and V.V. Prudnikov, Omsk State University]

#### UDC 539.612.001

[Abstract] Working within the framework of the density functional method, the authors of the study analyzed the adhesion characteristics of a system of two different metals separated by a dielectric layer. In essence, the functional density method entails solving a variational problem to find the minimum energy of the electron system examined against the background of a specified positive charge distribution. In the present study, the authors considered two semibounded metals occupying the regions z < -D and z > D with an intermediate dielectric layer with a thickness of 2D and a dielectric constant of  $\epsilon$ . By solving a linearized Thomas-Fermi equation using boundary conditions reflecting the continuity of the electrostatic potential  $\varphi(z)$  and electric induction  $\varepsilon d\phi/dz$  with z = +/-D and the finiteness of the potential in infinity, they derive an expression for the density of the electron distribution n(z) in the said system (assuming that  $\varphi(z) = -4\pi n(z)/\beta^2$ ). They also find the interface interaction energy and the adhesion energy and force of the adhesion interaction with consideration for the discreteness of the crystal lattice of the contacting metals as a function of the distance between the metal surfaces and the dielectric constant of the intermediate layer. The authors acknowledge that using the concept of the dielectric constant for a layer with a thickness on the order of interatomic quantities is not strictly correct but is instead a model abstraction. They further note that for  $\beta D/\epsilon^{1/2} >> 1$ , the adhesion properties of a metaldielectric-metal system will be determined by the characteristics of the metal-dielectric contact and that giving consideration to the vacuum gap between them will result in a replacement of repulsive forces by attractive forces. They conclude by stating that for distances of  $\beta D\epsilon^{1/2} >> 1$ , disperse attractive forces begin to come into play along with electrostatic forces and that these disperse attractive forces become decisive at values of D of about 100 angstroms or more. Figures 2; references 6: 5 Russian, 1 Western.

# Radiation Strength of Carbon-Carbon Composite Materials Under High-Temperature Neutron Irradiation

927D0068Q Moscow IZVESTIYA AKADEMII NAUK SSSR: SERIYA NEORGANICHESKIYE MATERIALY in Russian Vol 27 No 12, Dec 91 pp 2664-2666

[Article by R.G. Khanbekov, Kh.M. Rasulkulov, Yu.S. Virgilyev, I.P. Kalyagina, T.N. Shurshakova, Nuclear Physics Institute at the Uzbek Academy of Sciences]

**UDC 546.26** 

[Abstract] Fabric-based carbon-carbon composite materials (UUKM) which are distinguished from others by their structure and composition are studied in order to determine the following characteristics: density, bending strength and compressive strength, dynamic modulus of elasticity, thermal conductivity, electric resistivity, thermal coefficient of linear expansion, and the crystal lattice constant c. To this end, 4x4, 5x5, and 8x8 mm samples were irradiated in a helium atmosphere in the high-temperature chamber of a VVR-SM reactor at the Nuclear Physics Institute at the Uzbek Academy of Sciences at a temperature of 1,800-1,900 and 2,100-2,300K; the temperature was measured by W-Re thermocouples. The properties of fabric-based carboncarbon composites are summarized and tabulated and the relationship between the relative changes in resistivity and the fabric-based carbon-carbon composite material sample size is established and plotted. A slight anisotropy in properties of some materials is established. It is noted that in all fabric-based carbon-carbon composite materials and in the reactor-grade graphite, an improvement in resistivity may be attributed primarily to the compaction of the material. Irradiation of various fabric-based carbon-carbon composite material samples at 1,800-2,300K temperatures by a 1 x 10<sup>20</sup> neutron/cm<sup>2</sup> fluence leads to their shrinkage and decreases their resistivity due to a matrix compaction; the change in strength does not exceed 50%. Figures 1; tables 1; references 1.

#### An Investigation of Destruction of Composite Materials by Laser Radiation and a Supersonic Nitrogen Flow

927D0089G Moscow FIZIKA I KHIMIYA OBRABOTKI MATERIALOV in Russian No 6, Nov-Dec 91 (manuscript received 13 Jul 90) pp 58-65

[Article by A.A. Betev, V.T. Karpukhin, M.M. Malikov, and N.I. Shalnova, Moscow]

UDC 539.4:678.067

[Abstract] The authors of the study examined the combined effect of laser radiation and a supersonic nitrogen flow on specimens of composite materials (i.e., layered carbon-filled plastic and porous chlorosulfonated filled polyethylene) that included a phenol-formaldehyde resin binder. Composite specimens with an initial layered and porous structure were studied at oncoming flow Mach numbers of about 4.1, an impact temperature of 1,100 to 1,300 K, and an impact pressure of about 2.5 MPa. The laser radiation had a wavelength of 10.6  $\mu m$  and a radiating power of  $10^2$  to  $10^4$  W/cm<sup>2</sup>. The irradiation spot measured 30 x 40 mm in most of the experiments and had a diameter of 10 mm in some of the experiments. The duration of the irradiation was varied from 3 to 20 seconds and that of the supersonic flow was varied from 10 to 30 seconds. The effects of the nitrogen flow and the laser radiation were studied in combination and separately. A typical effect of the hot nitrogen flow on the chlorosulfonated filled polyethylene was that of uniform darkening (carbonization) of the specimen's entire surface area to a depth on the order of 0.1 to 0.2 mm. The surface of the carbon-filled plastic specimens cracked easily when subjected to a hot nitrogen flow, and some stratification of the said specimens was observed in individual places. The thickness of the carbonized layer carried away by the flow was on the order of 0.1 mm for both types of specimens. When the chlorosulfonated filled polyethylene specimens were subjected to a combination of laser radiation and the hot nitrogen flow, the burnthrough depth increased dramatically depending on the radiating power and duration of the radiation effect.

In the case of the carbon-filled plastics, combined laser radiation and nitrogen resulted in strong surface cracking and swelling, stratification, deformation, and a reduction in specimen mass (as opposed to when the nitrogen flow was used alone). The studies thus revealed that in the case of both types of composite specimens studied, most of the ablation of the materials was due to the laser radiation rather than to the nitrogen flow. The authors conclude by stating that the most likely mechanism of the effect of combined laser radiation and nitrogen flow treatment is that of pyrolysis of the binder under the effect of the laser radiation and "cleaning" of the surface layer of the coke by the supersonic flow. Figures 5; references 5 (Russian).

## The Effect of Argon Ion Channeling on the Sputtering of a Niobium Monocrystal Surface

927D0067A Moscow POVERKHNOST: FIZIKA, KHIMIYA, MEKHANIKA in Russian No 12, Dec 91 (manuscript received 27 Jun 90; after revision 4 Jun 90) pp 105-111

[Article by A.A. Kosyachkov, V.T. Cherepin, and S.M. Chichkan, Metal Physics Institute, UkSSR Academy of Sciences, Kiev]

#### UDC 537.534.8

[Abstract] The authors of the study used the method of secondary-ion emission [SIE] anisotropy to isolate the individual types of ion channels occurring during the sputtering of a niobium monocrystal surface and to subsequently determine the effect of argon ion channeling on the sputtering. During their studies they used a new angular resolution instrument that permitted freer selection of the direction of surface irradiation and analysis of the sputtered ions. The surfaces of welloriented Nb (100) and Nb (111) monocrystals were bombarded with Ar<sup>+</sup> ions with energies of 3, 5, and 7 keV at an ion current density of 5 x 10<sup>14</sup> cm<sup>-2</sup> x s<sup>-1</sup> in a beam with a spread not exceeding 1°. The polar and azimuthal bombardment angles were established with a precision of 0.5°. An electrostatic lens was used to level the spatial and energy anisotropy of the probability of the sputtered ions' ionization. The sputtering of clusters was taken into account by summing the yields of the  $Nb_n^+$  (n = 1 to 6) cluster ions. In accordance with the established practice, the effect of channeling on the anisotropy of SIE was determined as the relative difference between the maximum and minimum ion yields measured at one and the same polar glide angle. The contributions made by the individual channeling components to the reduction in output of secondary ions was assumed to be additive. The studies performed confirmed that channeling of bombarding Ar+ ions parallel to the most open (110) planes of the body-centered crystal lattice make the greatest contribution to the reduction in output of sputtered particles. When compared with this, the contribution of planar (100) channeling is insignificant. The studies also established that the amount of contrast may be altered by more than a factor of 2 depending on the slope of the channeling plane relative to the target surface. By analogy in the case of axial channeling, the incline of the axial channel relative to the crystal surface may have a more significant effect on SIE anisotropy than channel transparency does. The contribution from the most transparent channels, i.e., (111) and (100), is commensurate with that of planar channeling. The possible channeling along the (112), (113), and (115) axes, on the other hand, has no influence on the orientation effects of sputtering. Increasing the energy of the bombarding argon ions from 3 to 7 keV was found to improve contrast and reduce the angular half-widths of the minima of the azimuthal distributions of the SIE. The studies performed thus confirmed the feasibility of

the authors' proposed technique to quantitatively estimate the individual contributions of axial and planar channeling of Ar<sup>+</sup> ions. Figures 3, tables 2; references 7: 5 Russian, 2 Western.

# Development and Implementation of Low-Sulfur Steel-Making Pig Iron Smelting Under Southern USSR Conditions

927D0061B Moscow STAL in Russian No 12, Dec 91 pp 7-12

[Article by S.N. Pryadko, V.I. Malkin, S.L. Yaroshevskiy, V.V. Starov, I.D. Tsybulenko, Z.K. Afanasyeva, Kramatorsk Metallurgical Works, Donetsk Polytechnic Institute, and Bakal Ore Directorate]

#### UDC 669.162.2

[Abstract] The increasingly stringent requirements being imposed on the sulfur content in various brands of steel-making pig iron and the specific operating conditions of blast furnaces in the south of the USSR which in many respects are inferior to those in the east are discussed. The development and implementation of processes and materials for smelting low-sulfur steel-making pig iron in southern blast furnaces are addressed; to this end, the chemical composition of iron ore materials and coke characteristics for smelting steel with a low sulfur content are summarized and kinetic ore reduction curves are plotted. The dependence of slag viscosity and melting point on the magnesia concentration is examined. Comparative performance indicators of blast furnace No. 4 at the Kramatorsk Metallurgical Works with siderite added to the burden are cited and the chemical composition of magnesian slags at the Kramatorsk Metallurgical Works is analyzed. Curves of the dependence of slag basicity on the desulfurization coefficient and the dependence of the sulfur content in pig iron on the slag basicity and silicon content are plotted. An analysis shows that the use of low-melting stable magnesian slags is the most important and indispensable element for producing conversion pig iron with a sulfur content of 0.02% or below and that an increase in the MgO content to 6-12% in slag with a 1.35-1.45 basicity lowers the melting point by 20 to 100°C, reduces viscosity by 0.18-0.65 Pa x s, and increases the stability of the slag's physical properties by two- to sevenfold. The impact of siderite addition to the charge is assessed. Figures 5; tables 3; references 15.

#### Metal Jet Drop Height During In-Line Vacuum Degassing of Continuously Cast Steel: Discussion

927D0061F Moscow STAL in Russian No 12, Dec 91 pp 24-25

[Article by A.A. Smirnov, Uralmash Production Association]

UDC 621.74.047-982-715.6

[Abstract] Analyses of the degree of metal refining in a vacuum as a function of the jet drop height performed by

various authors are discussed and the design of units for continuous metal jet degassing is presented. It is shown that the hypothesis of the structure of short rimmed steel jet in a vacuum is poorly argumented and the efficiency of refining processes during in-line vacuum degassing in the course of continuous steel casting depends on the joint effect of vacuum on a short jet and the volume of metal in the vacuum chamber or intermediate ladle. Given the same jet drop height, the greater the duration of the elementary metal volume stay in the active layer, the greater the refining degree. A formula is derived for calculating the metal degassing duration in the active layer. Figures 1; references 4.

## Comprehensive Utilization of Natural Gas in Metallurgy

927D0061A Moscow STAL in Russian No 12, Dec 91 pp 4-7

[Article by G.Ye. Senko, Kharkov Engineering Teachers College]

UDC 669.162.2:662.9

[Abstract] The essence of comprehensive utilization of natural gas in metallurgy is defined as delivering it first to furnace coolers as a cooling medium, then completely expending the gas, warmed up due to heat losses in the process zone, as fuel, making it possible to utilize furnace losses and save fuel, improve working conditions and extend the cooler life, and considerably decrease the cooling water rate and prevent its ingress into the furnace area. Commercial experiments to cool the doublewall blast furnace nozzle by natural gas conducted by the Ferrous Metallurgy Institute at the Krivoy Rog Integrated Iron and Steel Works and the effect of the natural gas temperature and speed in pipes of various diameters on the heat transfer coefficient are summarized. The calculations were made on a computer using an algorithm developed in the Fortran language. The experiments demonstrate the high efficiency of using natural gas and make it possible to estimate the anticipated economic impact of the proposed method in blast furnace foundries. The method is recommended for widescale implementation. Tables 1; references 3.

### The Nitriding of a Nickel Alloy and Its Properties

927D0089N Moscow FIZIKA I KHIMIYA OBRABOTKI MATERIALOV in Russian No 6, Nov-Dec 91 (manuscript received 30 Nov 90) pp 145-149

[Article by Yu.V. Levinskiy, A.A. Nuzhdin, V.P. Zhabin, V.B. Latyshdev, and T.L. Tsuprun, Moscow]

UDC 669.245.26.295

[Abstract] The authors of the study reported herein examined the process of internal nitriding of nickelbased alloys with chromium and titanium dopants. Specifically, they nitrided alloys containing the following (% by mass): chromium, 24; titanium, 0.5 to 3.0; La, 0.1; C, 0.04; and O<sub>2</sub>, 0.05. After smelting, the ingots were forged and then rolled until sheets 1.5 mm thick were produced. Specimens were then prepared for testing in accordance with All-Union State Standard [GOST] 9657-73. A Neophot light microscope and Hitachi S-800 scanning electron microscope were used to study the structure of the nitrided alloy specimens. The studies performed established that "through" nitriding may be achieved in the temperature interval from 1,373 to 1,473 K in time periods that are acceptable from a technological standpoint. Test specimens nitrided at 1,453 K were found to have a nitride phase with a characteristic particle size of 0.1 to 1.0 µm. When low holding times and relatively low temperatures were used, the ratio of the metal elements in the nitride particles having an NaCl-type structure are approximately equal to that in the matrix. As the temperature of internal nitriding is increased, the titanium content in the particles of the hardening phase in the near-surface areas of the specimen increases, and the chromium content decreases. According to the authors' thermodynamic calculations, the free energy of the formation of complex titanium nitride (63% Ti, 17.0% Cr) at 1,173 K equals 190 kcal/mol. As the temperature is increased to 1,323 and 1,453, it reaches 170 and 140 kcal/mol, respectively. These elevated temperatures are also thermodynamically more conducive to the formation of phases richer in titanium. The free energy of their formation amounts to 175 and 170 kcal/mol for the specified temperatures. Internal nitriding also resulted in significant improvements in the test specimens' mechanical properties and microhardness and in a reduction in resistivity. Internal nitriding also resulted in improved heat resistance and resistance to oxidation. Figures 4, tables 2; references 4: 3 Russian, 1 Western.

The Formation of Mg<sub>32</sub>(Al, Zn)<sub>49</sub> and Al-Mg-Zn Phases in an Unsaturated Aluminum-Magnesium-Zinc Solid Solution Upon Electron Irradiation in a Diffraction Channeling Mode

927D0089F Moscow FIZIKA I KHIMIYA OBRABOTKI MATERIALOV in Russian No 6, Nov-Dec 91 (manuscript received 28 Sep 90) pp 50-52

[Article by V.V. Ivanov, V.M. Lazorenko, and Yu.M. Platov, Moscow]

UDC 621.791.85:620.18

[Abstract] The authors of the study examined the formation of the phases Mg<sub>32</sub>(Al, Zn)<sub>49</sub> and Al-Mg-Zn in an alloy containing 0.1% (atomic) Al and 0.06% (atomic) Zn during irradiation under a high-voltage microscope. Foils of the study alloy 0.2 mm thick were annealed in air at a temperature of 550° for 2 hours. The specimens were thinned in an electrolyte containing 20% HClO<sub>4</sub> + 80% C<sub>2</sub>H<sub>5</sub>OH at a temperature of 60°C. The foils were subjected to electron irradiation in a JEM-1000 highvoltage microscope with a power of 1 MeV at temperatures from 20 to 150°C. The intensity of the irradiation amounted to  $6.2 \times 10^{18} \text{cm}^{-2}/\text{s}$ , and the irradiation was performed in a channeling mode with the electron beam practically parallel to type (111), (100), and (110) planes and passing along the axes of the crystal zone. Transmission electron microscopy studies performed on the study specimens revealed that irradiation in doses of about 2.2 x 10<sup>-26</sup>/m<sup>2</sup> at a temperature of 100°C resulted in dislocation loops and zones of uniform contrast in the form of light spots with tetrahedral form vacancy accumulations inside them. The size of these zones and the tetrahedra were found to increase as the irradiation dose was increased; however, their density remained unchanged. Unlike aluminum-magnesium alloys, the study alloys were not found to exhibit any spatial correlation in the arrangement of the zones of uniform contrast and the tetrahedra on the one hand and the neighboring vacancytype dislocation loops on the other. The authors were only able to speculate as to the formation mechanism of Mg<sub>32</sub>(Al, Zn)<sub>49</sub> and Al-Mg-Zn phases upon electron irradiation. They hypothesized that it was either a segregation mechanism analogous to the phase formation during neutron irradiation or else a spinodal decomposition mechanism. Figure 1, table 1; references 5: 3 Russian, 2 Western.

### Gold Extraction With Low-Basicity Anion Exchangers

927D0030G Moscow TSVETNYYE METALLY in Russian No 6, Jun 91 pp 68-69

[Article by G.A. Stroganov, V.Ye. Dementyev, A.P. Tatarinov, D.A. Semenkov, and S.V. Valikov, Irkutsk State Scientific Research Institute of Rare Metals]

UDC 622.775:66.074.7

[Abstract] A method of regenerating saturated low-basicity anion exchanger for production of commercial gold-silver alloy containing 83 % Au by the desorption process has been developed. This involves treatment of the saturated anion exchanger with an alkali-cyanide solution, electrolysis of the eluate, roasting the auriferous carbonaceous wad, and floating-zone melting of the cinder. Treatment with aqueous NaOH-NaCN solution completes simultaneous desorption of the gold and regeneration of the low-basicity anion. A saturated anion exchanger contains typically 1.2 mg/g Au + 3.49 mg/g Fe + 0.23 mg/g Zn + 0.1 mg/g Ni + 0.1 mg/g Co + 0.04 mg/g

Cu + 0.01 mg/g Ag, a regenerated anion exchanger then containing only 1.1 mg/g Fe + 0.1 mg/g Zn + 0.1 mg/g Au. Electrolysis produces an extract which contains typically 82.76 % Au in the Au-Ag alloy, 9.94 % Au in the regenerated anion exchanger + 0.06 % Au in the residual electrolyte + 7.34 % Au in the slag. Hydrometallurgical reprocessing of the slag for extraction of gold from it involves crushing and grinding it to the -0.1 mm grain size fraction, leaching with water at 80-90°C for 32 h followed by cyaniding the cake with 2 g/dm³ NaCN for 48 h, and leaching with sulfuric acid at 90°C for 1 h followed by cyaniding the cake with 1.5 g/dm³ NaCN for 48 h. Up to 92 % Au can be thus extracted from the slag. Figures 2; tables 2.

# Producing Silicon Single Crystals With Uniformly Distributed Oxygen

927D0030F Moscow TSVETNYYE METALLY in Russian No 6, Jun 91 pp 48-50

[Article by Z.A. Salnik, Ye.S. Levshin, and Yu.A. Miklyayev, Perm Chemical Apparatus Manufacturing Plant (PKhMZ)

UDC 669.782

[Abstract] The process of growing silicon single crystals by the rotating crucible method for internal getters in fabrication of VLSI circuits is described, the speed of rotation being varied as the crystal grows so as to ensure optimum oxygen content and its most nearly uniform distribution over the crystal volume. In an experimental study of this proposed process two batches of Si(100) and Si(111) single crystals 105 mm in diameter were grown while being doped with boron or phosphorus in standard crucibles: "Redmet" (Rare Metal)-15 crucible 270 mm in diameter and "Redmet" (Rare Metal)-30 crucible 330 mm in diameter. The crucibles were charged with 15-22 kg of silicon melt, the speed of their rotation then being varied by a KM 111 microprocessor in accordance with a special control program. An analysis of oxygen distribution histograms reveals a highly uniform (within 10 %) axial oxygen concentration profile in 600-900 mm long grown single crystals. A statistical analysis of pointby-point electrical resistance (conductance) readings taken with an ASR-100C tester and indicating the radial spreadout of oxygen reveal a highly microuniform (within 4.5 %) radial oxygen concentration profile in crystals annealed at 430°C temperature for 75 h. Getters grown by this process are now used with success in production of VLSI circuits by either bipolar or MOS technology. Figures 3; references 4.

# Electrolyzer for Carnallite With Wider Separation Zone Between Products of Electrolysis

927D0030E Moscow TSVETNYYE METALLY in Russian No 6, Jun 91 pp 44-45

[Article by P.A. Donskikh, V.A. Kolesnikov, and D.F. Rakipov, BT Metallurgical Combine]

UDC 669.721

[Abstract] An electrolyzer for carnallite has been built with a 65 mm wide distance between graphitized anodes and 50-60 mm thick cathode plates, all electrodes being mounted equally high above the bottom pan for current feed from below. Such a construction is to ensure a more nearly complete separation of the two gaseous and liquid phases, with a resulting reduction of magnesium and chlorine losses. Such an electrolyzer was tested in standard operation over a 25.5-month period, after which interelectrode distance was found to have become 100-110 mm long. The thickness of the anodic graphite layer on the cast iron core had in this time decreased from the original 150 mm to not less than 65 mm, corresponding to 1.5-1.7 mm/month and thus lower than the normal rate of graphite consumption on each side. Two such electolyzers of the new version were subsequently tested over a 21-month period for both magnesium yield and energy consumption at a 0.225 A/cm<sup>2</sup> current density in an electrolyte with an electrical conductivity of 1.73 S. The voltage drop across the electrolyte had increased in time owing to the increase of the interelectrode distance only, calculations based on the experimental data indicating that the voltage drop due to dissolution of anodic iron and a consequently poorer iron-graphiye is negligible. Figures 1; tables 1.

# Results of Test Performed on Model of Cooler for Anodes of Magnesium Electrolyzer

927D0030D Moscow TSVETNYYE METALLY in Russian No 6, Jun 91 pp 41-44

[Article by V.F. Yalovoy, A.M. Sizonenko, M.M. Nikolayev, L.A. Orlova, and T.K. Kolesnik, Titanium Institute of UKT Metallurgical Combine]

UDC 669.721

[Abstract] A magnesium electrolyzer with evaporative water cooling of the anode assembly has been designed, and the water-vapor mixture entering a separator drum from which the water is pumped back into an array of jackets. These jackets, an array of semicylindrical tubes, are produced by lengthwise cutting cylindrical steel tubes in half (300 m long tubing for one electrolyzer) and welding the half-tubes with high-quality seams to a steel base. A gage pressure of 0.5 MPa and water temperature of 158°C are maintained in the system. A simple model of such a cooler was built and tested for design and performance evaluation, a 645 mm-long and 150 mmwide graphitized plate on top of a helical electric heater simulating the anode assembly with current leads on top and a 2.5 mm thick steel U-tube 32 mm in diameter encapsulated in an Al-Mg alloy pot on top of that plate simulating the cooler. Heat transfer from plate to cooler above it was improved by filling three 315 mm-deep and 40 mm-wide vertical holes drilled into the 340 mm-high plate with an Al-Mg alloy. The heater underneath the plate was thermally insulated with diatomite brick so as to minimize heat leakage into the surrounding air. The

model was placed inside a steel housing for the test. Measurements made over a 6 h period have yielded the essential cooler performance characteristic, namely the dependence of the quantity of heat dissipated on the plate temperature in three modes of operation: 1) heating without cooling, 2) simultaneous heating and cooling, 3) cooling without heating. The results of measurements are compared with and found to agree closely with the results of design calculations. The plateto-cooler heat transfer coefficient, a key cooler performance indicator, is 3500 W/(m<sup>2</sup> x °C) when calculated theoretically only and 4539 W/(m<sup>2</sup> x °C) when recalculated with use of test data. An analysis of the results indicates that the new cooler will raise the current capacity of anodes and thus also the productivity of an industrial electrolyzer by 14.5 % with a lower graphite consumption. Figures 5; tables 1; references 1.

### Behavior of Lead Anodes in Sulfuric Acid Solutions Containing Cobalt

927D0030C Moscow TSVETNYYE METALLY in Russian No 6, Jun 91 pp 25-28

[Article by A.A. Kucherov, A.D.Artemyev, N.A. Zaykova, and V.N. Kozhanov, Ural Scientific Research and Planning Institute of Copper Industry]

UDC 669.347

[Abstract] An experimental study of the behavior of lead anodes in sulfuric acid solutions ions was carried out

aimed at improving, by addition of cobalt ions, their corrosion resistance and thus their performance in production of electrolytic copper foil at the Kyshtym Electrolytic Copper Making Plant of the "Uralelektromed (Ural Electrocopper)" Combine. Such anodes were electrolytically polished in a weak HNO3 solution and then washed with distilled water. Laboratory tests were performed with an electrolyte containing 50+5 g/dm<sup>3</sup> CuSO<sub>4</sub> and/or 55+5 g/dm<sup>3</sup> H<sub>2</sub>SO<sub>4</sub>, for 5 h at a 2 kA/ m<sup>2</sup> anode current density so as to ensure formation of a 50 % protective surface layer. Industrial tests were then performed in a commercial solution of 75+/-20 kg/m<sup>3</sup>  $H_2SO_4$  with 62+/-11 kg/m<sup>3</sup> Cu and 0.025+/-0.008 kg/m<sup>3</sup> Cl ions at a 40+/-2.5°C temperature, for 2232 h with a 2600+/-400 A/m<sup>2</sup> anode current density under a 7.2+/ -0.4 V average electrolyzer voltage. Subsequent tests were performed in plain H<sub>2</sub>SO<sub>4</sub> solutions without Cu ions, so as to eliminate their effect on the corrosion rate, and CoSO<sub>4</sub> was added in successively larger amounts so that its concentration increased stepwise from 0.0003 to 0.03 kg/m<sup>3</sup>. The anode current density was varied stepwise from 2 to 18 kA/m<sup>2</sup>. The corrosion rate was measured by loss of mass method. The results indicate that corrosion of Pb anodes proceeds slower in an H<sub>2</sub>SO<sub>4</sub>:CuSO<sub>4</sub> electrolyte than in a plain H<sub>2</sub>SO<sub>4</sub> electrolyte and still slower in an H<sub>2</sub>SO<sub>4</sub>:CoSO<sub>4</sub> electrolyte, probably because of formation of a denser protective PbO<sub>2</sub> surface layer. The most likely mechanism of Pb-Co<sup>2+</sup> interaction is electrochemical adsorption at a high anode potential. Addition of CoSO<sub>4</sub> to the electrolyte decreased the electrical resistance of anodes by up to 8 %, with an equivalent energy saving, and decreased the loss of mass by up to 32 %. Figures 2; references 10.

### Efficiency of the Absorption of Radiation Point Defects by Pores Surrounded by Impurity Atmospheres

927D0089B Moscow FIZIKA I KHIMIYA OBRABOTKI MATERIALOV in Russian No 6, Nov-Dec 91 (manuscript received 16 Aug 90) pp 12-18

[Article by S.B. Kislitsin, Yu.S. Pyatiletov, and N.I. Yedemskiy, Alma-Ata]

#### UDC 621.039.531

[Abstract] The authors of the study examined the effects of the formation of equilibrium atmospheres of interstitial impurity atoms on the efficiency of the absorption of radiation point defects by vacancy and gas-filled pores in metals with a body-centered crystal structure irradiated under various conditions. Specifically, they performed a mathematical analysis of the following: the equilibrium impurity atmospheres close to pores, the concentrations of point defects close to pores surrounded by an impurity atmosphere, and the efficiency of absorption of point defects by pores surrounded by impurity atmospheres. The analysis performed led the authors to conclude that as a result of the formation of impurity atmospheres around vacancy and gas-filled pores, each pore becomes a sink with a preference for absorbing either titanium interstitial atoms or vacancies. Vacancy pores with an impurity atmosphere mainly absorb interstitial atoms, whereas gas-filled pores with a gas pressure exceeding 2γ/r<sub>u</sub> mainly absorb vacancies. The application of external tensile or compressive stresses does not change these absorption preferences; however, it does change the values of the absorption efficiency (Ya) and the pore preference parameter (B<sub>o</sub>). Figures 4; references 10: 8 Russian, 2 Western.

### Use of Cryogenic Technology To Produce Powders 927D0049J Moscow FIZIKA I KHIMIYA OBRABOTKI MATERIALOV in Russian No 3, May-Jun 91 (manuscript received 26 Jun 89) pp 121-123

[Article by A.F. Alekseyev, K.K. Palekha, S.G. Ponomarchuk, L.V. Chernyak, and V.Ya. Shlyuko, Kiev]

#### UDC 621.762.2

[Abstract] The authors of the study examined the various process variables affecting the dispersivity powders produced by cryogenic technology. Al<sub>2</sub>(SO<sub>4</sub>)<sub>3</sub> x 18H<sub>2</sub>O with a purity grading of good was used as the starting material to prepare the solutions. Solutions containing between 0.025 and 0.65 moles Al<sub>2</sub>(SO<sub>4</sub>)<sub>3</sub> x 18H<sub>2</sub>O per liter (obtained by diluting a saturated solution) were used to study the effect of concentration on specific surface. Tests revealed that decreasing the concentration of the starting solutions results in an increase in the specific surface of the resultant powder. The experiments also established that increasing the rate at which the starting solution is cooled results in an increase in specific

surface. A "hard" sublimation drying regimen was found to result in a specific surface of 92 m<sup>2</sup>/g, whereas a "moderate" regimen resulted in a specific surface of 116 m<sup>2</sup>/g. Derivative thermogravimetric analysis of the decomposition process of granules of sublimation-dried aluminum sulfate indicated that the process is completed at a temperature of about 1,000° within 60 to 90 minutes. A sharp decrease in specific surface was found to occur in the temperature interval from 1,050 to 1,200°, and it remained virtually unchanged upon further heating to 1,300°. At a temperature of 1,050°, average particle size ranged from 0.5 to 1 x 10<sup>-8</sup> m; at 1,300°, it ranged from 1 to 3 x 10<sup>-7</sup> m. The studies performed confirmed that cryogenic technology can indeed be used to produce powders with a high specific surface and that specific surface may be controlled within a broad interval of starting water-and-salt solution concentrations, cooling rates, and heat treatment conditions. Figures 2; references 4 (Russian).

# Preparation and X-Ray Phase Analysis of Thin Zinc Arsenide Films

927D0068B Moscow IZVESTIYA AKADEMII NAUK SSSR: SERIYA NEORGANICHESKIYE MATERIALY in Russian Vol 27 No 12, Dec 91 pp 2499-2500

[Article by N.S. Zhalilov, G.S. Yuryev, S.F. Marenkin, General and Inorganic Chemistry Institute imeni N.S. Kurnakov at the USSR Academy of Sciences]

#### UDC 539.27:546.48'19+546.47'18

[Abstract] Interest in Zn<sub>3</sub>As<sub>2</sub> compounds is due to their use as a component of Zn<sub>3</sub>As<sub>2</sub>-Cd<sub>3</sub>As<sub>2</sub> solid solutions and an analogue of CdTe-HgTe solid solutions. Zn<sub>3</sub>As<sub>2</sub> films for the study are prepared from Zn<sub>3</sub>As<sub>2</sub> single crystals; 24x10x05 mm vitreous and leucosapphire wafers are used as the substrate. Thin Zn<sub>3</sub>As<sub>2</sub> films are produced in a VUP-5 all-purpose vacuum chamber and their thickness is measured under a MII-4 interference microscope. The resistivity, Hall concentration, and carrier mobility of the films are measured in weak constant electric and magnetic fields. The results demonstrate that vacuum deposition can be used to produce amorphous and crystalline Zn<sub>3</sub>As<sub>2</sub> films. At substrate temperatures above 300°C, the films consist primarily of [224] oriented crystalline grains. An analysis demonstrates that the electric properties of the films are close to the properties of Zn<sub>3</sub>As<sub>2</sub> single crystals. Diffraction patterns of Zn<sub>3</sub>As<sub>2</sub> films are plotted. Figures 2; tables 1; references 7: 2 Russian; 5 Western.

### ZnSe Production by Self-Propagating High-Temperature Synthesis Method and ZnSe Properties

927D0068E Moscow IZVESTIYA AKADEMII NAUK SSSR: SERIYA NEORGANICHESKIYE MATERIALY in Russian Vol 27 No 12, Dec 91 pp 2516-2519

[Article by S.V. Kozitskiy, D.D. Polishchuk, V.P. Pisarskiy, S.V. Zubritskiy, N.M. Kompanichenko, I.S. Chaus,

V.G. Andreychenko, Odessa State University imeni I. Mechnikov and General and Inorganic Chemistry Institute at the Ukrainian Academy of Sciences]

#### UDC 546.661.847.23

[Abstract] The self-propagating high-temperature synthesis (SVS) method is used to produce solid blocks of zinc selenide. The burden is prepared from a standard zinc powder PTs-1 and chemically pure selenium ground in a mortar to a particle size of  $\leq 10 \,\mu m$ . Since the ZnSe quality depends primarily on the synthesis conditions as well as the combustion temperature and external pressure, these parameters were manipulated during the process. The results of chemical and X-ray phase analyses of ZnSe alloys, the response intensity of the superstructural ZnSe phase at various wavelengths, infrared transmission spectra measurements, diffuse reflection spectra of polycrystalline ZnSe, and emission spectra of polycrystalline ZnSe are cited. Radiographic studies are performed by the powder method in a DRON-2 under  $CuK_{\alpha}$  radiation while infrared spectroscopy analyses are carried out in a Specord M-80 instrument. Forbidden gap width measurement data attest to the presence of perfect crystals in synthesized ZnSe product. Photoconduction is measured on freshly cleaved surfaces while photoluminescence is analyzed in a special unit under a He-Cd laser. Analytical data indicate that stoichiometric ZnSe with a yield of over 97% can be produced by self-propagating high-temperature synthesis and that the resulting polycrystalline blocks have effective emissivity in the visible and near infrared spectra, making them promising for use in phosphor preparation. Figures 3; tables 2; references 7: 5 Russian, 2 Western.

### Photoluminescence of ZnSe/GaAs (100) Heterostructures

927D0068F Moscow IZVESTIYA AKADEMII NAUK SSSR: SERIYA NEORGANICHESKIYE MATERIALY in Russian Vol 27 No 12, Dec 91 pp 2520-2522

[Article by N.V. Bondar, A.V. Kovalenko, V.V. Tishchenko, A.Yu. Mekekechko, Dnepropetrovsk State University named after the 300th anniversary of the unification of Ukraine and Russia]

#### UDC 541.148

[Abstract] Chemical precipitation from the gaseous phase, epitaxy from organometallic compounds, and molecular beam epitaxy are the most promising methods of producing heterostructures; consequently, the effect of growth parameters (TRP) on the structure and photoluminescence spectra (FL) of epitaxial zinc selenide layers deposited on GaAs (100) substrates by the chemical gaseous phase precipitation method is studied. Multiply purified (by zone melting) ZnSe powder was vaporized in a quartz horizontal reactor in a purified hydrogen current. A 1 µm-thick cleaved ZnSe/GaAs (100) film was

examined by microphotography and reflection and photoluminescence spectra of two epitaxial ZnSe films on GaAs (100) substrates were plotted. As a result of the studies, bar charts characterizing the effect of the growth process parameters on the photoluminescence spectra of epitaxial ZnSe/GaAs (100) layers at a 300K temperature under ultraviolet excitation are plotted; the charts make it possible to identify the optimum growth parameters as being a 235-310°C temperature range and a carrier gas rate of 0.9-1.4 l/min. The exciton photoluminescence process is intensified under exposure to a He-Cd laser whose scattered radiation is aimed at the GaAs substrate. At a 4.2K temperature, only excitons are present in the ZnSe/GaAs photoluminescence spectra. Figures 3; references 8: 1 Russian; 7 Western.

## Eu<sub>2</sub>Ti<sub>2</sub>O<sub>7</sub> Phase Produced at High Pressures and Its Ferroelectric Properties

927D0068J Moscow IZVESTIYA AKADEMII NAUK SSSR: SERIYA NEORGANICHESKIYE MATERIALY in Russian Vol 27 No 12, Dec 91 pp 2597-2599

[Article by A.M. Sych, S.Yu. Stefanovich, Yu.A. Titov, T.N. Bondarenko, V.M. Melnik, Kiev State University imeni T.G. Shevchenko, Scientific Research Institute of Physical Chemistry imeni L.Ya. Karpov, and Institute of Materials Science Problems at the USSR Academy of Sciences]

#### UDC 548.312.3

[Abstract] The ability of titanates of rare earth elements (r.z.e.) to crystallize as two modifications, pyrochlore (PKh) and flaky perovskite-like structures (SLPS) with a polar symmetry, is discussed and an attempt is made to produce an individual high-pressure phase (f.v.d.) of Eu<sub>2</sub>Ti<sub>2</sub>O<sub>7</sub> with a flaky perovskite-like structure and investigate its ferroelectric properties. Eu<sub>2</sub>Ti<sub>2</sub>O<sub>7</sub> with a pyrochlore structure was converted to a polar modification by a two-stage treatment at a 3-4 GPa pressure and a 298K temperature and 8 x 10<sup>9</sup> Pa pressure at a 2,020K temperature. A radiographic analysis demonstrates that the high-pressure phase of Eu<sub>2</sub>Ti<sub>2</sub>O<sub>7</sub> with a flaky perovskite-like structure is crystallized in a monoclinic syngony. The temperature dependence of the relative second harmonic generation signal strength of high-pressure phases is examined; it is shown that the phase transition in the ferroelectric high-pressure phase of Eu<sub>2</sub>Ti<sub>2</sub>O<sub>7</sub> with a flaky perovskite-like structure is similar to the secondkind phase transition. The linear character of the second harmonic signal strength as a function of temperature is characteristic of intrinsic ferroelectrics near the phase transition. Eu<sub>2</sub>Ti<sub>2</sub>O<sub>7</sub> has a Curie temperature of close to 1,520K and a spontaneous polarization of 2.7 µCl/cm<sup>2</sup>. Figures 1; references 7: 5 Russian; 2 Western.

# Growing of Single Crystals of CuI and Its Certain Properties

927D0068K Moscow IZVESTIYA AKADEMII NAUK SSSR: SERIYA NEORGANICHESKIYE MATERIALY in Russian Vol 27 No 12, Dec 91 pp 2624-2628

[Article by V.I. Popolitov, Crystallography Institute imeni A.V. Shubnikov at the USSR Academy of Sciences]

#### **UDC 542.65**

[Abstract] The changes in the structure and lattice constants of copper monoiodide single crystals with an increase in temperature whereby the cubic lattice of the γ-phase is reordered into a wurtzite-type lattice of the β-phase, then again becomes cubic while the hightemperature CuI a-phase has a superionic conduction, are investigated and the solubility of copper iodide in aqueous solutions of HI is examined in a 200-300°C temperature range at a constant 5.05 x 10<sup>7</sup> Pa pressure. The dependence of the single crystals of copper iodide on the HI concentration at various temperatures, the dependence of the solubility logarithm of the copper iodide crystals on the inverse value of temperature at various concentrations of HI, the dependence of the (111) face growth rate of CuI single crystals on the HI concentration at various temperature gradients, the exciton reflection spectra of CuI single crystals under optimum and nonoptimum conditions, and CuI single crystal photoluminescence spectra are plotted. An analysis reveals the following optimum growth conditions of the principal tetrahedral face of CuI single crystals: an HI concentration of 32-25% by mass, a temperature of 230-270°C, and a temperature drop of 25-30°. The dependence of the growth rate of the fast growing tetrahedral (111) face on the HI concentration and temperature is exponential, and linear on the temperature drop. Figures 5; references

# Growing of MgGa<sub>2</sub>S<sub>4</sub> Single Crystals and Their Photoelectric Properties

927D0068O Moscow IZVESTIYA AKADEMII NAUK SSSR: SERIYA NEORGANICHESKIYE MATERIALY in Russian Vol 27 No 12, Dec 91 pp 2655-2656

[Article by N.A. Moldovin, Applied Physics Institute at the Moldova Academy of Sciences]

#### UDC 546.784'231

[Abstract] The issue of developing detectors with a spectral response in the ultraviolet (UF) band for solid-state photoelectronics applications is addressed and an attempt to grow MgGa<sub>2</sub>S<sub>4</sub> single crystals and examine their photoelectric properties is described. The single crystals were produced in a closed system by the method of iodide chemical transport with preliminary fusion of a charge of elementary components taken in a stoichiometric ratio. The photoconduction and transmission

spectra of  $MgGa_2S_4$  and  $MgAl_{0.2}Ga_{1.8}S_4$  crystals are investigated and plotted. The photoconduction mechanism which determines the position of the red photoelectric threshold is examined and the limit of aluminum atom concentration at which the  $MgAl_xGa_{2-x}S_4$  single crystal stability is maintained under exposure to moisture and air is established. It is demonstrated that  $MgGa_2S_4$  crystals are characterized by considerable photosensitivity to ultraviolet radiation and their photoconduction is intrinsic in origin. This compound's forbidden gap width is found to be equal to  $E_g = 3.4$  eV at a 300K temperature. Figures 1; references 4: 3 Russian, 1 Western.

### Production of Promising Types of Metal Products by Continuous Horizontal Two-Sided Casting Method

927D0061C Moscow STAL in Russian No 12, Dec 91 pp 16-17

[Article by V.M. Sinitskiy, A.I. Mayorov, L.P. Zakov, M.V. Panin, M.D. Zharnitskiy, All-Union Science Research Institute of Metallurgical Machine-Building]

#### UDC 621.746.27.047

[Abstract] The advantages of two-sided continuous horizontal casting are outlined and recent development in the field of making thin steel slabs by this method are discussed; the principal factors affecting the stability of the casting process and products are examined. The microstructure of a thin slab cast from transformer steel and the microstructure of bimetal produced by this method are investigated. The process makes it possible to cast 40-50 mm steel slabs and two-layered clad metal billets with a 1:2.5 ratio of base metal to cladding in a continuous casting machine (MNLZ); the method also makes it possible to expand the range of slab brands and dimensions, including those from electrical sheet and transformer steel with a 3% silicon content and corrosion resistant steel. Studies demonstrate the good ductility of the resulting slabs. The use of the method is especially efficient at small-scale metal works and other specialty steel plants. Figures 2; references 3.

# Correcting Titanium Content Within Narrow Range in Continuous Casting Machine During Pipe Steel Making

927D0061D Moscow STAL in Russian No 12, Dec 91 pp 18-19

[Article by A.I. Trotsan, B.F. Belov, V.M. Dolgan, D.Yu. Levin, O.V. Nosochenko, G.A. Nikolayev, Mechanics Problems Institute at the Ukrainian Academy of Sciences, Central Scientific Research Institute of Ferrous Metallurgy, and Azovstal Integrated Iron and Steel Works]

UDC 621.746.27.047

[Abstract] A method to correct the titanium concentration in pipe steel 09G2BT and 10G2BT within a narrow range of 0.05-0.09 and 0.07-0.09% Ti, respectively during the steel-making process by adding powder wire to the intermediate ladle in the continuous casting machine (MNLZ) is discussed and the titanium powder wire addition conditions are summarized allowing for the titanium composition in the ready product and its mean loss in the refining unit (UDM). For comparison, the titanium concentration in steel after its treatment with FeTi in the refining machine ladle and by adding titanium powder wire to a conventional intermediate ladle is tabulated and the method of correcting the titanium concentration in tube steel by adding titanium wire is summarized. An analysis shows that the titanium concentration in pipe steel 09G2BT and 10G2BT decreases by 0.01% during its exposure in the ladle and during continuous casting; an addition of titanium powder wire to the intermediate ladle ensures a uniform titanium distribution throughout the slab length where titanium assimilation reaches 70-75%. It is shown that in correcting the titanium concentration, powder wire should be added at a differentiated rate of 0.9 of the optimum in the beginning, 1.0 in the middle, and 1.1 at the end of the process. Tables 3.

## **Conductive Electromagnetic Metal Stirring During Continuous Slab Casting**

927D0061E Moscow STAL in Russian No 12, Dec 91 pp 21-24

[Article by V.M. Niskovskikh, A.A. Smirnov, V.V. Ryabov, V.P. Klak, Z.K. Kabakov, A.V. Larin, V.G. Dorofeyev, Uralmash Production Association, Central Scientific Research Institute of Ferrous Metallurgy, Novolipetsk Integrated Iron and Steel Works, and All-Union Scientific Research Institute of Metallurgical Technology]

#### UDC 621.746.638.047

[Abstract] The use of inductive methods of electromagnetic stirring (EMP) in order to improve the surface quality and internal structure of cast metal and thus expand the range of brands and dimensions of products made in continuous casting machines (MNLZ) and their shortcomings—primarily high energy outlays and the need for expensive equipment—are discussed and a new conductive electromagnetic stirring method (KEMP) which is free of these shortcomings is introduced. The feasibility study, development, and physical modeling were performed by Yu.A. Samoylovich at the All-Union Scientific Research Institute of Metallurgical Technology. The design of a unit for conductive electromagnetic stirring of metal in continuous casting machines and the microstructure of samples from steel Stsp produced with and without conductive electromagnetic stirring are presented. The distribution of nonmetallic inclusions in carbon and low alloyed steel cast with and

without conductive electromagnetic stirring as well as the temperature fields and flow structure in the slab's liquid core during the metal solidification with and without conductive electromagnetic stirring are plotted. The power required by the conductive electromagnetic stirring is 140-160 kW, which is lower than that of the inductive method by five- to sixfold. Full-scale tests show that the conductive electromagnetic stirring method makes it possible to expand the equiaxial crystal zone by 40-50% and decrease the amount of nonmetallic inclusions by 30-40%. Figures 5; references 5.

### Amorphous Precision Alloys: Technology, Properties, Applications

927D0061J Moscow STAL in Russian No 12, Dec 91 p 71-70

[Article by A.M. Glezer, A.G. Kozlov, Central Scientific Research Institute of Ferrous Metallurgy]

[Abstract] The fifth all-union conference organized by the Engineering Center of Amorphous and Microcrystalline Materials at the Central Scientific Research Institute of Ferrous Metallurgy was held in Rostov Velikiy on 23-27 September 1991 and attracted close to 200 experts from the USSR as well as Bulgaria, Hungary, mainland China, Lithuania, Vietnam, Germany, and France. The conference addressed the issues of production processes, properties and structure, and applications of amorphous and microcrystalline materials. The effect of the melt state on the quality and properties and amorphous alloy strips was featured in a number of reports; considerable attention was focused on the problem of producing microcrystalline materials by rapid quenching in rollers. The use of nontraditional methods for producing amorphous and microcrystalline alloys was discussed. In addition to engineering problems, the issue of decreasing the cost of amorphous alloys was addressed. Several reports dealt with the issue of using amorphous alloys as magnetic, brazing structural, and corrosion-resistant materials. A new class of soft magnetic materials was discussed. The next conference is expected to be held in

Method of Making Wire From Low-Carbon Steel 927D0061G Moscow STAL in Russian No 12, Dec 91 pp 56-57

[Article by V.Ya. Chinokalov, V.P. Kolpak, V.Z. Smakotina, L.M. Poltoratskiy, Western Siberian Integrated Iron and Steel Works and Eastern Branch of the Ferrous Metallurgy Institute]

UDC 621.778.1:621.785.1

[Abstract] The shortcomings of process annealing of wires for cold upsetting are discussed and the results of studies to improve the technology of wire production

according to GOST 5663—79 from steel 10 and 20, which involves drawing to size with subsequent low-temperature annealing, are presented. The microstructure of a wire rod from steel 20 and of wire after annealing with different degrees of straining are examined and the dependence of the mechanical characteristics of wires from steel 10 and 20 on the degree of strain (i.e., percent reduction of area) and annealing temperature is plotted. Certification tests reveal the stability of

the wires' mechanical properties from batch to batch and the uniformity of their length; the mean values of ultimate strength, percent reduction of area, and cold upsetting are 550 N/mm², 67%, and 72%, respectively. The use of the new process makes it possible to produce wire with the requisite quality and increase its output by 20%. The economic impact from its implementation in a steel wire plant is close to 400,000 rubles per year. Figures 4; references 1.

### The Effect of Cycling on the Crack Formation of Austenite Chromium Manganese Steel Intended for Use in a Controlled Thermonuclear Reactor

927D0049K Moscow FIZIKA I KHIMIYA OBRABOTKI MATERIALOV in Russian No 3, May-Jun 91 (manuscript received 14 May 90) pp 135-139

[Article by S.Ye. Gurevich, Ye.V. Demina, L.D. Yedidovich, and M.D. Prusakova, Moscow]

UDC 669.018.6:539.43

[Abstract] The authors of the study examined the cyclic crack resistance of Cr12Mn14Ni4AlMo austenite chromium-manganese low-nickel steel in five versions. The five versions of Cr12Mn14Ni4AlMo steel studied differed from one another with respect to boron, cerium, and scandium content. The test steels were smelted by the method of open induction melting by using the conventional charge materials. Cerium and boron were added to the melt after it had been killed. They were added in form of ferrocerium and ferroboron. The scandium was added in its metallic form directly to the stream of molten metal as it was poured into the ladle. The resultant ingots (weight, 150 kg) were subjected to hot and cold rolling into sheets 1.5 mm thick under standard plant conditions. Cyclic crack resistance was studied at room temperature, and the mechanical properties of the five versions of the steel were determined in specimens with a working section 22 mm long and 3 mm wide. When subjected to static stretching, all of the specimens had very similar mechanical properties. The steel with the greatest cyclic crack resistance (both in a work-hardened state and after annealing) had the following chemical composition (% by weight): Sc, 0.15; C, 0.055; Si, 0.67; Mn, 13.8; Cr, 12.3; Mo, 0.45; Ni, 4.32; and Al, 1.31. In general, additions of scandium to the basic steel composition were found to increase cyclic crack resistance. Adding extra scandium in place of boron was found to reduce the threshold amplitude of the stress intensity coefficient ( $\Delta K_{th}$ ) and the actual amplitude of the stress intensity coefficient ( $\Delta K_a$ ). Combining scandium and boron was found to reduce  $\Delta K_{th}$ somewhat but did not have any negative effect on  $\Delta K_a$ . Replacing boron by scandium when cerium was present did not increase resistance to the formation and growth of fatigue cracks. The reduction in  $\Delta K_a$  and  $\Delta K_{th}$ amounted to 11.0-12.7% for material in its shipped state and 11.7-12.7% after annealing. Cold deformation of Cr12Mn14Ni4AlMo steel in the amount of 10% was found to have a positive effect on cyclic crack resistance: it increased the amplitude and threshold amplitude of the stress intensity coefficient and noticeably reduced the rate of fatigue crack formation. Figures 4, tables 4; references 7: 4 Russian, 3 Western.

## Structural Changes in Polycrystalline Scandium Oxide Upon Ion Irradiation

927D0089A Moscow FIZIKA I KHIMIYA
OBRABOTKI MATERIALOV in Russian No 6,
Nov-Dec 91 (manuscript received 14 May 90) pp 5-11

[Article by A.Ye. Solovyeva, E.M. Diasamidze, V.L. Markov, Sukhumi]

#### UDC 661.863.1:620.181.001.5

[Abstract] The authors of the study examined the structural changes occurring in polycrystalline scandium oxide after irradiation by Xe<sup>+</sup> ions at an energy up to 300 keV. Polycrystalline test specimens were prepared from type OS-99.9 Sc<sub>2</sub>O<sub>3</sub> powder in accordance with a method described elsewhere and then annealed at 1.800° in a vacuum (holding time, 5 hours) and oxidized at 1,400° in air until a constant weight was achieved. The specimens prepared for the irradiation represented a mixture of two phases—an ordered phase and a type C disordered phase as described elsewhere. Ion irradiation was found to result in an alteration of the scandium oxide's chemical composition that was accompanied by phase transformations. After irradiation, the specimens' cubic structure was found to contain macro- and microstresses that were highly dependent on irradiation energy. An increase in the relative integral intensity of the specimens' reflecting planes was observed, with the maximal values recorded at a depth of 3 to 4.6 µm (which is connected with a change in the atoms' electron density). Analysis of the change in free energy of the processes of the reduction of scandium oxide after irradiation by Xe+ ions revealed that after ion irradiation in the amount of 140 keV, the free energy changes with an amplitude that becomes weaker deeper into the specimen until a depth of 3.5 µm (in the interval from 3.5 to 6 µm the lines virtually disappeared). Irradiation at an energy of 300 keV was found to result in small fluctuations of free energy to a specimen depth of 3 um. Figures 6, table 1; references 15: 11 Russian, 4 Western.

# The Erosion of Quartz Under the Effect of High-Power Nanosecond Ion Beams

927D0089C Moscow FIZIKA I KHIMIYA OBRABOTKI MATERIALOV in Russian No 6, Nov-Dec 91 (manuscript received 29 Jan 91) pp 25-32

[Article by V.P. Krivobokov, O.V. Pashchenko, G.A. Sapulskaya, and B.P. Stepanov, Tomsk]

### UDC 537.534.9:621.785.5

[Abstract] The authors of the study performed a series of calculations to establish the erosion kinetics and phase transformations of quartz surfaces irradiated by high-power nanosecond ion beams. The calculations established that nanosecond beams of accelerated ions in the energy interval studied cause intensive erosion of quartz surfaces due to vaporization. The erosion coefficient was

three to four orders of magnitude greater than the sputtering coefficient as a result of scattering of the accelerated ions on the atoms of the lattice. When a quartz surface is irradiated in a close-to-optimal mode, it is possible to achieve a minimal β-phase layer thickness (i.e., a thickness not exceeding several lengths of the projective run of the accelerated ions). The optimal ion energy values were found to range from 0.5 to 2 MeV, the optimal current density was found to lie between 100 and 1,000 A/cm<sup>2</sup>, and the optimal pulse duration was determined to be between 100 and 200 ns. Irradiation of polished quartz surfaces by a high-power nanosecond ion beam was found to have no detrimental effects on surface relief and, in some cases, even improved it. The researchers proposed a thermal erosion model that adequately describes the vaporization of silicon dioxide molecules and phase transformation kinetics occurring in irradiated quartz. Figures 5; references 9: 5 Russian, 4 Western.

# Sets of Radiation Effect Functions in the Problem of Predicting the Stability of Materials and Instruments in Ionizing Radiation Fields

927D0089D Moscow FIZIKA I KHIMIYA OBRABOTKI MATERIALOV in Russian No 6, Nov-Dec 91 (manuscript received 14 May 90) pp 33-38

[Article by V.I. Ostroumov, G.G. Solovyev, and A.I. Trufanov, Irkutsk, Moscow, and Leningrad]

#### UDC 539.1.043

[Abstract] Several approaches have been taken to the problem of predicting the damage inflicted on different materials and equipment subjected to ionizing radiation fields such as those existing in outer space. One such approach is based on the concept of the radiation effect function. The concept of the radiation effect function is in turn based on the assumption that in a material whose primary damage mechanism is one of shock damage, the first atoms knocked off by bombarding particles that possess an identical energy contribute identically to the ensuing changes in the given substance's properties. Although the approach does have its limitations, it has been used as a framework for examining all types of ionizing radiation (including electron, positron, gammaquantum, proton, neutron, etc.) with an arbitrary energy distribution. The authors of the study examined the possibility of expanding the set of problems that may be solved by using a previously developed method of predicting the degradation of the electrophysical parameters of materials and equipment based on the concept of a radiation effect function. They focused their analysis on the problems of giving adequate consideration to the effect of fluence and the intensity of irradiation. Their analysis led them to conclude that the radiation effect function approach to predicting radiation stability may be extended to the solution of most problems concerned with damage sustained by materials and equipment in ionizing radiation fields. Specifically, they concluded that the approach is valid in such practically important problems as problems in which materials are subjected to extensive variations in fluence and bombarding particle flux density or else to simultaneous irradiation by several types of particles. The analysis presented further demonstrated that radiation effect functions may be reconstructed on the basis of data from independent ground experiments on readily accessible and economical testing units. Figure 1; references 11 (Russian).

# The Effect of γ- and Electron Irradiation on the Optical Properties of Barium-Sodium-Niobate (Ba<sub>2</sub>NaNb<sub>5</sub>O<sub>15</sub>) Crystals

927D0089E Moscow FIZIKA I KHIMIYA OBRABOTKI MATERIALOV in Russian No 6, Nov-Dec 91 (manuscript received 15 May 90) pp 39-42

[Article by S.A. Baryshev, G.A. Yermakov, V.N. Karasev, V.P. Nosov, and S.V. Protasova, Moscow]

#### UDC 535/34:621

[Abstract] The authors of the study examined the effect of electron and γ-irradiation on the process of the twinning of Ba<sub>2</sub>NaNb<sub>5</sub>O<sub>15</sub> crystals and on the magnitude of the optical loss coefficient (K) in crystals at the wavelength of a neodymium laser (1,064 nm). Ba<sub>2</sub>NaNb<sub>5</sub>O<sub>15</sub> crystals in the form of parallelepipeds measuring 12 x 5.0 x 3.5 mm along the X, Y, and Z axes were grown by the Czochralski method. They were irradiated with a γ-quantum in the amount of 1.25 MeV. During the irradiation, the specimens' temperature did not exceed 30°C. The irradiated specimens then underwent a twinning process that included heating to a temperature of 260-300°C, holding at the said temperature under a load applied perpendicular to the (100) plane of a tetragonal crystal cell, and cooling (also under a load) to room temperature. Nonirradiated control specimens were subjected to the same twinning regimen. Both before and after the twinning, the researchers measured the test and control specimens' refractivity gradient ( $\Delta n$ ) along the direction (010) at  $\lambda = 632.8$  nm and the transmission coefficients at the wavelengths  $\lambda$  = 532 and 1,064 nm. Preliminary γ-irradiation of the Ba<sub>2</sub>NaNb<sub>5</sub>O<sub>15</sub> crystals was found to have a significant effect on their twinning process. The refractivity gradient of the irradiated crystals after twinning did not exceed 10<sup>-5</sup>, whereas that of the nonirradiated crystals was between 10-4 and 10-5. Notably, the period for which the irradiated crystals were held under a load was much shorter (by a factor of 3 to 5). The measurements of the transmission coefficient at  $\lambda = 532.8$  nm revealed that preliminary γ-irradiation followed by thermomechanical treatment resulted in a 10% reduction in the Ba<sub>2</sub>NaNb<sub>5</sub>O<sub>15</sub> crystals' optical sensitivity to irradiation in the dose range from 10<sup>2</sup> to 10<sup>6</sup> Gy. The same effect was achieved by heat treatment in air at 650°C for 5 to 15 hours. The transmission coefficients of both the test and control specimens measured at  $\lambda = 1,064$  nm remained virtually unchanged from their starting values.

 $\gamma$ -Irradiation of Ba<sub>2</sub>NaNb<sub>5</sub>O<sub>15</sub> crystals in doses from 50 to  $10^5$  Gy made it possible to reduce the mechanical load placed on them during the twinning process by a factor of 2 to 3. Figure 1, table 1; references 12: 10 Russian, 2 Western.

### The Properties and Use of Uranium Fluoride Plasma

927D0089H Moscow FIZIKA I KHIMIYA
OBRABOTKI MATERIALOV in Russian No 6,
Nov-Dec 91 (manuscript received 20 Mar 91) pp 66-72

[Article by Yu.N. Tumanov and K.V. Tsirelnikov, Moscow]

#### UDC 621.039.61:669.822

[Abstract] The authors of the study examined the physicochemical processes occurring in uranium fluoride plasma and in uranium hexafluoride at high temperatures. Specifically, they attempted to systematize existing information on the properties of uranium fluoride plasma with respect to chemical and metallurgy applications related to the fuel elements of nuclear reactors. First, they describe the thermal dissociation of uranium hexafluoride and the formation of uranium fluoride plasma in terms of a set of 10 equations. After analyzing available data on the properties of uranium fluoride plasma, they conclude the following: 1) as the number of fluorine ligands in UF<sub>n</sub> molecules decreases, the average bond energy increases and the volatility of the compound decreases (this applies to stable uranium fluorides such as UF<sub>6</sub>, UF<sub>5</sub>, UF<sub>4</sub>, and UF<sub>3</sub>); 2) if dissociation of UF<sub>6</sub> occurs in nonisothermal plasma, then condensation of weakly volatile fragments of UF<sub>6</sub> and recombination of the volatile fluorides UF<sub>6</sub> and UF<sub>5</sub> may occur in segments of a plasma zone with a reduced neutral particle temperature (such as in the plasma located near a reactor wall); and 3) at atmospheric temperature, uranium hexafluoride begins noticeable dissociation at temperatures of about 1,850 K, and increasing the pressure shifts these maxima to the range of higher temperatures. After examining existing information regarding the electrical conduction of uranium fluoride plasma, the authors conclude that it is comparatively low at temperatures below 6,000 K because of the adhesion of electrons to the fluorine atoms and the formation of F' ions, thanks to which the contribution of ions to total electric conduction is greater than that of electrons at the said temperatures; at higher temperatures, the ion concentration decreases, and the contribution of electron conduction increases. The available information regarding the formation kinetics of uranium fluoride plasma enabled the authors to describe the destruction of UF<sub>6</sub> molecules and their fragments in terms of a Lindemann scheme and to present an equation describing complex multiatomic molecules with high bond-breaking energies. They used these equations

to calculate the rate constants of the reactions of the decomposition of  $UF_6$  to  $UF_5 + F$ ,  $UF_5$  to  $UF_4 + F$ , and so on down to  $UF \rightarrow U + F$ . These rate constants are presented in table form for temperatures from 1,000 to 6,000 K, inclusively. Figures 3, tables 2; references 16: 8 Russian, 8 Western.

An Experimental Investigation of the Discharge Occurring During the Effect of Continuous-Wave Radio-Frequency Radiation on Dielectric Materials

927D0089J Moscow FIZIKA I KHIMIYA OBRABOTKI MATERIALOV in Russian No 6, Nov-Dec 91 (manuscript received 16 May 90) pp 107-112

[Article by Yu.V. Bykov, A.G. Yeremeyev, and A.A. Sorokin, Gorkiy]

#### UDC 536.2

[Abstract] The authors of the study conducted a series of experiments to establish the mechanism of the formation and burning of a near-surface radio-frequency [RF] discharge during the treatment of dielectric materials with continuous-wave radiation. A gyrotron with a power output of about 5 kW at a wavelength of 3 mm operating in a mode of controlled pulse durations (from 1 second to 15 minutes) was used as the radiation source. Two groups of materials were used to test the authors' hypothesis that the discharge formation process would conform to a vaporization model: comparatively weakly absorbing dielectrics (steatite ceramic, electrovacuum glass, pyroceram) and dielectrics with a high absorption coefficient (textolite and chamotte). A nozzle providing air speeds up to about 10<sup>4</sup> cm/s was used. The threshold values found for the intensity of RF radiation at which a discharge occurs close to a dielectric surface heated by air at atmospheric pressure were around 10<sup>3</sup> W/cm<sup>2</sup>. The said values differed by more than three orders of magnitude from the intensities corresponding to the breakdown of air in a free space. A similar significant reduction in intensities corresponding to the occurrence of a breakdown (disruptive discharge) have also been observed when solids are subjected to laser irradiation. The experiments confirmed that the discharge formation process studied does indeed conform to a vaporization model. The discharge was determined to have a quasiequilibrium nature, the plasma temperature was between 3,000 and 4,000 K, and the electron concentration amounted to about 1013/cm3. The authors also determined the parameter that a gas stream lengthwise to the irradiated surface must have in order to ensure the absence of a discharge at radiation intensities of about 5 x 10<sup>3</sup> W/cm<sup>2</sup> or less. Figures 2, table 1; references 10: 9 Russian, 1 Western.

### Substantiating the Hydrogenation Absorption Regimens of Titanium Alloys To Improve Their Machinability

927D0090G Ordzhonikidze IZVESTIYA VYSSHIKH UCHEBNYKH ZAVEDENIY: TSVETNAYA METALLURGIYA in Russian No 2, Apr 91 (manuscript received 21 May 90) pp 90-94

[Article by B.A. Kolachev, Yu.B. Yegorova, V.I. Sedov, and A.N. Kravchenko, Department of Metal Science and Hot Metal Working, Moscow Aviation Technology Institute]

### UDC 669.295.017:669.788

[Abstract] The authors of the study reported herein compared different hydrogen absorption regimens in order to find the best way of adding hydrogen to titanium alloys and thus make them easier to machine. Electrolytic hydrogen absorption regimens were found to have two principal shortcomings: At room temperature, hydrogen only penetrates titanium alloys to a depth on the order of hundreds of fractions of a millimeter at concentrations that are sufficient to cause surface flaking and the formation of titanium hydrides, and distribution of the absorbed hydrogen throughout the treated blank's cross section is very uneven. Adding hydrogen to ingots is another option, but it has proved to be more complicated than the process of adding hydrogen to solid metal. As an alternative, the researchers investigated hydrogen

absorption in a hydrogen gas medium. Specifically, they calculated the distribution of hydrogen throughout the cross sections of cylindrical blanks made of the titanium alloys VT6 and VT3-1 with a radius of 30 mm after hydrogen absorption at 700, 800, and 900°C for different amounts of time. Even distributions were only obtained after rather long holding times (35 hours). The studies further revealed that achieving hydrogen absorption throughout titanium alloy layers commensurate with machining depths requires creating a hydrogen concentration gradient by varying the duration of hydrogen absorption and the rate at which a blank is cooled. On the basis of their experiments, the researchers worked out optimal hydrogen absorption regimens for blanks made of the following titanium alloys: VT5-1, VT6, VT8 and VT25, VT3-1, and VT20. A table detailing the hydrogen absorption times and temperatures for different-diameter blanks of each of the aforesaid alloys is presented. The researchers recommended that the hydrogen absorption guidelines be used with intermediate products whose thicknesses (diameter) do not exceed 60 to 80 mm so that the duration of hydrogen absorption required does not exceed 6 to 8 hours and thus become impracticable. In cases where these thicknesses (diameters) are exceeded, the researchers recommended hydrogen absorption of just surface layers inasmuch as machining allowances do not generally exceed 10 to 15 mm. They conclude by stating that the most effective method of adding hydrogen is hydrogen absorption during the melting process but that much more research is required before the technique can be used. Figures 4, tables 2; references 4 (Russian).

### The Problem of Creating an Integrated Technology To Reprocess Platinum-Bearing Chromatites—A New Mineral Ore Containing Platinum Metals

927D0090D Ordzhonikidze IZVESTIYA VYSSHIKH UCHEBNYKH ZAVEDENIY: TSVETNAYA METALLURGIYA in Russian No 2, Apr 91 (manuscript received 21 Aug 90) pp 17-24

[Article by L.V. Razin, T.N. Greyver, O.N. Tikhonov, S.A. Gladkov, and T.A. Kozyreva (deceased), Moscow Geological Prospecting Institute and Leningrad Mining Institute]

UDC 669.23

[Abstract] The authors of the study reported herein worked to develop a profitable technology for integrated reprocessing of platinum-bearing chromatites, which are likely to be the main industrial mineral source of platinum metals in the next 10 to 20 years. As an experimental model they selected laboratory and commercial samples of chromatites from rock masses located in the Aldan craton that are similar to the Ural type. Along with platinum-group elements, the samples were also found to contain small amounts of gold and silver, up to 0.1-0.3% (by mass) Ni and Cu, up to 0.1-0.2% (by mass) Co, up to 1% Ti and Mn, up to 20% Fe, up to 8% Al, up to 12% Mg, and up to 25% Si. After reviewing existing literature on the reprocessing of platinum-containing chromatites, the researchers decided to base their new process on gravitation methods. They developed a process entailing disintegration by crushing, followed by sieve separation of the disintegration products by grain size. Both the fine and coarse fractions were subjected to enrichment on a concentration table, and the coarse fraction was also subjected to magnetic separation and special enrichment. The initial experiments revealed that combining magnetic and gravitation enrichment methods does not result in significant extraction of platinum-group elements into the concentrate. Further experiments were conducted to refine the new process. On the basis of the studies performed, the authors recommended the following regimen for breaking down chromospinelide concentrates: temperature, 160°C; duration, 4 hours; CrO<sub>3</sub> flow rate, 30% of the chromium content in the sample; and grist size, 74 µm. The said process parameters resulted in good recovery of chromium and iron, platinum-group elements, and gold and silver. The noble metals were then concentrated in the form of a rich product that was transferred to an insoluble residue that may in turn be reprocessed at a special enterprise. The chromium in the process solutions was extracted in accordance with the standard process. Figures 3, tables 2; references 6: 4 Russian, 2 Western.

## Operation of the Nonreturn Valve in a Separator for Regenerating Magnetic Fluids

927D0090C Ordzhonikidze IZVESTIYA VYSSHIKH UCHEBNYKH ZAVEDENIY: TSVETNAYA METALLURGIYA in Russian No 2, Apr 91 (manuscript received 20 Aug 90) pp 14-17

[Article by V.N. Gubarevich and S.V. Vidsota, State Scientific Research and Design Institute of Coal Enrichment Equipment]

#### UDC 622.778.002.5

[Abstract] A new magnetic separator has been developed for use in recovering the magnetic fluid used in processes of enriching materials in magnetic fluid. The new separator consists of an electromagnetic with polar terminals that form a nonuniform magnetic field. A working chamber is located in the gap between the poles. Mounted to the chamber bottom is a nonreturn valve intended to automatically drain the magnetic fluid as it accumulates in the working chamber during the regeneration process. The nonreturn valve is simple in design: It consists of a weight made of a nonmagnetic material connected by a rod to a separator that covers the drain line. In the valve's working mode, the drain line is covered by the separator under the effect of the weight. As the emulsion moves along the working chamber, droplets of magnetic fluid are extracted from it under the effect of magnetic force as they accumulate up to the top level of the weight. The weight of the material floats up. thus opening the drain line to allow free drainage of the accumulated magnetic fluid. When the fluid level drops under the effect of the weight through the rod, the separator closes the drain line once again. The valve's operation is based on two nearly identical competing forces: the upward-directed Archimedian force of the weight pushing outward and the force of the pressure of the column of magnetic fluid on the upper surface of the separator. The authors of the study reported herein calculate these opposing forces and derive an expression for use in optimizing the new nonreturn valve's design and selecting its geometric parameters. Figures 3.

### An Analytic Method of Calculating the Parameters of the Magnetic Field in the Live Zone of a Magnetic-Gravitation Separator Based on Permanent Magnets

927D0090B Ordzhonikidze IZVESTIYA VYSSHIKH UCHEBNYKH ZAVEDENIY: TSVETNAYA METALLURGIYA in Russian No 2, Apr 91 (manuscript received 5 Jul 90) pp 5-10

[Article by A.B. Solodenko, Useful Minerals Enrichment Department, Northern Caucuses Mining and Metallurgy Institute]

UDC 622.778.002.5

[Abstract] Calculating the design parameters of a magnetic-gravitation [MG] separator based on permanent

magnets and the process indicators of a magnetic separation process requires knowing the nature of the change in the key parameters of the magnetic field in the separator's live zone. Analytic methods of describing the said parameters by proceeding from the condition of the equipotentiality of the poles' surface is available for use with electromagnetic magnetic-gravitation separators. This condition of equipotentiality is violated in magnetic systems consisting of flat permanent magnets because the force lines in such cases are not at a 90° angle to the pole surface. A new method of calculating the distribution of magnetic potential in a system of permanent magnets has been developed to allow for the force lines that occur when flat permanent magnets are used. The new method is based on the familiar method of mirror representations and is modified to allow for two additional assumptions. These assumptions are as follows: 1) the opposing magnetic circuit planes do not distort the permanent magnets' field, and 2) the magnetic circuit has a resistance of zero. An analytical description of a system of two magnets located in a homogeneous medium with a magnetic permeability of  $\mu_0$  is then derived by using the concept of complex magnetic potential. To estimate the error of their new method, the researchers tested it on physical models of magnetic systems using KSP-37 permanent magnets with an induction of 0.1 T on the central part of their surface. The new method proved to be highly reliable in describing the magnetic field in the interpolar gap of a system consisting of flat permanent magnets. The new method was deemed effective for quickly determining the optimal magnet dimensions and distance and angle of the gap between the two magnetis in both wedgeshaped and plane open systems. The new method has been used to develop a number of flat permanent magnet-based magnetic-gravitation separators that are being used successfully to enrich gold-containing microsections. Figures 5; references 2 (Russian).

### The Effect of pH on the State of Fatty Acid Collectors of Heavy Metal Ions in Solutions

927D0090A Ordzhonikidze IZVESTIYA VYSSHIKH UCHEBNYKH ZAVEDENIY: TSVETNAYA METALLURGIYA in Russian No 2, Apr 91 (manuscript received 28 Aug 90) pp 2-5

[Article by L.D. Skrylev, V.F. Sazonova, T.L. Skryleva, and Ye.A. Yakhova, Physical and Colloidal Chemistry Department, Odessa State University]

UDC 622.765:541.183

[Abstract] The authors of the study reported herein performed a mathematical analysis demonstrating that a quantitative link between the pH of aqueous solutions of alkaline metal soaps and their critical concentration of micelle formation may be easily established by considering the process of micelle formation from the principles of phase equilibrium and by assuming that the "solubility product" concept is applicable to micelles of soaps. They presented both calculated and experimental data confirming that there is a straightline dependence (with a slope of ½ to the abscissa) existing between the log of the critical concentration of micelle formation of alkaline metal soaps and the pH of their solutions within the range of pH values ensuring adequate stability of the soap micelles and meeting the requirement that [H<sup>+</sup>] >> K<sub>c</sub> (K<sub>c</sub>) being the total concentration of RCOO ions and RCOOH molecules in a saturated soap solution. This finding led them to further hypothesize that when [H<sup>+</sup>] >> K<sub>c</sub> still holds true but the micelle solution also contains fatty acids, the dependence between pH and the log of the critical concentration of micelle formation will be described by an equation represented by a straight line with a slope of 1 to the abscissa. This did not turn out to be the case, however. Instead, the critical concentration of micelle formation remained virtually unchanged as the pH changed. This led the authors to hypothesize that in media with a rather high concentration of hydrogen ions, the dissociation of fatty acids is essentially completely suppressed, and the critical concentration of micelle formation of fatty acids is in fact not dependent on the pH of the medium. The studies performed thus led the researchers to conclude that the colloid-chemical state of fatty acid ion collectors of heavy metals in a solution (which by and large determines their technological characteristics) depends on the pH of the solution. They further concluded that when the solution's pH drops below a certain limit (as determined by the nature of the collector) there is a marked decrease in the collector's critical concentration of micelle formation that in turn has an adverse impact on its effectiveness. Figures 2; references 10 (Russian).

### Learning To Use the First Domestically Manufactured Ladle Furnace

927D0016A Kiev PROBLEMY SPETSIALNOY ELEKTROMETALLURGII in Russian No 4, 91 pp 74-76

[Abstract of article by V. P. Denisenko, Yu. A. Koval, A. Z. Shevtsov, K. P. Verbitskiy, and S. S. Kazakov]

UDC 669.187.56.001.6

[Abstract] The Dneprospetsstal steelworks has designed and manufactured the first domestically produced ladle furnace, which was jointly put into operation by Dneprospetsstal and the Ukrainian Scientific Research Institute of Specialty Steels. The installation. which is to be used for the final ladle treatment of electric-arc furnace steels, is essentially a heating station with a 15 MV-A transformer and electrodes 350 mm in diameter. The station has a system of hoppers for storing and accurately dispensing alloying elements into the ladle, a lance for blowing argon through the melt, and a wire-feeding device for dispensing aluminum wire into the melt. A buggy equipped with an argon supply system is used to transport the metalfilled ladle to the heating and pouring stations. The ladle bottom is made with a block of porous material through which argon can be blown through the melt. In order to learn how to use the installation and make final adjustments to the equipment, more than 100 heats of machine and bearing steel, including steel for critical applications, were processed in it. Steelmaking time was reduced 30 to 60 minutes, depending on the type of refining slag used (white furnace slag, synthetic liquid slag, or slag made from solid slag-forming materials). It was possible to control the rate at which the metal was heated as well as the desulfurization process. Manganese and silicon assimilation was increased, and the concentration of alloying elements in the metal was

optimized. No metal was rejected because of nonmetallic inclusions. The bearing steel had a lower oxygen concentration than conventionally made bearing steel. The mechanical properties and surface quality of the machine steel was also greatly improved. Refractory lining and electrode service life was satisfactory. Figures 3.

### Data Bank for Electroslag Remelting and Related Technologies

927D0016B Kiev PROBLEMY SPETSIALNOY ELEKTROMETALLURGII in Russian No 4, 91 pp 86-87

[Abstract of article by V. M. Litvinchuk]

[Abstract] The Ye. O. Paton Institute of Electric Welding of the Ukrainian Academy of Sciences has created a data bank for electroslag remelting and related technologies. It has nine major directories (e.g. electroslag technology, vacuum-arc remelting and other special electrometallurgical processes, continuous casting, and so forth) and more than 12,000 files compiled from the journal METLLURGIYA dating from January 1, 1988. Average document size is 2000 bytes and contains complete bibliographical information, key words, and synopses. The data is stored on magnetic tapes, which are distributed by the All-Union Institute of Scientific and Technical Information. The software, which was designed for use on MSDOSequipped PC/AT personal computers, features a userfriendly dialog interface. The user can access a document through any of its bibliographic information by utilizing an electronic dictionary. Documents or related information can be retrieved in printed form or on diskette in any of a number of forms convenient to the user, including author and company indices, lists of topically related files, and so forth. More information can be obtained by writing to the Paton Institute at the following address: 252650, Kiev-5, GSP, 11 Bozhenko St., Department of Electroslag Technology. The telex number is 131139 RAKOTs CYu.

### 5285 PORT ROYAL RO SPRINGFIELD VA

22161

This is a U.S. Government publication. Its contents in no way represent the policies, views, or attitudes of the U.S. Government. Users of this publication may cite FBIS or JPRS provided they do so in a manner clearly identifying them as the secondary source.

Foreign Broadcast Information Service (FBIS) and Joint Publications Research Service (JPRS) publications contain political, military, economic, environmental, and sociological news, commentary, and other information, as well as scientific and technical data and reports. All information has been obtained from foreign radio and television broadcasts, news agency transmissions, newspapers, books, and periodicals. Items generally are processed from the first or best available sources. It should not be inferred that they have been disseminated only in the medium, in the language, or to the area indicated. Items from foreign language sources are translated; those from English-language sources are transcribed. Except for excluding certain diacritics, FBIS renders personal names and place-names in accordance with the romanization systems approved for U.S. Government publications by the U.S. Board of Geographic Names.

Headlines, editorial reports, and material enclosed in brackets [] are supplied by FBIS/JPRS. Processing indicators such as [Text] or [Excerpts] in the first line of each item indicate how the information was processed from the original. Unfamiliar names rendered phonetically are enclosed in parentheses. Words or names preceded by a question mark and enclosed in parentheses were not clear from the original source but have been supplied as appropriate to the context. Other unattributed parenthetical notes within the body of an item originate with the source. Times within items are as given by the source. Passages in boldface or italics are as published.

### SUBSCRIPTION/PROCUREMENT INFORMATION

The FBIS DAILY REPORT contains current news and information and is published Monday through Friday in eight volumes: China, East Europe, Central Eurasia, East Asia, Near East & South Asia, Sub-Saharan Africa, Latin America, and West Europe. Supplements to the DAILY REPORTs may also be available periodically and will be distributed to regular DAILY REPORT subscribers. JPRS publications, which include approximately 50 regional, worldwide, and topical reports, generally contain less time-sensitive information and are published periodically.

Current DAILY REPORTs and JPRS publications are listed in *Government Reports Announcements* issued semimonthly by the National Technical Information Service (NTIS), 5285 Port Royal Road, Springfield, Virginia 22161 and the *Monthly Catalog of U.S. Government Publications* issued by the Superintendent of Documents, U.S. Government Printing Office, Washington, D.C. 20402.

The public may subscribe to either hardcover or microfiche versions of the DAILY REPORTs and JPRS publications through NTIS at the above address or by calling (703) 487-4630. Subscription rates will be

provided by NTIS upon request. Subscriptions are available outside the United States from NTIS or appointed foreign dealers. New subscribers should expect a 30-day delay in receipt of the first issue.

U.S. Government offices may obtain subscriptions to the DAILY REPORTs or JPRS publications (hardcover or microfiche) at no charge through their sponsoring organizations. For additional information or assistance, call FBIS, (202) 338-6735,or write to P.O. Box 2604, Washington, D.C. 20013. Department of Defense consumers are required to submit requests through appropriate command validation channels to DIA, RTS-2C, Washington, D.C. 20301. (Telephone: (202) 373-3771, Autovon: 243-3771.)

Back issues or single copies of the DAILY REPORTs and JPRS publications are not available. Both the DAILY REPORTs and the JPRS publications are on file for public reference at the Library of Congress and at many Federal Depository Libraries. Reference copies may also be seen at many public and university libraries throughout the United States.